[redacted]

OTS: 60-11,080

JPRS: L-1188-N

STAT

25 December 1959

[redacted]

STAT

SELECTED TRANSLATIONS ON

SOVIET ROCKET ENGINEERING

Distributed by:

OFFICE OF TECHNICAL SERVICES
U. S. DEPARTMENT OF COMMERCE
WASHINGTON 25, D. C.

U. S. JOINT PUBLICATIONS RESEARCH SERVICE
205 EAST 42nd STREET, SUITE 300
NEW YORK 17, N. Y.

[redacted]

STAT

JPRS: L-1188-N

CSO : 3905-N/2

SELECTED TRANSLATIONS

ON

SOVIET ROCKET ENGINEERING

This series includes translations of selected items from the Soviet literature on hypersonic aerodynamics, magnetohydrodynamics, space flight mechanics, propulsion systems (liquid, solid, nuclear, ion, plasma), propellants and combustion, instrumentation and control, guidance and navigation, materials and structures, and space communications. The series is published as an aid to U. S. Government research.

ON THE THEORY OF GAS FLOW IN THE LAYER BETWEEN THE SURFACE OF A SHOCK WAVE AND THE BLUNT SURFACE OF A ROTATING BODY

N. A. Slezkin

Izvestiya Akademii Nauk SSR, Otdeleniye Tekhnicheskikh Nauk, Mekhanika i Mashinostroyeniye, [News of the Academy of Sciences USSR, Department of Technical Sciences, Mechanics and Machine Building], No. 2, Mar-Apr 1959, Moscow, pages 3-12

As is known, when a body moves in air with a velocity exceeding the velocity of sound, a shock wave is produced. If the forward portion of the surface of the body is blunted, then the surface of the shock wave is located in its forward portion at a small distance from the surface of the body. In 1946, we proposed in one of our articles [1] to consider this intermediate layer between the surface of the shock wave and the surface of the blunting of the body as a Reynolds layer, i.e., as a layer in which the flow of gas is affected essentially by the pressure and by viscosity forces. This assumption can be justified in the following manner. It is known that the influence of viscosity is of importance not only for the flow of gas near solid walls, but also for the flow within the limits of the pressure jump itself. As long as the considered intermediate layer is bounded on one hand by a solid wall and on the other hand by the surface of the pressure peak, then the viscosity of the gas should exert a substantial influence on the flow of gas in such a layer. Therefore, the problem may concern merely whether the viscosity should be computed in accordance with the Prandtl-layer model or in accordance with the Reynolds-layer model. In our second article [2] we have shown that the Reynolds equations, which he proposed in the approximate hydrodynamic theory of flow in a lubricating layer [3], are applicable not only for small Reynolds numbers, but also Reynolds numbers on the order of ε^{-1}, where ε is the ratio of the mean thickness of the layer to the length of the longitudinal extent of the layer. On the other hand, the Prandtl equations for the boundary layer are correct for Reynolds numbers having an order ε^{-2}. In both cases the characteristic dimension of length, ℓ, is taken to be the length of the longitudinal extent of the layer, and the characteristic velocity is taken to be the maximum value of the modulus of the velocity within the confines of the layer. The coordinate x axis is taken to be a curved coordinate along the surface of the body, where the y coordinate is taken to be the length of the segment along the normal to the surface of the body.

We shall henceforth use two ideas in the investigation. The first is that it is useful in certain cases to stratify the region of

gas flow not only in the longitudinal direction, separating the laminar sublayer, the turbulent layer, and the region of the external flow, but also in the transverse direction, separating the following portions of the layer: 1) the Reynolds layer, 2) the Oseen layer, and, 3) the Prandtl layer. The second idea is to use the method of successive examination of the development of the phenomenon within the limits of the individual sections of the layer, with a transition from one section to the other. This idea makes it possible to employ linearized equations.

1. Statement of the problem. We shall consider that the body is stationary, and that the flow of gas has a velocity U_∞ at infinity, directed parallel to the symmetry axis of the body from left to right (see Figure). We denote the angle between the tangents to the surface of the shock wave and the velocity vector of the external stream by β, while the angle between the tangent to the surface of the body and the same direction of the velocity vector we denote by θ. If we use the known formulas for an oblique shock wave [4], derived under the assumption that the viscosity and the heat conduction of the gas are not taken into account, we can obtain the following equations:

$$u_A = U_\infty\left[\frac{\rho_\infty}{\rho_A}\sin\beta\sin(\beta-\theta)+\cos\beta\cos(\beta-\theta)\right]$$
$$v_A = U_\infty\left[-\frac{\rho_\infty}{\rho_A}\sin\beta\cos(\beta-\theta)+\cos\beta\sin(\beta-\theta)\right] \qquad (1.1)$$
$$U_A = U_\infty\sqrt{\cos^2\beta+\left(\frac{\rho_\infty}{\rho_A}\right)^2\sin^2\beta},\quad p_A = p_\infty+\rho_\infty U_\infty^2\sin^2\beta\left(1-\frac{\rho_\infty}{\rho_A}\right)$$

where the index A denotes the values after the passage of the shock wave, i.e., on the outer boundary of the intermediate layer considered by us, the variable thickness of this layer being denoted by h. It follows from Eq. (1.1) for the modulus of velocity U_A that for values of angle β that differ little from $\pi/2$, the maximum value of the velocity modulus U_A will differ little from the value $U_\infty\rho_\infty/\rho_A$

$$U_A \sim U_\infty\frac{\rho_\infty}{\rho_A} \qquad (1.2)$$

The ratio of the coefficient of viscosity to the density, μ/ρ will not agree within the limits of the layer with the value μ_∞/ρ_∞; in the layer $T_A > T_\infty$ we have $\rho_A > \rho_\infty$. The viscosity coefficient increases with increasing temperature, i.e., $\mu_A > \mu_\infty$.

Thus, it can be assumed that the order of the values μ_A/ρ_A is close to the order of μ_∞/ρ_∞. In this case we obtain for the Reynolds in the layer the following relation

$$R_A = \frac{\rho_A U_A l}{\mu_A} \sim \frac{\rho_\infty}{\mu_\infty}\frac{\rho_\infty}{\rho_A}U_\infty l = \frac{\rho_\infty}{\rho_A}R_\infty \qquad (1.3)$$

If we consider the ratio ρ_∞/ρ_A small and of the same order as ε, and if we assume that the Reynolds number of the external stream R_∞ has an order of ε^{-2}, the Reynolds number for the flow of gas inside the intermediate layer considered by us will be of the order ε^{-1}, and this means in turn that under these assumptions the layer between the surface shock wave and the blunted forward portion of the surface of the body can be considered as a Reynolds layer.

In the note/1/ we considered the case when $\theta = \pi/2$ and the angle β is almost $\pi/2$, and did not take into account the variability of the density within the limits of the layer. The latter premise was also the starting point in other investigations devoted to the same topic; thus, in a recently published paper by Lee-Ting-i and Geiger/5/, the distance between the surface of the shock wave to the critical point on the surface of the body is also determined by using the equations of motion of the gas without taking into account the variability of the density in the layer and without taking into account the viscosity terms.

We propose that when the surface of the shock wave is closely adjacent to the surface of the blunted body, the influence of viscosity should be taken into account not only in the equations of motion of the gas, but also in the derivation of the relations on the surface of the shock wave. The purpose of this article is indeed the derivation of the approximate equations of the Reynolds type, suitable in certain cases for the flow of gas in a thin layer between a surface of a shock wave and a blunted surface of the body, and to use in the solution of these equations the conditions on the peak, with allowance for the viscosity and heat conduction of the gas.

2. Equations of Reynolds for the flow of gas in the layer.

We shall consider a section of the layer with abscissa $x_B = l$. In this section we take the point B, at which the longitudinal velocity u has a maximum value U_B. The values of the other quantities at the same point will be denoted by ρ_B, ρ_B, T_B, μ_B, and λ_B. We introduce the dimensionless variables and the dimensionless characteristics of gas flow in the layer as follows: (2.1)

$$x = lx_1,\quad y = \varepsilon l y_1,\quad u = U_B u_1,\quad v = \varepsilon U_B v_1,\quad p = p_B p_1,\quad \rho = \rho_B\rho_1,$$
$$T = T_B T_1,\quad \mu = \mu_B\mu_1,\quad \lambda = \lambda_B\lambda_1,\quad c_p = c_{pB}c_1,\quad \gamma = \frac{c_{pB}}{c_{vB}},$$
$$M_B^2 = \frac{\rho_B U_B^2}{\gamma p_B},\quad \frac{AU_B^2}{gc_{pB}T_B} = (\gamma-1)M_B^2,\quad R_B = \frac{l\rho_B U_B}{\mu_B},\quad P_B = \frac{g\mu_B}{\rho_B}\frac{\rho_B}{\gamma_B}$$

We shall consider the case of a plane-parallel steady-state flow of a viscous and heat-conducting gas without taking into account the mass forces. In this case the known equations of motion of the gas/6/, when using (2.1), are expressed in the following form

$$R_B \rho_1 \varepsilon^2 \left(u_1 \frac{\partial u_1}{\partial x_1} + v_1 \frac{\partial u_1}{\partial y_1}\right) = -\frac{R_B}{\gamma M_B^2} \varepsilon^2 \frac{\partial p_1}{\partial x_1} + \frac{\partial}{\partial y_1}\left(\mu_1 \frac{\partial u_1}{\partial y_1}\right) + \varepsilon^2 \left\{\frac{\partial}{\partial x_1}\left[\frac{2\mu_1}{3}\left(2\frac{\partial u_1}{\partial x_1} - \frac{\partial v_1}{\partial y_1}\right)\right] + \frac{\partial}{\partial y_1}\left(\mu_1 \frac{\partial v_1}{\partial x_1}\right)\right\}$$

$$\varepsilon^2 \rho_1 \left(u_1 \frac{\partial v_1}{\partial x_1} + v_1 \frac{\partial v_1}{\partial y_1}\right) = -\frac{1}{\gamma M_B^2} \frac{\partial p_1}{\partial y_1} + \frac{1}{R_B}\left\{\frac{\partial}{\partial x_1}\left(\mu_1 \frac{\partial u_1}{\partial y_1}\right) + \varepsilon^2 \frac{\partial}{\partial x_1}\left(\mu_1 \frac{\partial v_1}{\partial x_1}\right) + \frac{\partial}{\partial y_1}\left[\frac{2\mu_1}{3}\left(2\frac{\partial v_1}{\partial y_1} - \frac{\partial u_1}{\partial x_1}\right)\right]\right\}$$

$$\frac{\partial (\rho_1 u_1)}{\partial x_1} + \frac{\partial (\rho_1 v_1)}{\partial y_1} = 0 \qquad (2.2)$$

$$p_1 = \rho_1 T_1, \qquad \mu_1 = \mu_1(T_1), \qquad \lambda_1 = \lambda_1(T_1)$$

$$R_B \varepsilon^2 \rho_1 \left[u_1 \frac{\partial}{\partial x_1}(c_1 T_1) + v_1 \frac{\partial}{\partial y_1}(c_1 T_1)\right] = \varepsilon^2 R_B \frac{\gamma - 1}{\gamma}\left(u_1 \frac{\partial p_1}{\partial x_1} + v_1 \frac{\partial p_1}{\partial y_1}\right) + \frac{1}{P_B}\left[\varepsilon^2 \frac{\partial}{\partial x_1}\left(\lambda_1 \frac{\partial T_1}{\partial x_1}\right) + \frac{\partial}{\partial y_1}\left(\lambda_1 \frac{\partial T_1}{\partial y_1}\right)\right] + \frac{\gamma - 1}{\gamma}\mu_1 \left(\frac{\partial u_1}{\partial y_1}\right)^2 + \frac{\gamma - 1}{\gamma}\varepsilon^2 \mu_1 \left\{\varepsilon^2 \left(\frac{\partial v_1}{\partial x_1}\right)^2 + \frac{4}{3}\left[\left(\frac{\partial u_1}{\partial x_1}\right)^2 + \left(\frac{\partial v_1}{\partial y_1}\right)^2 + \frac{3}{2}\frac{\partial v_1}{\partial x_1}\frac{\partial u_1}{\partial y_1} - \frac{1}{2}\frac{\partial u_1}{\partial x_1}\frac{\partial v_1}{\partial y_1}\right]\right\}$$

where A is the heat equivalent of work. To obtain from Eqs. (2.2) the well known equations of the boundary layer, it is necessary to put

$$R_B = \frac{1}{\varepsilon^2} \qquad (2.3)$$

and assume that the numbers M_B and P_B are on the order of unity.

$$M_B \sim 1, \qquad P_B \sim 1 \qquad (2.4)$$

Putting then $\varepsilon \to 0$, we obtain equations for the flow in the Prandtl boundary layer. Since at $\varepsilon \to 0$ the Reynolds number increases to infinity, then the equations for the flow in the boundary layer will be the asymptotic equations of flow of a viscous and heat conducting gas. On the other hand if we put

$$R_B = \frac{1}{\varepsilon}, \qquad M_B^2 = 0, \qquad P_B \sim 1 \qquad (2.5)$$

and then decrease the parameter ε to 0, we obtain from Eqs. (2.2) the well known Reynolds equations for the flow of gas in a layer, which

after transformation to dimensional variables assume the following form

$$\frac{\partial p}{\partial x} = \frac{\partial}{\partial y}\left(\mu \frac{\partial u}{\partial y}\right), \qquad \frac{\partial p}{\partial y} = 0, \qquad \frac{\partial (\rho u)}{\partial x} + \frac{\partial (\rho v)}{\partial y} = 0 \qquad (2.6)$$

$$p = g R \rho T$$

$$0 = \frac{\partial}{\partial y}\left(\lambda \frac{\partial T}{\partial y}\right) + A\mu\left(\frac{\partial u}{\partial y}\right)^2, \qquad \mu = \mu(T), \qquad \lambda = \lambda(T)$$

Inasmuch as Eqs. (2.6) were also obtained by taking the limit $R_B \to \infty$, these equations can also be called asymptotic equations for the flow of viscous and heat-conducting gas in a thin layer. The difference between the Prandtl and Reynolds equations consist merely in the order in which the Reynolds number goes to infinity, or the order in which the ratio of the mean thickness of the layer to its longitudinal extent diminishes.

We assume that to study the flow of gas in the vicinity of the forward critical point on the body there are many grounds for using Eqs. (2.6) rather than the Prandtl equations.

In reference/2/ we have shown that for the case of an incompressible liquid it is easy to improve the solutions of Eqs. (2.6) by using successive approximations. In individual cases of gas flow in a layer, the solutions of Eqs. (2.6) can also be made more accurate by representing the solutions of Eqs. (2.2) in the form of series in powers of the small parameter ε.

3. Linearized equations for the flow of gas in the layer. Eqs. (2.6) are in general nonlinear. In order to obtain from Eqs. (2.2) linearized equations for the flow of gas in a layer, we shall proceed with the following argument. For the nearest vicinity of the considered point B we assume that the dimensionless variables are represented in the form

$$u_1 = 1 + \varepsilon u', \quad v_1 = \varepsilon v', \quad \rho_1 = 1 + \varepsilon^2 \rho', \quad p_1 = 1 + \varepsilon p'$$
$$T_1 = 1 + \varepsilon T', \quad \mu_1 = 1 + \varepsilon \mu', \quad \lambda_1 = 1 + \varepsilon \lambda', \quad c_1 = 1 + \varepsilon c_1' \qquad (3.1)$$

Inserting (3.1) into (2.2), using the assumptions (2.5) and retaining only the terms with the lowest power of the parameter ε, we obtain the following equations

$$\frac{\varepsilon}{\gamma M_B^2}\frac{\partial p'}{\partial x_1} = \frac{1}{\varepsilon R_B}\frac{\partial u'}{\partial y_1^2}, \qquad \frac{\partial p'}{\partial y_1} = 0, \qquad \frac{\partial u'}{\partial x_1} + \frac{\partial v'}{\partial y_1} = 0, \qquad p' = T', \qquad \frac{\partial^2 T'}{\partial y_1^2} = 0 \qquad (3.2)$$

If in the resultant Eqs. (3.2) we return to the initial dimensional variables, i.e., we put

$$x_1 = \frac{x}{l}, \quad y_1 = \frac{y}{\varepsilon l}, \quad u' = \frac{u - U_B}{\varepsilon U_B}, \quad v' = \frac{v}{\varepsilon U_B}$$
$$p' = \frac{p - p_B}{\varepsilon p_B}, \quad T' = \frac{T - T_B}{\varepsilon T_B}, \quad A\gamma \frac{p_B}{\rho_B} = gT_B c_{pB}(\gamma - 1) \tag{3.3}$$

then we get the simplest linearized Reynolds equations for the flow of gas in a layer

$$\frac{\partial p}{\partial x} = \mu_B \frac{\partial^2 u}{\partial y^2}, \quad \frac{\partial p}{\partial y} = 0, \quad \frac{\partial u}{\partial x} + \frac{\partial v}{\partial y} = 0, \quad p = \frac{p_B}{T_B} T \tag{3.4}$$

On the otherhand, if we put

$$\rho_1 = 1 + \varepsilon\rho' \tag{3.5}$$

we retain all the remaining equations in (3.1) and the assumption (2.5), make the substitution in Eqs. (2.2), retain the terms with the lowest power of the parameter ε, and return in the resultant equations to the initial dimensional variables, we obtain a new simple form of linearized Reynolds equations

$$\frac{\partial p}{\partial x} = \mu_B \frac{\partial^2 u}{\partial y^2}, \quad \frac{\partial p}{\partial y} = 0$$
$$\frac{\partial u}{\partial x} + \frac{\partial v}{\partial y} + U_B\left(\frac{1}{p_B}\frac{\partial p}{\partial x} - \frac{1}{T_B}\frac{\partial T}{\partial x}\right) = 0, \quad \frac{\partial^2 T}{\partial y^2} = 0 \tag{3.6}$$

We eliminate the density from the continuity equation with the aid of the equation of state

$$\frac{p}{p_B} + 1 = \frac{T}{T_B} + \frac{\rho}{\rho_B}$$

On the other hand, if we use instead of assumptions (2.5) the assumptions in (2.3) and (2.4), again make use of all the equations in (3.1), and repeat all the preceding calculations, we can obtain the following Oseen-type equations

$$\rho_B U_B \frac{\partial u}{\partial x} = -\frac{\partial p}{\partial x} + \mu_B \frac{\partial^2 u}{\partial y^2}, \quad \frac{\partial p}{\partial y} = 0, \quad \frac{\partial u}{\partial x} + \frac{\partial v}{\partial y} = 0, \quad p = \frac{p_B}{T_B} T$$
$$g\rho_B U_B\left[c_{pB} + T_B\left(\frac{dc_p}{dT}\right)_B\right]\frac{\partial T}{\partial x} = AU_B \frac{\partial p}{\partial x} \tag{3.7}$$

If however we use assumptions (3.5), the Oseen-type equations are represented in the form

$$\rho_B U_B \frac{\partial u}{\partial x} = -\frac{\partial p}{\partial x} + \mu_B \frac{\partial^2 u}{\partial y^2}, \quad \frac{\partial p}{\partial y} = 0$$
$$\frac{\partial u}{\partial x} + \frac{\partial v}{\partial y} + U_B\left(\frac{1}{p_B}\frac{\partial p}{\partial x} - \frac{1}{T_B}\frac{\partial T}{\partial x}\right) = 0 \tag{3.8}$$
$$g\rho_B U_B\left[c_{pB} + T_B\left(\frac{dc_p}{dT}\right)_B\right]\frac{\partial T}{\partial x} = AU_B\frac{\partial p}{\partial x} + \lambda_B \frac{\partial^2 T}{\partial y^2}$$

The linearized equations (3.7) were used extensively in the monograph of Targ/7/ to solve problems in the development of flow of an incompressible liquid in tubes and diffusors. The results of the calculations were in satisfactory agreement with the results of the experiments, not only with respect to the length of the initial portion, but also in respect to the development of the profile of the velocity distribution over the sections. For this reason one can assume that the foregoing linearized equations (3.6) or (3.8) can be used to solve certain types of problems in the flow of gas in a layer.

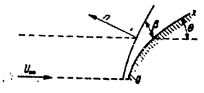

4. Dynamic conditions on the surface of the shock wave. The dynamic conditions that relate the characteristics of gas motion with the velocity of discontinuity propagation, with allowance for viscosity, were carried out by Duhame and considered in detail in the work by N. Ye Kochin/8/. These conditions can be written in symbolic form as follows

$$[\rho\theta^*] = 0, \qquad \rho\theta^*[\mathbf{V}] + [\mathbf{p}_n] = 0$$
$$\frac{1}{2}[\rho\theta^*(\mathbf{V}\cdot\mathbf{V})] + \rho\theta^*[cT] + [\mathbf{p}_n\cdot\mathbf{V}] - \left[\lambda\frac{\partial T}{\partial n}\right] = 0 \tag{4.1}$$

where β^* is the speed of propagation of the wave front, $\mathbf{V}$ the velocity vector of gas motion, and $\mathbf{p}_n$ is the stress vector on an area adjacent to the surface of the wave; the vector normal to the area is directed towards the outer flow (see figure). In the case under consideration by us, of a plane-parallel flow of gas, these conditions (4.1), after certain transformations, can be represented as

$$p_A = p_\infty + \left(1 - \frac{\rho_\infty}{\rho_A}\right)\rho_\infty U_\infty^2 \sin^2\beta + (\tau_{nn})_A \qquad (4.2)$$

$$u_A = U_\infty\left[\cos\beta\cos(\beta-\theta) + \frac{\rho_\infty}{\rho_A}\sin\beta\sin(\beta-\theta)\right] - \frac{\cos(\beta-\theta)}{\sin\beta}\frac{(\tau_{ns})_A}{\rho_\infty U_\infty} \qquad (4.3)$$

$$v_A = U_\infty\left[\cos\beta\sin(\beta-\theta) - \frac{\rho_\infty}{\rho_A}\sin\beta\cos(\beta-\theta)\right] - \frac{\sin(\beta-\theta)}{\sin\beta}\frac{(\tau_{ns})_A}{\rho_\infty U_\infty}$$

$$\rho_\infty U_\infty \sin\beta\left[\frac{1}{2}A(U_\infty^2 - U_A^2) + c_{p\infty}T_\infty - c_{pA}T_A + A\left(\frac{p_\infty}{\rho_\infty} - \frac{p_A}{\rho_A}\right) + A\frac{(\tau_{nn})_A}{\rho_A}\right] - \lambda_A\left(\frac{\partial T}{\partial n}\right)_A - A(\tau_{ns})_A[u_A\cos(\beta-\theta) + v_A\sin(\beta-\theta)] = 0 \qquad (4.4)$$

The projections of the vector of the deviator stress on the normal, τ_{nn}, and on the tangent, τ_{ns}, will be represented in the following form

$$\tau_{nn} = -\frac{2}{3}\mu\left(\frac{\partial u}{\partial x} + \frac{\partial v}{\partial y}\right) + 2\mu\left[\frac{\partial u}{\partial x}\sin^2(\beta-\theta) + \frac{\partial v}{\partial y}\cos^2(\beta-\theta) - \frac{1}{2}\left(\frac{\partial v}{\partial x} + \frac{\partial u}{\partial y}\right)\sin 2(\beta-\theta)\right] \qquad (4.5)$$

$$\tau_{ns} = \mu\left(\frac{\partial v}{\partial y} - \frac{\partial u}{\partial x}\right)\sin 2(\beta-\theta) + \mu\left(\frac{\partial v}{\partial x} + \frac{\partial u}{\partial y}\right)\cos 2(\beta-\theta)$$

If in the right halves of Eq. (4.5) we go to dimensionless quantities, using (2.1), and retain the terms of highest order, we can obtain the following approximate expressions for the projections of the deviator stress

$$\tau_{nn} \approx -\mu\frac{\partial u}{\partial y}\sin 2(\beta-\theta), \qquad \tau_{ns} \approx \mu\frac{\partial u}{\partial y}\cos 2(\beta-\theta) \qquad (4.6)$$

Thus, the relations on the surface of the shock wave, with allowance for viscosity and heat conduction, are represented by Eqs. (4.2), (4.3), (4.4), and (4.6).

5. General expressions for the characteristics of gas flow in the intermediate layer. The simplest linearized equations (3.4) were used in our article /1/ under certain supplementary assumptions. We shall now consider the use of the system of Eqs. (3.6) with partial allowance for the variability of the density.

If we retain the previous notation, but consider not a plane-parallel flow but a gas flow with a symmetry axis, then the linearized equations, with partial allowance for the variability of the density and with approximate replacement of r by the lengths of the arc x, will be represented in the following form

$$\frac{\partial p}{\partial x} = \mu_B\frac{\partial^2 u}{\partial y^2}, \quad \frac{\partial}{\partial y}(xv) + \frac{\partial}{\partial x}\left[x\left(u + U_B\frac{\rho}{\rho_B} - U_B\frac{T}{T_B}\right)\right] = 0$$

$$\frac{\partial p}{\partial y} = 0, \quad \frac{\partial^2 T}{\partial y^2} = 0, \quad \frac{p}{p_B} + 1 = \frac{T}{T_B} + \frac{\rho}{\rho_B} \qquad (5.1)$$

The boundary conditions on the surface of the body and on the surface of the shock wave will have the form

$$u = 0, \quad v = 0, \quad T = T_0 \quad \text{при } y = 0$$
$$u = u_A, \quad v = v_A, \quad T = T_A \quad \text{при } y = h \tag{5.2}$$

The solutions of Eqs. (5.1) subject to boundary conditions (5.2) will be given by the equations

$$u = \frac{1}{2\mu_B}\frac{\partial p_A}{\partial x}(y^2 - hy) + \frac{u_A}{h}y$$
$$xv = -\int_0^y \frac{\partial}{\partial x}\left[x\left(u + U_B\frac{\rho_A}{\rho_B} - U_B\frac{T}{T_B}\right)dy\right] \tag{5.3}$$
$$T = T_0 + (T_A - T_0)\frac{y}{h}$$

If in the second equation of (5.3) the upper limit y is replaced by h, the operation of differentiation with respect to the variable x is taken outside the integral sign, and the first and third equations of (5.3) are used then used together with the boundary condition (5.2) for v, we obtain an equation for the pressure

$$\frac{1}{x}\frac{d}{dx}\left(xh^3\frac{dp_A}{dx}\right) = 12\mu_B\left\{\rho_A - \frac{1}{2}u_A\frac{dh}{dx} + \frac{h}{2}\left(\frac{du_A}{dx} + \frac{u_A}{x}\right) - \right.$$
$$\left. - \frac{1}{2}\frac{U_B}{T_B}\left[(T_0 - T_A)\left(\frac{dh}{dx} + \frac{h}{x}\right) - h\left(\frac{dT_A}{dx} - \frac{dT_0}{dx}\right)\right]\right\} \tag{5.4}$$

From the first Eq. (5.3) we get

$$\left(\frac{\partial u}{\partial y}\right)_A = \frac{h}{2\mu_B}\frac{dp_A}{dx} + \frac{u_A}{h} \tag{5.5}$$

Inserting (5.5) into (4.6) and then into (4.2), (4.3), and (4.5) we obtain the following expressions for the characteristics of gas flow on the very surface of the shock wave

$$\rho_A = \rho_\infty + \left(1 - \frac{\rho_\infty}{\rho_A}\right)\rho_\infty U_\infty^2 \sin^2\beta - \sin 2(\beta - \theta)\left[\frac{h}{2}\frac{dp_A}{dx} + \frac{\mu_B u_A}{h}\right] \tag{5.6}$$

$$u_A\left[1 + \frac{\mu_B}{\rho_\infty U_\infty h}\frac{\cos(\beta - \theta)\cos 2(\beta - \theta)}{\sin\beta}\right] =$$
$$= U_\infty\left[\cos\beta\cos(\beta - \theta) + \frac{\rho_\infty}{\rho_A}\sin\beta\sin(\beta - \theta)\right] -$$
$$- \frac{h}{2\rho_\infty U_\infty}\frac{dp_A}{dx}\frac{\cos(\beta - \theta)\cos 2(\beta - \theta)}{\sin\beta}$$

$$v_A = U_\infty\left[\cos\beta\sin(\beta - \theta) - \frac{\rho_\infty}{\rho_A}\sin\beta\cos(\beta - \theta)\right] -$$
$$- \frac{\mu_B}{\rho_\infty U_\infty h}u_A\frac{\sin(\beta - \theta)\cos 2(\beta - \theta)}{\sin\beta} - \frac{h}{2\rho_\infty U_\infty}\frac{dp_A}{dx}\frac{\sin(\beta - \theta)\cos 2(\beta - \theta)}{\sin\beta}$$
$$c_{pA}T_A - c_{p\infty}T_\infty + \frac{\lambda_A}{\rho_\infty U_\infty \sin\beta}\frac{T_A - T_0}{h} = A\left\{\frac{1}{2}(U_\infty^2 - U_A^2) + \right.$$
$$+ \frac{p_\infty}{\rho_\infty} - \frac{p_A}{\rho_A} - \frac{\mu_B}{\rho_A}\left(\frac{u_A}{h} + \frac{h}{2\mu_B}\frac{dp_A}{dx}\right)\sin 2(\beta - \theta) -$$
$$\left. - \cos 2(\beta - \theta)\left[\frac{h}{2}\frac{dp_A}{dx} + \frac{\mu_B u_A}{h}\right]\right\}[u_A\cos(\beta - \theta) + v_A\sin(\beta - \theta)]$$

Eqs. (5.4) and (5.6) must be used in conjunction with the geometric relation

$$\frac{dh}{dx} = \operatorname{tg}(\beta - \theta) \tag{5.7}$$

We chose as the characteristic velocity U_B in section 2 the maximum value of the longitudinal velocity u in the section with abscissa $x_B = \ell$. Since we have

$$\frac{\partial u}{\partial y} = \frac{1}{2\mu_B}\frac{dp_A}{dx}(2y - h) + \frac{u_A}{h}$$

be from the ordinate of the point B will determined by the equality

$$y_B = \frac{h}{2} - \frac{\mu_B u_A}{h\,dp_A/dx} \tag{5.8}$$

Inserting (5.8) into the first and last equations of (5.3) we get

$$U_B = -\frac{1}{2\mu_B}\frac{dp_A}{dx}\left(\frac{h}{2} - \frac{\mu_B u_A}{h\,dp_A/dx}\right)^2$$
$$T_B = T_0 + (T_A - T_0)\left[\frac{1}{2} - \frac{\mu_B u_A}{h^2\,dp_A/dx}\right] \tag{5.9}$$

If we use the approximate equation of state in this case, we obtain the following expression for the density

$$\rho_B = \rho_A\frac{T_B}{2T_B - T_A} \tag{5.10}$$

Since the initial equations (5.1) are correct for a section with abscissa x_B 1, then the relation (5.4) and relations (5.6), (5.9), and (5.10) are correct, generally speaking, for $\mathcal{A}$ small vicinity of the intermediate layer considered by us near the fixed section. As one moves away from the given section towards the broadening of the layer, the velocity U_B increases and the Reynolds number

$$R_B = \frac{\rho_B U_B x_B}{\mu_B} \tag{5.11}$$

will also increase; as one approaches the symmetry axis, this Reynolds number (5.11) will decrease. Consequently, the vicinity of the layer for which the foregoing relations are valid can be extended with lesser error towards the symmetry axis than towards removal away from this axis.

6. Limiting relations for the symmetry axis. Let us assume that the relations established in section 5 are correct also for those sections of the intermediate layer considered by us, which are sufficiently close to the symmetry axis of the blunted body. Subject to this assumption, we perform in these relations the transition to the limit, decreasing the abscissa x to 0, increasing the angle to $\pi/2$, and putting $\beta = \pi/2$. We then have

$$\begin{array}{llll} \sin\beta \to 1, & \cos\beta \to 0, & \sin(\beta-\theta) \to 0 & \\ \cos(\beta-\theta) \to 1, & \sin 2(\beta-\theta) \to 0, & \cos 2(\beta-\theta) \to 1 & \end{array} \tag{6.1}$$

Using the L'Hospital rule we get

$$\left(\frac{\cos\beta}{x}\right)_{\substack{x\to 0\\ \beta\to\pi/2}} = -\frac{d\beta}{dx}, \qquad \left[\frac{\sin(\beta-\theta)}{x}\right]_{\substack{x\to 0\\ \beta-\theta\to\pi/2}} = \frac{d\beta}{dx} - \frac{d\theta}{dx} \tag{6.2}$$

Since on the symmetry axis the pressure should have a maximum value, we get

$$\left(\frac{dp_A}{dx}\right)_{x=0} = 0 \tag{6.3}$$

From Eq. (5.7) we get

$$h \to h^*, \quad \left(\frac{dh}{dx}\right)_{x=0} = 0 \tag{6.4}$$

Using (6.1) and (6.3) we obtain from (5.6) the following limiting relations

$$(u_A)_{x=0} = 0$$

$$(v_A)_{x=0} = -\frac{\rho_\infty}{\rho_A} U_\infty = -kU_\infty \tag{6.5}$$

$$(p_A)_{x=0} = p_\infty + (1-k)\rho_\infty U_\infty^2$$

$$\left(c_{vA} T_A - c_{v\infty} T_\infty + \lambda_A \frac{T'_A - T_B}{\rho_\infty U_\infty h}\right)_{x=0} = A\left[\frac{p_\infty}{\rho_\infty}(1-k) + \frac{1}{2}U_\infty^2(1-k)^2\right]$$

Differentiating the second Eq. (5.6) and using the foregoing equations for the limiting transitions, we get

$$\left(\frac{du_A}{dx}\right)_{x=0}\left[1 + \frac{\mu_B}{\rho_\infty h^* U_\infty}\right] = U_\infty\left[-\frac{d\beta}{dx} + k\left(\frac{d\beta}{dx} - \frac{d\theta}{dx}\right) - \frac{h^*}{2\rho_\infty U_\infty}\frac{d^2 p_A}{dx^2}\right]_{x=0} \tag{6.6}$$

If we start with the first Eq. (5.3), we find that the longitudinal velocity along the entire symmetry axis equals 0, and consequently we can put

$$U_B = 0 \tag{6.7}$$

From the L'Hospital rule we get

$$\lim\left(\frac{v_A}{x}\right)_{x\to 0} = \frac{du_A}{dx}, \qquad \lim\left[\frac{1}{x}\frac{dp_A}{dx}\right]_{x\to 0} = \frac{d^2 p_A}{dx^2} \tag{6.8}$$

Making the limiting transition in Eq. (5.4) and using (6.5), (6.3), (6.4), (6.8) and (6.7) we get

$$-kU_\infty = \left[\frac{h^{*2}}{6\mu_B}\frac{d^2 p_A}{dx^2} - h^*\frac{du_A}{dx}\right]_{x=0} \tag{6.9}$$

If we differentiate the first equation of (5.6) twice and then make the transition to the limit, we obtain

$$\left(\frac{d^3 p_A}{dx^3}\right)_{x=0} = -\left\{2(1-k)\rho_\infty U_\infty^2\left(\frac{d\beta}{dx}\right)^2 + 4\left(\frac{d\beta}{dx} - \frac{d\theta}{dx}\right)\left[\frac{h^*}{2}\frac{d^2 p_A}{dx^2} + \frac{\mu_B}{h^*}\frac{du_A}{dx}\right]\right\}_{x=0} \tag{6.10}$$

Inserting (6.9) into (6.6) and (6.10), we obtain the following two relations

$$\left(\frac{d^2p_A}{dx^2}\right)_0\left(\frac{h^{*2}}{6\mu_B}+\frac{2h^*}{\rho_\infty U_\infty}\right)= \tag{6.11}$$

$$= -U_\infty\left[\frac{d\beta}{dx}(1-k)+k\frac{d\theta}{dx}+\frac{k}{h^*}+k\frac{\mu_B}{\rho_\infty U_\infty h^{*2}}\right]_{x=0}$$

$$\left(\frac{d^2p_A}{dx^2}\right)_0\left[1+\frac{k}{3}h^*\left(\frac{d\beta}{dx}-\frac{d\theta}{dx}\right)\right]_0=$$

$$= -U'_\infty\left[2\rho_\infty U_\infty(1-k)\left(\frac{d\beta}{dx}\right)^2+\frac{4k\mu_B}{h^{*2}}\left(\frac{d\beta}{dx}-\frac{d\theta}{dx}\right)\right]_{x=0}$$

Eliminating d^2p/dx^2 from (6.11) we get

$$a\left(\frac{d\beta}{dx}\right)^2+2b\frac{d\beta}{dx}+c=0 \tag{6.12}$$

where

$$a=\frac{1}{3}(1-k)h^*\left(\frac{\rho_\infty U_\infty h^*}{\mu_B}-1\right)$$

$$b=-\frac{1}{2}\left[k+1-\frac{8}{3}(1-2k)h^*\frac{d\theta}{dx}\right] \tag{6.13}$$

$$c=-k\left[\frac{1}{h^*}+\frac{\mu_B}{\rho_\infty U_\infty h^{*2}}-\frac{d\theta}{dx}-\frac{8}{3}h^*\left(\frac{d\theta}{dx}\right)^2\right]$$

Solving Eq. (6.12) and selecting the sign in front of the square root in this solution on the basis of the condition that the angle β must decrease with increasing x, we get

$$\left(\frac{d\beta}{dx}\right)_0=-\frac{1}{a}(b+\sqrt{b^2-ac}) \tag{6.14}$$

Thus, if we assume ρ_∞, U_∞, and $(d\theta/dx)_0$ known, specify preliminary values of h^*, k, and μ_B on the basis of some other considerations, we can determine the value of $(d\beta/dy)_0$ from Eq. (6.14), and will therefore have in the nearest vicinity of the symmetry axis

$$\beta=\frac{\pi}{2}+\left(\frac{d\beta}{dx}\right)_0 x \tag{6.15}$$

From the foregoing data and from the value of $(d\beta/dx)_0$ as obtained from (6.14) we can determine $(d^2p_A/dx^2)_0$ from the first Eq. (6.11), and determine the value of $(du_A/dx)_0$ from (6.6). We then have for the vicinity of the symmetry axis

$$p=(p_A)_0+\frac{1}{2}x^2\left(\frac{d^2p}{dx^2}\right)_0,\quad u_A=\left(\frac{du_A}{dx}\right)_0 x \tag{6.16}$$

Next, going to the section close to the axis and determining the angle β for this section from (6.15), we can repeat the entire argument and derive formulas analogous to (6.14), (6.15), and (6.16). The last equation of (6.5) contains the temperature T_0 on the wall, which cannot be considered assumed. In the first approximation this temperature can be assumed equal to the temperature T_A. If one assumes that the coefficient of heat capacity c_v is represented by a definite dependence on T, it is possible to determine from the last equation of (6.5) the temperature T_A in terms of T_0, P_∞, U_∞, ρ_∞, and k. In this case it is possible to determine from the temperature T_A the viscosity coefficient μ_A on the axis and put $\mu_B=\mu_A$ in Eqs. (6.13). Then, if Eqs. (6.13) are used, it is enough to specify the tentative value of the thickness of the layer h^* on the symmetry axis.

Received 17 February 1958.

BIBLIOGRAPHY

1. Slezkin N. A. Concerning the Problem of Determining the Distribution of Pressure on the Blunting Area of a Shell, DAN SSSR (Reports of the Academy of Sciences USSR), vol 54, no 7, pp 583-585, 1946.

2. Slezkin N. A. Concerning the Problem of Refining the Solution of the Reynolds Equation, DAN SSSR, vol 54, no 2, pp 121-124, 1946.

3. Reynolds, O. Hydrodynamic Theory of Lubrication and its Application to the Tower Experiments. Coll. Gidrodinamicheskaya teoriya smazki (Hydrodynamic Theory of Lubrication), GTTI, pp 249-360, 1934.

4. Loytsyanskiy L. G. Mekhanika zhidkosti i gaza (Mechanics of Liquids and Gases) GITTL, p 326 (1957).

5. Li Ting-i, Geiger R. Critical Point of a Blunt-Nose Body in a Hypersonic Stream. Coll. of Translations "Mekhanika"(Mechanics) 5, pp 33-48 (1957).

6. Schlichting G. Teoriya pogranichnovo sloya (Boundary Layer Theory) Russ. Transl. from German, IL, p 254, 1956.

7. Targ S. M. Osnovnyye zadachi teorii laminarnykh techeniy (Principal problems of the Theory of Laminar Flow), GITTL, 1951.

8. Kochin N. Ye. Sobraniye sochineniy (Collected Works), vol II, pp 5--42, Izd. AN SSSR, 1949.

Approximation Method of Calculating Shock Waves and Their Interactions

G. M. Iyakhov
N. I. Polyakova

Izvestiya Akademii Nauk SSR, Otdeleniye Tekhnicheskikh Nauk, Mekhanika i Mashinostroyeniye, [News of the Academy of Sciences USSR, Department of Technical Sciences, Mechanics and Machine Building], No 2, Mar-Apr 1959, Moscow, pages 13-18.

1. Description of the method. The problem of propagation of known stationary shock wave has at present not been solved in general form even for unidimensional plane flow. The system of three quasi-linear first-order partial differential equations

$$\frac{\partial u}{\partial t}+u\frac{\partial u}{\partial x}+\frac{1}{\rho}\frac{\partial p}{\partial x}=0,\quad \frac{\partial \rho}{\partial t}+u\frac{\partial \rho}{\partial x}+\rho\frac{\partial u}{\partial x}=0,\quad \frac{\partial s}{\partial t}+u\frac{\partial s}{\partial x}=0 \qquad (1.1)$$

which describes the non-stationary shock wave, should be solved subject to the boundary conditions on the front of the wave, i.e., on the line that is also sought and must itself be determined from the considered system of equations. This circumstance complicates the exact solution of the problem considerably.

The method proposed is based on the fact that the curve that expresses the law of compressibility of the medium, $p=p(\rho)$, is replaced by a broken line with segments of the type

$$p=-A^2\rho^{-1}+B \qquad (1.2)$$

where A and B are constant within the limits of each segment of the broken line.

Such an approximation was first used by Chaplygin/1/ in a consideration of steady-state flow of gas, and was also used by L.I. Sedov/2/ and, in the case of unsteady flow, by K.P. Stanyukovich/3/.

In dense media the heat losses can be neglected at pressures on the order of tens or even hundreds of atmospheres, and therefore this method can find wide use here. However, such an approximation is possible also in an analysis of shock waves in air, in the case when the pressure on the front does not exceed 2 or 3 kg/cm^2. The Hugoniot adiabat, which gives the connection between the pressure p and the specific volume V on the front of the wave

$$V=V_0\frac{(k-1)p+(k+1)p_0}{(k+1)p+(k-1)p_0} \qquad (1.3)$$

differs in this case little from the Poisson adiabat

$$pV^k=p_0V_0^k \qquad (1.4)$$

For illustration, we give the values of the volume V, calculated in accordance with (1.3) and (1.4), for certain values of p/p_0

$p/p_0 = 1.0$	1.5	2.0	2.5		
$V/V_0 = 1$	0.750	0.615	0.531	according to	(1.3)
$V/V_0 = 1$	0.748	0.609	0.525	according to	(1.4)

We write down the basic equations for one-dimensional plane case in the Lagrange system of coordinates

$$\frac{\partial u}{\partial t} + \frac{\partial p}{\partial h} = 0, \qquad \frac{\partial u}{\partial h} - \frac{\partial V}{\partial t} = 0 \tag{1.5}$$

Here h is the mass of the substance between the initial and the current sections

$$h = \int_0^{x_0} \rho_0 dx = \int_0^x \rho dx, \quad \rho \frac{dx}{\partial h} = 1 \tag{1.6}$$

Let the equation of state of the medium be

$$p = -A^2 V + B$$

Then the system of equations becomes

$$\frac{\partial u}{\partial t} + \frac{\partial p}{\partial h} = 0, \qquad \frac{\partial u}{\partial h} + \frac{1}{A^2}\frac{\partial p}{\partial t} = 0$$

From this we readily obtain the well known wave equation

$$\frac{\partial^2 p}{\partial h^2} = \frac{1}{A^2}\frac{\partial^2 p}{\partial t^2} \tag{1.7}$$

the solution of which has the form

$$p = F_1(h - At) + F_2(h + At), \quad u = \frac{1}{A}\left[F_1(h - At) - F_2(h + At)\right] \tag{1.8}$$

Here F_1 and F_2 are arbitrary functions, which should be determined from the boundary conditions, A is the velocity of propagation of small disturbances in coordinates h,t. The quantity A corresponds to the acoustic impedance of the medium ρc for a given section of the approximation of the isentropic curve.

2. Propagation of shock waves. We consider the propagation of a plane shock wave in a medium, the equation of state of which is given in the form $p = p(V)$ while the pressure, as a function of time, is defined at a certain section of this medium, which we shall consider the initial section. The boundary conditions are

specified in the initial section and on the front of the wave. The law of motion of the front is not known beforehand and must itself be determined from the system of the principal equations.

The boundary conditions on the front of the shock wave are of the form

$$\rho_0 D = \rho(D - u), \qquad p - p_0 = \rho_0 D u \tag{2.1}$$

Here p_0, ρ_0 are the paremeters of the medium in front of the wave front, while p, ρ, D, and u are the parameters on the front of the wave.

Eliminating u from these equations we get

$$p - p_0 = \rho_0^2 D^2 (V_0 - V)$$

If the curve $p = p(V)$ is approximated by a straight line $p - p_0 = -A^2 (V - V_0)$, then $\rho_0 D = A$, i.e., the velocity of the front of the wave coincides with the speed of propagation of the weak discontinuities. In this case all the states behind the front of the wave move with equal velocity, equal to the velocity of the front. The wave will proceed without damping and without a change in its front. Let us consider the case when the curve $p = p(V)$ is approximated by a broken line (Fig. 1). On the section closest to the front we have

$$p = -A_0^2 V + B_0 \tag{2.2}$$

Ahead of the front we have

$$p = -A_0^2 V + B_0 \tag{2.3}$$

The velocity of the front in Lagrangian coordinates is

$$h'_\phi = \rho_0 D = \sqrt{\frac{p - p_0}{V_0 - V}} \tag{2.4}$$

It is obvious that

$$A_n = \sqrt{\frac{p - p_{n-1}}{V_{n-1} - V}} > h'_\phi > A_1 = \sqrt{\frac{p_1 - p_0}{V_0 - V_1}} \tag{2.5}$$

where A_1 corresponds to the speed of propagation of the states on the first section, and A_n corresponds to the last section of the approximation. It follows from this that the states behind the front of themselves propagates more rapidly than the front itself, and the front itself moves more rapidly than the weak disturbances in front of it. Thus, when the curve p=p (V) is replaced by a broken line with several segments, the shock wave changes its shape as it propagates. The magnitude of the maximum pressure will decrease. By reducing the sizes of the segments, it is possible to obtain any degree of accuracy in the determination of the wave parameters.

It follows from (2.1) and (2.4) that

$$p - p_0 = h_{\varphi}^2 (V_0 - V_n), \qquad u = h_{\varphi} (V_0 - V_n)$$

Taking (2.2) and (2.3) into account, we get

$$p - p_0 = \frac{a_n h^2_{\varphi}}{A^2_n - h^2_{\varphi}}, \qquad u = \frac{a_n h_{\varphi}}{A_n^2 - h^2_{\varphi}}$$
$$\left(a_0 = \frac{A_n^2 B_0 - A^2_0 B_n - \rho_0 (A_n^2 - A_0^2)}{A_0^2} \right) \qquad (2.6)$$

The flow between the section h=0 and the front of the wave is determined by expressions (1.8). Hence we have on the front of the wave

$$2F_1 = p + A_n u, \qquad 2F_2 = p - A_n u$$

In accordance with (2.6) we have on the front of the wave

$$2F_1 = p_0 + a_n \varphi_1 \qquad 2F_2 = p_0 - a_n \varphi_2$$

Here

$$\varphi_1 = \frac{h_{\varphi}}{A_n - h_{\varphi}}, \qquad \varphi_2 = \frac{h_{\varphi}}{A_n + h_{\varphi}} \qquad (2.7)$$

If the approximation segments are sufficiently small, then, as calculations show, the function φ_1 can be replaced on each of the

segments by a straight line, while φ_2 can be assumed constant. Such a linearization of the boundary conditions makes it possible to obtain a solution in an explicit and readily visualized form.

If $\varphi_2 (h_{\varphi}) = \text{const}$, then $F_2 (h + A_n t) = \text{const}$ on the line of the front, and consequently, in the entire region 1 (Fig. 2). From the condition at the section h=0 we determine the function $F_1 (h - A_n t)$. Let, for example, the change in the pressure be specified in the section h=0 in the following form

$$p = a + bt \qquad \left(a = p_0 + \rho_m, \quad b = -\frac{\rho_m}{\theta} \right) \qquad (2.8)$$

We then have in the section h=0

$$F_1 (-A_n t) + F_2 = a + bt$$

Hence in the entire region 1

$$F_1 (h - A_n t) = a - F_2 - \frac{b}{A_n} (h - A_n t) \qquad (2.9)$$

$$p = F_1 + F_2 = a - \frac{b}{A_n} (h - A_n t) \qquad (2.10)$$

$$u = \frac{1}{A_n} (F_1 - F_2) = \frac{1}{A_n} \left[a - 2F_2 - \frac{b}{A_n} (h - A_n t) \right] \qquad (2.11)$$

The solution obtained will be correct in region 1 between the section h=0, the front of the wave, in the straight line

$$h = A_n (t - \tau_{n-1}), \qquad \tau_{n-1} = \frac{p_{n-1} - a}{b}$$

where τ_{n-1} is the instant of time when the pressure in section h=0 drops to a value p_{n-1} corresponding to the lower limit of the pressure on the n-th section of the approximation.

Let us find the second boundary of the region 1 — the front of the shock wave. Since the function F_1 is determined by (2.9), then, inserting (2.9) into (2.7), we obtain a differential equation for the motion of the wave front

$$\frac{dq}{dt} = 2b \left(1 - \frac{q}{a_n + q} \right)$$

where

$$q = k_n - \frac{2bA}{A_n} + 2bt, \qquad k_n = 2a - 2F_{2n} - p_0 - A_n u_0 \qquad (2.12)$$

Solving this equation and taking into account the fact that $h_f=0$ when $t=0$, we obtain the law of motion of the front of the shock wave

$$h_f = \frac{A_n}{2b}\left[2bt + k_n + \alpha_n - \sqrt{(k_n+\alpha_n)^2 + 4\alpha_n bt}\right] \qquad (2.13)$$

Let now $p = p_{n-1}$ in the section $h=0$. The region 3 in the h,t plane, where the pressure corresponds to the $(n-1)$-th approximation segment, cannot make direct contact with region 1, since the straight line on which $p=\text{const}$ has a different slope in the new region than in 1. Between the regions 1 and 3 there should lie a region 2 of constant parameters, bounded by the characteristics. For the region 3 the corresponding calculations yield

$$p = a - \frac{b}{A_{n-1}}(h - A_{n-1}t), \qquad u = \frac{1}{A_{n-1}}\left[a - 2F_2\frac{b}{A_{n-1}}(h - A_{n-1}t)\right] \qquad (2.14)$$

$$h_f = \frac{A_{n-1}}{2b}\left[2b(t-\tau) + k_{n-1} + \alpha_{n-1} - \sqrt{(k_{n-1}+\alpha_{n-1})^2 + 4\alpha_{n-1}b(t-\tau)}\right] + h_f' \qquad (2.15)$$

Here h_f' and τ are the values of h and t at the point where the front starts out in region 3.

We determine analogously the flow in the succeeding regions.

Thus, for the pressure specified at a given section of the medium, we determine the law of motion of the front of the wave and the flow behind the front.

3. Reflection of shock wave. Let us consider the reflection of a plane shock wave from a rigid partition. In the case of dense single-component multi-component media, there is no doubt that the approximate method considered above is applicable to the solution of this problem, since the heat losses due to reflection are small. In air the problem can be solved by this method only at small pressures. However, as the front of the wave reflected from the partition moves into the incident wave, the pressure on the front of the reflected wave decreases, and with it the entropy jump. To the contrary, the entropy of the particles in the incident wave increases with the distance from the partition. Therefore there occurs during the reflection an equalization of the entropy at various particles of the medium.

On the front of the reflected shock wave we have

$$\rho_1(D - u_1) = \rho_2(D - u_2), \qquad p_2 - p_1 = \rho_1(D - u_1)(u_2 - u_1) \qquad (3.1)$$

where the index 1 corresponds to the incident wave and the index 2 to the reflected one.

Let the states behind the front of the reflected and incident waves lie in different sections of the approximation

$$p_1 = -A_1^2 V_1 + B_1, \qquad p_2 = -A_2^2 V_2 + B_2$$

Assuming $u_2 = 0$, we obtain an expression for the pressure p_{02} in the reflected wave, acting on the partition during the initial instant of reflection

$$p_{02} = \frac{A_2^2}{2}\left\{-\left[\frac{B_1}{A_1^2} - \frac{B_2}{A_2^2} - p_1\left(\frac{1}{A_1^2} + \frac{1}{A_2^2}\right)\right] \pm \right.$$
$$\left. \pm \left(\left[\frac{B_1}{A_1^2} - \frac{B_2}{A_2^2} - p_1\left(\frac{1}{A_1^2} + \frac{1}{A_2^2}\right)\right]^2 - \frac{4}{A_2^2}\left[\frac{p_1}{A_1^2} - p_1\left(\frac{B_1}{A_1^2} - \frac{B_2}{A_2^2}\right) - u_1^2\right]\right)^{1/2}\right\} \qquad (3.2)$$

In the case of air this p formula is practically the same as the Izmaylov formula. Taking into account the connection between the pressure in the incident and reflected waves at $A_1 \to A_2$, we find that the plus sign should be taken here.

Let us denote the line of the front of the reflected wave by $\tau_f = h_f(t)$. The solution in the region of the reflected wave has the form

$$F_1(h - A_2 t) = \frac{1}{2}(p_2 + A_2 u_2), \qquad F_2(h + A_2 t) = \frac{1}{2}(p_2 - A_2 u_2)$$

The arbitrary functions must be found from the boundary conditions. The conditions on the front yield

$$2F_1 = p_1 + A_2 u_1 + a\varphi_1, \qquad 2F_2 = p_1 - A_2 u_1 - a\varphi_2 \qquad (3.3)$$

Here

$$\varphi_1 = \frac{k'_f}{A_2 - k'_f}, \qquad \varphi_2 = \frac{k'_f}{A_2 + k'_f}, \qquad a = \frac{p_1(A_1^2 - A_2^2) + A_1^2 B_1 - A_2^2 B_2}{A_1^2} \qquad (3.4)$$

Unlike the incident wave, the variables in the expressions F_1 and F_2 are not only the functions φ_1 and φ_2, but also u_1 and p_1, which complicates the solution.

If the reflection is from a stationary partition, the second

boundary condition yields

$$u_2 = 0, \qquad F_1(h^* - A_2 t) = F_2(h^* + A_2 t) \tag{3.5}$$

where h* is the coordinate of the partition.

If the reflection is from a moving partition

$$u_2 = u_3 = u, \qquad m\frac{du}{dt} = p_2(t) - p_3(t)$$

$$\frac{1}{A_2\rho_2}[F_1(h^* - A_2 t) - F_2(h^* + A_2 t)] = \frac{1}{A_3\rho_3}[\Phi_1(h - A_3 t) - \Phi_2(h + A_3 t)] \tag{3.6}$$

where the index 3 corresponds to the parameters of the medium behind the partition, m is the mass of the partition, and u is its velocity.

Let us consider the reflection of a non-stationary shock wave from a stationary partition. Without limiting the generality, we can assume that the incident wave reaches the partition on that section of the path, where it is stationary (Fig. 2). In region 4 all the parameters are constant. Then they will also be constant in region 5. The velocity of the particles in region 5 is $u_5 = 0$, and the pressure is determined by (3.2). The velocity of the front of the reflected wave is

$$h'_\phi = \rho_1(D - u_1) = \frac{p_{02} - p_1}{u_1} \tag{3.7}$$

The boundary of region 5 is the characteristic a

$$h - A_2 t = \text{const}$$

where

which is drawn from the point [illegible] the line of the front of the reflected wave meets the line that bounds region 4. The characteristic b limits the region 7 on the side of region 8 and intersects the front of the reflected wave. The equation of this characteristic is

$$h + A_2 t = \text{const}$$

Both in region 5 and in region 7 we have $\Phi_2(h + A_2 t) = p_{02}/2$.

The boundary condition on the front of the wave is

$$2\Phi_2(h + A_2 t) = p_2 - A_2\rho_2 u_2 = p_1 - A_2\rho_1 u - \alpha\frac{h'_\phi}{A_2 + h'_\phi} \tag{3.8}$$

Considering that in the incident wave the pressure and velocity of the particles are determined by (2.14), we obtain the differential equation for the motion of the front

$$\frac{dq}{dt} = -\frac{\alpha}{\beta q + \gamma} \tag{3.9}$$

Here

$$\alpha = (2F_2 - p_{02})\left(1 + \frac{A_1}{A_2}\right) - B_1\frac{A_1}{A_1} + B_2\frac{A_1}{A_2}, \qquad \beta = \frac{b}{A_1^3}\left(\frac{A_2}{A_1} - 1\right)$$

$$\gamma = \frac{p_{02}}{A_2} - \frac{2F_2}{A_1} + \frac{B_1}{A_1}\left(1 - \frac{A_2}{A_1}\right) + \frac{B_1 A_2}{A_1^2} - \frac{B_2}{A_2}$$

The solution of the equation is

$$\frac{\gamma}{\alpha}(h - A_1 t) + \frac{\beta}{2\alpha}(h - A_1 t)^2 = t + \text{const} \tag{3.10}$$

Thus, the line of the front of the reflected wave represents a second-order curve. The function $F_1(h - A_2 t)$ in region 7 is determined from the relation

$$2F_1(h - A_2 t) = p_{02} + A_2\rho_2 u =$$

$$= p_1 + A_2\rho_1 u + \left[\rho_1\left(\frac{1}{A_2^2} - \frac{1}{A_1^2}\right) + \frac{B_1}{A_1^3} - \frac{B_2}{A_2^3}\right]\frac{A_2 h'_\phi}{A_2 - h'_\phi}$$

which is satisfied on the now known line of the front of the reflected wave.

The limit of region 7 is the characteristic

$$h + A_2 t = \text{const}$$

which is drawn from the partition and intersects the line of the wave front. In region 8 between this characteristic and the partition, the function $\Phi_1(h - A_2 t)$ will be the same as in region 7. The function $\Phi_2(h + A_2 t)$ is determined from the condition that u=0 on the partition. The solution in the succeeding regions (Fig. 2) is obtained in a similar manner, with simultaneous determination of the line of the front.

We assume that a certain instant of time the pressure on the partition in the reflected wave has dropped to a value p*, starting with which it is necessary to go to the second section of the approximation of the isentropic curve.

On the line $p(h,t) = p^*$ (dotted line), which is not a charac-

teristic, all the parameters are known, and therefore the flow behind this line, in the regions bounded by the corresponding characteristics, is fully determined. If, as in the examples considered above, the functions F_1 and F_2 are linear, then the line $p=p^*$ will be broken, and will consist of straight-line segments (shown dotted in Fig. 2). The flow in regions 10 and 11 is determined starting with the conditions on the lines $p=p^*$. The flow in region 12 is determined starting with the conditions on the characteristic and on the partition, while in region 14 it is determined from the conditions on the characteristic and on the front, in region 13 it is determined from the conditions on the two characteristics. The further flow is built up in an analogous manner.

The authors are grateful to L.I. Sedov and K.P. Stanyukovich for attention and interest in this investigation.

Received 9 September 1958.

BIBLIOGRAPHY

1. Chaplygin S. A. O gazovykh struyakh (On Gas Jets), Gostekhizdat, 1949.

2. Sedov L. I. Ploskiye zadachi gidrodinamiki i aerodinamiki (Plane Problems in Hydrodynamics and Aerodynamics), Gostekhizdat, 1950.

3. Stanyukovich K. P. New Approximate Method of Integrating Certain Hyperbolic Equations, DAN SSSR, vol XCIII, no 6, 1953.

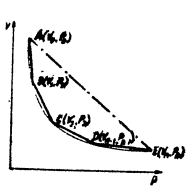

Fig. 1. Scheme for approximating the curve $p = p(V)$

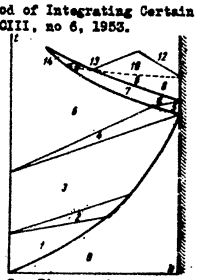

Fig. 2. Diagram showing the regions of the various solutions.

Deceleration of a Supersonic Flow in Wind Tunnel Diffusers

N. N. Shirokov

Izvestiya Akademii Nauk SSR, Otdeleniye Tekhnicheskikh Nauk, Mekhanika i Mashinostroyeniye, [News of the Academy of Sciences USSR, Department of Technical Sciences, Mechanics and Machine Building], No 2, Mar-Apr 1959, Moscow, pages 19-24.

We report in this paper the results of an investigation of the process of deceleration of supersonic flow in the converging portion of diffuser channels of wind tunnels. Criteria are determined for the maximum possible deceleration of the flow to the narrow section of the diffuser, which will be called henceforth the throat. The effect of the Reynolds number on the characteristics of the diffuser is investigated. Based on the experimental data, an approximate procedure is proposed for the calculation, making it possible to determine the effectiveness of a diffuser channel of a given geometry.

An experimental verification of the computation procedure is made for different Mach numbers.

A characteristic feature of the published results of research devoted to the problem of deceleration of supersonic flow in wind-tunnel diffusers is the absence of any method whatever for the preliminary calculation of the coefficient of pressure restoration, with the exception of flow calculation based on an ideal liquid, the results of which, as a rule, are quite far from the experimental data obtained. This is evidence that the problem of preliminary calculation of the pressure recovery coefficient depends essentially on a knowledge of the laws of the influence of viscosity on the deceleration process.

The process of deceleration of supersonic flow in a diffuser can be broken up into two stages -- the reduction in the supersonic speed in front of the blocking shock in the converging portion of the channel, and the deceleration in the blocking jump itself and in the channel behind it. In investigations of the adjustable diffusers of wind tunnels there is always a clearly pronounced maximum in the relation $\sigma = f(\bar{F})$, where σ is the recovery coefficient of total pressure, and F is the relative area of the diffuser throat, i.e., beyond a certain value of the throat area, further deceleration of the flow in the converging channel does not lead to an increase in σ, but, to the contrary, it leads to a sharp decrease in the pressure recovery coefficient. Various authors have explained the character of the curve $\sigma = f(\bar{F})$ by the fact that as the velocity in the throat is decreased, the losses in the blocking shock decrease more slowly than the increase in loss in the flow behind the

blocking shock. However, experimental data do not confirm this hypothesis. Among the problems still unsolved concerning the deceleration process are two principal ones -- what determines the maximum possible deceleration of flow in the converging channel, i.e., F_{min}, and what determines the maximum in the relation $\sigma = f(\bar{F})$, i.e., the optimum geometry of the diffuser. The present paper is devoted to a clarification of these problems.

Description of the experimental setup. The investigations were carried out in experimental setup (Fig. 1) consisting of receiver 1, in which a regulating valve 2 was used to maintain a given pressure, which is registered with a standard manometer 3. The air for the experiment was taken from a bank of high pressure air flasks. Connected to the receiver were interchangeable flat nozzles 4. The investigated diffuser channel were connected to the nozzles. These consisted of stationary sidewalls 5 and movable eyelids 6, the number and shapes of which could be varied from experiment to experiment over a wide range. The cross sections of the diffuser channel were changed by means of special screws 7 and the accuracy of the displacement of the eyelids was $\pm$ 0.1 mm on each side, and was registered with indicators 8. A non-adjustable subsonic diffuser 9 with a throttle 10 on its outlet was then attached to the movable eyelids. During the time of the experiments, a measurement was made of the pressure in the receiver, using manometer 3, while the distribution of the static pressure along the symmetry axis of the latter walls and of the moving eyelids was measured with mercury differential manometers 11. The fields were traversed by fittings for total and static pressure in two mutually-perpendicular directions, 12, at fixed time intervals along the length of the diffuser.

It was possible to observe and photograph the flow through an IAB-451 instrument and to photograph the process with motion picture camera SKS-1. The principal investigations were carried out at flow velocities corresponding to $M = 3.0$.

Results of the experiment and their analysis. Fig. 2 shows the distribution of the static pressure along the axis of the sidewall of the diffuser at a minimum value of throat area for a given channel geometry, along with the shadow photograph corresponding to this distribution. Judging from the shadow pattern, the reflection of the jumps from the walls occurs even in the subcritical region, where the influence of the viscosity does not go beyond the limits of the boundary limit.* The same figures shows the pressure distribution calculated for a flow of an ideal liquid in the same channel, with a correction introduced for the thickness of the volume displacement.

* The results of the investigation of the interaction between

Let us estimate the calculated flow pattern from the point of view of the critical ratio of the pressure in the shock waves. The value of the relative pressure in the shock waves when the latter are reflected from the walls and when they intersect the sidewalls are shown in Fig. 3, which also shows the curve of the critical pressure ratio. It is seen that in the investigated channel the pressure ratio in the shocks at a minimum throat area does not reach critical value and consequently the curve of the critical pressure ratios for this case is not a criterion capable of determining the maximum possible braking of the flow.

Let us consider the change of the velocity field in the field of the diffuser as the throat area is reduced (Fig. 4), and the change in the velocity field along the length of the diffuser for a minimum throat (Fig. 5). It follows from the examination that as the throat is reduced the velocity profile between the stationary lateral walls becomes substantially less filled, and approaches a detachment profile. The velocity profile between the movable eyelids is also deformed, but much less. The deformation of the profiles occurs principally on the finite portion of the converging part of the diffuser. After the swing of the stream in the throat, there occurs in the diverging channel of the diffuser a filling of the velocity profile on both walls. It follows therefore that the weakest place in the channel, from the point of view of a closeness to detachment, is the velocity profile on the lateral wall in the throat of the diffuser. It was shown in reference/1/ that upon detachment of a stream moving with a positive pressure gradient, the criterion that characterizes the state of the boundary layer, namely

$$\bar{\zeta} = \frac{\bar{z} p'_x}{\rho u^2}$$

with respect to where p'_x is the first derivative of the pressure the length in a given section of the boundary layer, z is the characteristic dimension of the boundary layer, ρ is the density, and u is the velocity of flow on the limit of the boundary layer, depends little on the Mach number (in the investigated range) and, when calculated in accordance with the aerodynamic volume displacement δ^*, has an approximate value of 0.014 or 0.015.

A calculation of the values of $\bar{\zeta}$ in our experiments shows that as the throat area is decreased, the value of $\bar{\zeta}$ increases and reaches a maximum value at F_{min}, approaching in absolute

the boundary layer and the shocks and the determination of the curve of critical pressure ratio in shock waves were reported in a paper by G. I. Petrov at the session of the Department of Technical Sciences of the Academy of Sciences U S S R in June 1958.

magnitude the critical value ζ_* (Fig. 6). In our experiments, after measuring the velocity field, it is impossible to fix directly the detachment of the stream, i.e., to obtain $\zeta = \zeta_*$, since the detachment of the stream in the throat disturbs the supersonic flow in the converging portion of the diffuser channel and partially in the nozzle.

To confirm the foregoing premise concerning the detachment from the lateral walls, we took a high speed motion picture of the shadow pattern of the flow in the region of the diffuser throat. The pictures were taken at 4,000 frames per second. Fig. 7 shows frames of the motion picture film, fixing the flow at the instant of detachment.

Photograph 1 shows the normal flow pattern prior to the detachment a supersonic flow with oblique shock waves in the converging portion, turning of the flow in the throat of the diffuser, and the acceleration of the flow in the diverging portion of the diffuser channel (flow from left to right). Photographs 3 to 6 show in the throat of the diffuser on the sidewall the formation of the detachment zone (dark spot , which moves against the flow (photos 9 -- 11, 13, 16).

Photographs 11, 13, and 16 show clearly that the detachment zone follows the produced shock wave, changing its shape as it moves towards the converging channel. During the motion of this shock, supersonic flow is retained in the throat of the diffuser and in the diverging portion of the channel. Photographs 18 and 20 show the formation and the motion of the second shock wave, which differs in shape from the first one, since the velocities in the converging channel have been reduced after the passage of the first shock wave. This is followed by the formation of new compression waves, photographs 23, 24, and 27 and finally, the velocity of sound is established in the throat, photograph 32.

All this complicated system of shock waves stops moving after it reaches the corresponding section in the nozzle, and a subsonic flow is established in the converging portion, photograph 37.

It should be noted that during the entire time of the separation process, approximately 0.01 seconds, supersonic flow is retained in the diverging channel, with a corresponding blocking shock.

The results of this experiment give direct confirmation of the fact that the maximum possible retardation of the flow in the converging channel is determined by ζ_* on the lateral wall.

Measurement of at F_{min} was carried out in addition in channels with different lengths of converging portion and with different boundary layers at the inlet to the diffuser. The results of the measure-

are shown in Fig. 8 and confirm the assumption of weak dependence of ζ_* on the Mach number (in the investigated range).

The usual procedure of investigation of diffuser channels provides for a reduction in the pressure in the receiver after the starting of the tube and the establishment of the necessary through sections in the diffuser. Thus, the determination of the relationships $\sigma = f(\bar{F})$ occurs at variable R numbers. To eliminate the influence of the variation in the R number, the characteristic $\bar{\sigma} = f(\bar{F})$ was plotted at a constant pressure in the receiver, and a throttle at the outlet from the diffuser was used for the determination of $\bar{\sigma}$. It was found in these investigations that the descending branches in the characteristic $\bar{\sigma} = f(\bar{F})$ are absent (Fig. 9). What is the same, at different pressures p_0 in the receiver for a channel of given geometry.

Approximate calculation of the characteristic $\bar{\sigma} = f(\bar{F})$. Based on the data of the preceding sections, we can calculate approximately the effectiveness of the diffuser channel with an accuracy sufficient for practical purposes. The calculation is broken up into two stages: the first is the determination of the limiting curve $\bar{F}_{min} = f(p_0)$, which depends on the Mach number of the nozzle and on the thickness of the boundary layer, on the shape and dimensions of the converging channel. The second stage is the determination of $\bar{F}_{min}$ corresponding to the maximum pressure recovery at a given geometry of diverging channel.

In the determination of ζ it is necessary to know the change in the throat of M, p'_x, and δ^*; this can be obtained by calculating the flow in the converging channel with allowance for the boundary layer.

To calculate δ^* it is possible to use the well known procedures of calculations of turbulent boundary layer, specifying merely the change in the parameter $H = \delta^*/\delta^{**}$, where δ^{**} is the thickness of the momentum loss, characteristic of the braking process. The change in the parameter H along the length of the converging channel at $\bar{F}_{min}$ (Fig. 10) shows that the principal deformation of the profile occurs in the throat region. A further small decrease in the throat leads to the formation of a detachment profile, i.e., the parameter H on curve 10 should increase almost vertically. Assuming that a detachment profile occurs on the throat on the lateral wall and taking H (x) as shown in Fig. 10, we can calculate the change in relative to $\bar{F}$. The throat area, at which $\zeta = \zeta_*$, will be a minimum for a given value of p_0.

The best shape of the diverging channel was shown experimentally to the cylindrical. For this case it is easy to determine the total-pressure losses, after determining by previous calculation

the parameters of the flow at the inlet to a cylindrical channel, solving simultaneously the equations of conservation of flow, energy, and momentum, without allowance for friction forces.

To verify the approximate procedure of calculation, we calculated and tested experimentally channels for M=2.5, 3.0, and 3.5. The calculation and experimental results are shown in Fig. 11, from which it follows that F_{min} is determined by computation with accuracy 3 — 5%, while the accuracy of σ_{max} reaches 6%.

Received 21 November 1958

BIBLIOGRAPHY

1. Baw-Zelikovich G. M. Calculation of the Detachment of the Boundary Layer. Izv. AN SSSR, OTN (News of the Academy of Sciences USSR, Dept. of Tech. Sciences) no 12, 1954.

Figure Captions

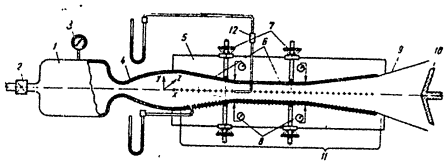

Fig. 1. Diagram of experimental setup.

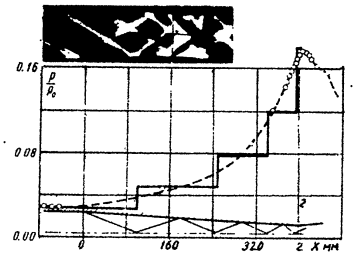

Fig. 2. Flow pattern in converging channel; — — — calculation flow of an ideal liquid, o–o — experiment.

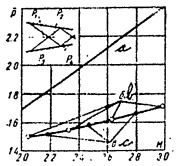

Fig. 3. Comparison of the flow in converging channel with curve a of critical pressure ratio; the points b and c correspond to $\bar{p}=p_2/p_1$ and $\bar{p}=p_4/p_3$.

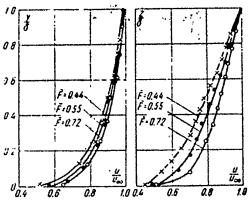

Fig. 4. Change in velocity profile in the throat with changing throat area.

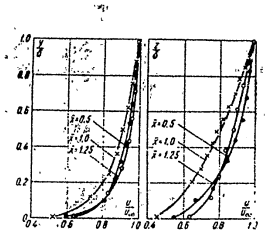

Fig. 5. Change in the velocity profile along the length of the channel at F_{min} ($\bar{x}=1.0$ corresponds to the section of the diffuser throat).

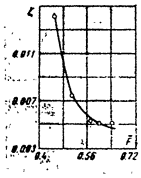

Fig. 6. Variation of along the sidewall in the throat with changing F.

Fig. 7. Process of detachment of flow in diffuser.

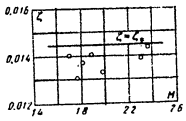

Fig. 8. Values of ζ obtained in various channels at $\overline{F}_{min}$.

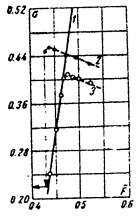

Fig. 9. Influence of the Reynolds number R on the characteristic $\sigma = f(\overline{F})$; 1 — $\overline{F}_{min} = f(p_0)$, 2 — $\sigma = f(\overline{F})$ for R=const, P_0=4.55 atmos, 3 — $\sigma = f(\overline{F})$ at R=var, P_0=5 to 2.42 atmos.

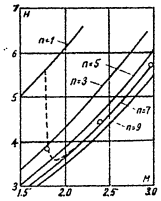

Fig. 10. Dependence of H=f (M) for power-law profiles; dotted -- experimental values.

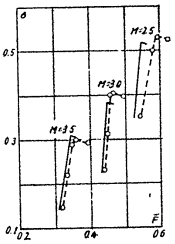

Fig. 11. Comparison of the results of calculations (solid lines) with the experimental data (dotted).

Shock Tubes for Measuring Drag Coefficients of Bodies in Free Flight

Yu. A. Dunayev
G. I. Mishin

Izvestiya Akademii Nauk SSR, Otdeleniye Tekhnicheskikh Nauk, Mekhanika i Mashinostroyeniye, [News of the Academy of Sciences USSR, Department of Technical Sciences, Mechanics and Machine Building], No. 2, Mar-Apr 1959, Moscow, pages 188-190.

A brief description is given of a shock tube 4 meters long with four stations for plotting the space-time variation of flying bodies. The setup makes it possible to measure the drag coefficients and simultaneously photograph the spectra of flow of various gases over high-speed axially-symmetrical bodies.

1. An investigation of the flight of bodies under condition of maximum approach to natural can be carried out in ballistic (shock) installations/1 — 4/. In a closed polygon, it is possible to create any desired atmospheric conditions and to vary independently the similarity criteria such as the Mach numbers and the Reynolds numbers over the widest possible range.

The use of various gases in a shock tube makes it possible to establish the role of aero-physical parameters $h\vartheta/kT$ — the ratio of the characteristic temperature of the gas to the impact temperature and $L/u\tau$ — the ratio of the characteristic dimension of the body to the width of the relaxation region (u is the gas velocity, τ the relaxation time), during the dynamics of the flight. Fig. 1 shows an overall view and Fig. 2 shows the diagram of a shock tube for the measurement of resistance coefficients.

High initial velocities of the bodies were accomplished by shooting from a rifle one of 14.5 mm caliber, using large batches of special powders and a corresponding fastening of the butt. To soften the blow during the shooting, the rifle was placed on slides, permitting it to recoil. The sound of the shot was reduced by placing the butt in a vacuum tank 2 through a rubber seal, making it possible for the butt to move horizontally. The tank was evacuated by means of forevacuum pump 3 of type VN-1 to a pressure on the order of 1 mm mercury, controlled by means of manometer 4.

Steel, duraluminum, magnesium and bakelite balls 9.46 mm were shot with the gun. The balls were pressed in wads made of delta wood. At small velocities, to facilitate the removal of the balls from the wads, the latter were cut along the diametral plane.

The outlet from the vacuum tank and the entrance into the shock tube were covered with collophane films 0.04 mm thick; such diaphragms produce no deformation even in the case of magnesium balls.

The shock tube consisted of four sections of a total length of 4 meters. The internal diameter of the tube was 300 mm, thus guaranteeing absence of the influence of the walls on the flight of the bodies.

Three sections had two rectangular windows each, measuring 720 x 100 mm, located diametrically opposite, and two round flanges each, 150 mm in diameter, to connect the pump, the manometer, the vacuum meter, and the gas inlet.

Before entering the polygon, the body passed through a shield, an angle sector 6, and vacuum chamber 7, serving for rapid removal of the air from the surface of the body during shooting in various gases.

Before the experiment, the tube was evacuated by forevacuum pump VN-1, 8, to a pressure of approximately 10^{-2} mm mercury. The pressure was registered with a thermocouple vacuum meter 9. The gas was then let out of flask 10, and the pressure and temperature of the gas were measured by manometer 11 and thermometer 12, located near the trajectory.

The rifle was triggered by relay 26, using a signal received from the gun-control panel 24.

2. The values of the drag coefficients were calculated after measurement made with instantaneous photographs of the positions of the ball along the trajectory, at known specified time intervals. Such a method of plotting the space-time dependence of the flight of the ball was adopted by us because it is easier to obtain by electronic means calibrated time intervals, than to measure the time when a body passes the fields of light beams with the same accuracy.

Simultaneous photography of the sphere and of the coordinate rule were made with light transmitted through plexiglas rectangular windows 13, by means of cameras "Kiev", 14. To obtain clear photographs of a body moving with a velocity greater than 100 meters per second, it is necessary to have exposures on the order of 0.5×10^{-6} seconds. Mechanical shutters cannot produce such short exposures, and therefore, prior to the firing, the lenses of the cameras were opened by means of relay 25, and the exposure time was determined by the length of the light flash.

Illuminating apparatus 15 had a system of mirrors 16 and condenser lenses 17, insuring illumination of the entire field of each station from a single source 18.

Transparent coordinate rules with millimeter divisions were mounted inside the tube below the flight trajectory. The setting of the rules was checked by means of a 1-1/2 meter beam compass.

The cameras were placed relative to the trajectory in such a way, that their fields of view overlapped. In the case of deviation of the ball from the mean trajectory, the photograph of its position relative to the rule was seen displaced. This displacement is small near the axis of the lens. The position of a ball that deflects away from the axis of the lens is recorded simultaneously by two cameras, making it possible to determine accurately its exact coordinates by simple computations. Correction for the taper of the rifle could also be made by measuring the deviation of the ball at the exit from the polygon.

It must be noted that in many experiments the deviation was less than 1 cm, and consequently the correction was necessary only in rare cases.

At the first station, which had a round field of 150 mm diameter, the procedure was not only to measure the coordinate, but also to photograph the shadow spectrum of flow around the ball. A condenser lens and a point-source spark illuminator of the type "cylinder-electrode" 19 produced a parallel beam of light, which was projected on the ground surface of a plane-parallel plate, which was provided with a vertical coordinate reference. The scale of the photographs was determined by first photographing a millimeter grid. The measurements were carried out directly on the negatives using the MIR-12 measuring microscope, which has an accuracy of ± 0.3 mm.

The most suitable circuit for spark production was one employing a discharge of a capacitor, first charged to 14 — 16 kv, through a pulsed hydrogen thyratron TGI-1-325/16. Such a circuit produces a minimum spread in time between the passage of the triggering pulse and the instant of appearance of the spark since the process of initiation is lacking. The pulsed hydrogen thyratron permits exact control, realized by applying a low positive voltage to the grid (the time spread in operation, based on the rated data, is not more than 0.04×10^{-6} seconds, even with only 6 kv on the anode).

To improve the breakdown conditions, pointed electrodes were

used.

In view of the small power of the spark, the glow of the plasma was rapidly damped by the surrounding air, and the effect of afterglow was limited by the finite sensitivity of the film.

3. A series of pulses, arriving in sequence to the spark devices at exactly-known time intervals, was generated by a multichannel electronic synchronizer 22, the block diagram of which is shown in Fig. 3. The signal b, applied to photorelay 23 when the bullet crossed the light beam, was applied to a starting trigger c, which controlled the impact-excitation generator d.

After the trigger was turned, the generator started operating with the same initial phase, with constant amplitude and frequency. In the next stage, e, the sinusoidal voltage was converted into brief, almost rectangular pulses. These pulses pass then through a frequency divider f with a division coefficient 32, from which they were applied to univibrator g, which formed broad pulses, equal in duration to the period of the master generator.

The pulse from the univibrator separated, in a coincidence circuit, one of the pulses that come directly from the shaping stage e, thereby eliminating the "floating" of the output signals with time, through the use of a binary-type divider with a large division coefficient.

The pulses from the coincidence circuit passed to a distributing block, which served four spark devices. After the operation of the last of the stages of the distributing block, the starting trigger returned to its initial position and the oscillations of the generator were quenched. For the spark devices to operate with a minimum spread in time, pulses with an amplitude of 350 volts and a current of 0.5 amp were fed from the output stages of the synchronizer to the grids of the hydrogen thyratrons.

calibrated

The generator frequency was controlled by a quarts heterodyne calibrator type VS-221T. The relative accuracy of the measurement of the frequency was 0.1%.

The electronic circuit ensured the appearance of light flashes at known time intervals, differing from each other by tenths of a microsecond.

4. The drag coefficient of a ball flying in a gas, by definition, equals

$$C_x = \frac{8ma}{\rho v^2 \pi d^2}$$

where m is the mass of the ball, a the deceleration, ρ the gas density, v the ball velocity, and d the ball diameter.

It is interesting to note that the time does not enter directly into the expression for C_x, since $v \sim t^{-1}$ and $a \sim t^{-2}$.

Knowing the pressure of the gas p and its temperature T in the tube, it is possible to determine the density from the equation of state

$$\rho = 0.3594\, \rho_0 \frac{P}{T}$$

Here ρ_0 is the gas density at 0°C and a pressure of 760 mm mercury.

The mass of the ball was determined by weighing on an analytic balance, and the diameter was measured with a micrometer.

The magnitudes of the deceleration and of the velocity were determined from the dependence of the ball coordinate on the time of flight either by the method of averages or by the method of least squares. The number M is found after calculating the velocity of sound, with allowance for the temperature correction or through the use of available tabular values of the velocity of sound. Fig. 4 shows the results of the measurement of C_x in air at atmospheric pressure, using magnesium balls for Mach numbers from 2.4 to 6.1 and Reynolds numbers from 5.0×10^5 to 1.0×10^6. The Reynolds number varied in proportion to the velocity.

The average deviation of the measured values from the mean curve amounts in this case approximately to ±1%.

When the investigation was performed in a gas of high molecular weight, such as Freon, the mean error rarely exceeded 0.5%.

Basedoon the above, it can be concluded that the shock tube is a convenient method for measuring the flight of bodies with supersonic velocities.

In conclusion, I express my gratitude to A.A. Sokolov, who has rendered great help in the wiring and operation of the apparatus.

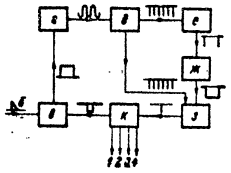

Fig. 3.

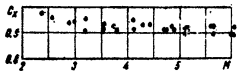

Fig. 4.

BIBLIOGRAPHY

1. Charters A. s. Thomas R. The Aerodynamic Performance of Small Spheres from Subsonic to High Supersonic Velocities. JAS, v. 12, № 4, 468, 1945.
2. Seeger R. J. On Aerophisics Research, Amer. Journ. of Physics, v. 19, № 8, 459, 1951.
3. May A. a. Witt B. Free-Flight Determinations of the Drag Coefficients of Spheres. JAS, v. 20, № 9, 635, 1953.
4. Hodges A. J. The Drag Coefficient of very high Velocity Spheres. JAS, v. 24, № 10, p. 755, 1957.

INFORMATION ON THE STATUS OF SOVIET RESEARCH IN HYPERSONICS

M. S. Solomonov

Izvestiya Akademii Nauk SSSR,
Otdeleniye Tekhnicheskikh Nauk

/News of the Academy of Sciences USSR,
Department of Technical Sciences/,
No 9, September 1958, Moscow,
Pages 157-159

/The following material is an extract translation of an article entitled "June General Meeting of the Department of Technical Sciences of the Academy of Sciences USSR."/

On 16-17 June 1958, under the chairmanship of Academician A. A. Blagonravov, a general session of the Department of Technical Sciences was held, at which two scientific reports of considerable significance were examined. The first report, by Corresponding Member of the Academy G. I. Petrov, was devoted to the problem of the motion of a real gas at velocities considerably exceeding that of sound.

The rapid development of aeronautical and rocket technology has presented aerodynamic science with many new and difficult problems and resulted in increased requirements for accuracy of experimentally obtained data. For the analysis and design of vehicles flying through the atmosphere at high supersonic speeds, and also for the design of power plants, the study of the motion of a gas in close proximity

to the surface skin, where the effects of viscosity and heat conductivity become evident, is of great importance. This matter arises because the boundary layer in supersonic flow can significantly change the nature of the shock waves generated by the body, and this is especially important when flying at high velocities.

A basic question, frequently determining the "to be or not to be" of any vehicle, is the matter of protection from aerodynamic heating. The initial experimental investigations of the velocity distribution in a supersonic boundary layer, conducted with "microtubes" and basically by quantitative optical methods, showed that the velocity distribution in both a laminar and a turbulent boundary layer, for velocities at the boundary exceeding that of sound, is similar to that in a subsonic boundary layer. The velocity distribution in a turbulent layer is well described by exponential laws.

In supersonic flow, in regions characterized by a sharp longitudinal variation in the flow parameters (the base of the shock wave, flow around an obtuse angle), the fundamental propositions of boundary layer theory fail. In these regions it is impossible to neglect the pressure change across the layer and the possibility of transmitting the effect of disturbances forward against the flow. Consequently, the equations for the boundary layer, equations of a parabolic type, cannot describe the phenomena taking place here. In these regions it is possible to apply the basic equations for a non-viscous gas, but under conditions of mixed vortex flow.

The study of the interaction of strong pressure jumps with the boundary layer has permitted the establishment of the general mechanism of the onset of this special kind of "crisis" wherein, at the time of the attainment of a critical ratio of the pressure behind the jump to the pressure before the jump, the shock wave changes in nature so that an additional jump is formed; or, in the case of emission into the fluid with back pressure, the pressure jump is transferred into a region of lower Mach number, so that the ratio of the pressures does not exceed the critical. This critical ratio for a turbulent boundary layer is a function only of the Mach number of the approaching flow and has been determined experimentally over a wide range of Reynolds numbers for Mach numbers from 1.5 - 6.

The discovery of this effect and the obtained universal relationship for the critical pressure ratio as a function of Mach number has permitted the clarification and the predicting of a series of other effects connected with flows in diffusors, altitude chambers, around airfoils, around braking flaps and other cases of practical importance. This has also permitted the development of a method of calculating the thrust of a nozzle in the uncalculated regime.

When studying the deceleration of flow in diffusors and the exhaust of nozzles, of fundamental importance is the study of the laws of motion of a "closing" pressure jump, i.e., a jump which can be displaced or deformed by the action of a back pressure. The relation-

ships which have been obtained permit the determination of the statically stable positions of a closing jump and the calculation of the losses in ducts.

During experiments on the maximum deceleration of a supersonic flow in converging channels by N. N. Shirokov, a new phenomenon was detected: the formation of a new pressure jump on the side walls of the channel due to the breaking away of the boundary layer. This determines the maximum possible increase of pressure as a function of the Mach and Reynolds numbers and of the shape of the channel.

As the author showed, the numerous semi-empirical methods of calculating the coefficients of heat transfer and friction with supersonic flow in the turbulent boundary layer are based upon the application of integral relationships and the establishment of a connection between the local characteristics of the boundary layer and the local coefficients of heat transfer and friction. These relationships, obtained from a finite number of experiments at low speeds, have been broadly extrapolated over a wide range of Mach numbers and ratios between the wall temperature and the stagnation temperature. The results of calculations based upon these methods differ widely amongst each other as the Mach number increases.

For an experimental investigation of heat transfer and friction in turbulent supersonic flow, the working out and development of an extremely precise methodology for the direct measurement of the

local coefficients of heat transfer and friction is required. The experiments which have been carried out have permitted the establishment of reliable criteria for the physical relationships and even for a comparison of the various methods of calculation. Of the existing methods of calculating, the best agreement with experiment over a wide range of experimental conditions is given by a method developed by V. M. Iyevlev, which takes into account the molecular dissociation of the gas.

During an investigation of the flow and heat transfer on a blunt nose on a body flying at a high supersonic velocity, there was established the law of the constancy of the relative distribution of pressure as the Mach number is varied over a wide range, and there was also determined the coefficients of heat transfer on bith rigidly supported and free-floating bodies. Rather high coefficients of heat transfer on free-floating models were obtained by virtue of the roughness of the surface at the time of its disintegration.

The methods which have been developed, together with experiments which have already been carried out, have permitted the establishment of the existence of anomalies in the boundary layer structure during evaporation on the wall or during the injection of another gas through a porous wall, and have further permitted an evaluation of [the effect of] a reduction in the thermal flow which is important when developing methods for protecting structures from thermal effects at very great flight velocities.

The author of the report pointed out that the investigation of the transition of the laminar boundary layer into a turbulent boundary layer is still only in a rudimentary state, and we have only partial information on the effect of the various factors on the Reynolds number of the transition. But evidently, as the Mach number increases beyond 5, with a relative reduction in the wall temperature the transition will be delayed. Special importance can be ascribed to the fact that with a high longitudinal velocity gradient, the reverse transition can take place, namely from turbulent into laminar. This was detected in experiments with the boundary layer when investigating the losses in the nozzle of an engine.

Flow Around a Conic Body During Motion of a Gas With High Supersonic Speed

A. L. Gonor

Izvestiya Akademii Nauk SSR, Otdeleniye Tekhnicheskikh Nauk, Mekhanika i Mashinostroyeniye, [News of the Academy of Sciences USSR, Department of Technical Sciences, Mechanics and Machine Building], No. 1, Jan-Feb 1959, Moscow, pages 34-40.

1. Description of the general method. We shall consider the flow around a conical body by a supersonic gas stream with the associated shock wave. The surface of the body is given by the equation $F(x/z, y/z) = 0$.

To derive the equations of motion we choose an orthogonal system of coordinates, in which the following holds: a) the first coordinate family is the spheres $r^2 = x^2+y^2+z^2$; b) the surface of the body coincides with one of the coordinate surfaces of the first family. Such a system can be determined if the second family is taken to be the surfaces $F(x/z, y/z, \theta) = 0$, obtained by introducing in the first equation the parameter θ, and if the third family is taken to be the conical surfaces $\Phi(x/z, y/z, \varphi) = 0$, superimposed on the orthogonal trajectories to the surfaces of this second family (Fig. 1). Considering that the conic flow is self-similar with respect to the radius r, we obtain after several simple derivations from the general Lagrange second type equations [1] the following system

$$\begin{gathered}
\frac{r}{A_1}\frac{\partial u}{\partial \theta}+\frac{w}{A_2}\frac{\partial u}{\partial \varphi}-r^2-u^2=0 \qquad \left(A_1=\frac{\sqrt{x_0^2+y_0^2+z_0^2}}{r}\right)\\
\frac{v}{A_1}\frac{\partial v}{\partial \theta}+\frac{w}{A_2}\frac{\partial v}{\partial \varphi}+uv+vw\frac{(\ln A_1)_\varphi}{A_2}-w^2\frac{(\ln A_2)_\theta}{A_1}=-\frac{1}{\rho A_1}\frac{\partial p}{\partial \theta}\\
\frac{r}{A_1}\frac{\partial}{\partial \theta}\left[\frac{v}{\gamma-1}\frac{p}{\rho}+\frac{u^2+v^2+w^2}{2}\right]+\frac{w}{A_2}\frac{\partial}{\partial \varphi}\left[\frac{\gamma}{\gamma-1}\frac{p}{\rho}+\frac{u^2+v^2+w^2}{2}\right]=0 \qquad (1.1)\\
\frac{v}{A_1}\frac{\partial}{\partial \theta}\left(\frac{p}{\rho^\gamma}\right)+\frac{w}{A_2}\frac{\partial}{\partial \varphi}\left(\frac{p}{\rho^\gamma}\right)=0 \qquad \left(A_2=\frac{\sqrt{x_0^2+y_0^2+z_0^2}}{r}\right)\\
2\rho u+\frac{r}{A_1}\frac{\partial \rho}{\partial \theta}+\frac{w}{A_2}\frac{\partial \rho}{\partial \varphi}+\frac{\rho}{A_1A_2}\left[\frac{\partial (vA_1)}{\partial \theta}+\frac{\partial (wA_2)}{\partial \varphi}\right]=0
\end{gathered}$$

The first two equations are the projections of Euler's equations along the axes r and θ. The last three equations express the condition of conservation of energy, entropy, and mass of the particles, respectively. The functions A_1 and A_2 are the Lame coefficients, calculated on the surface of the unit sphere; u, v, and w denote respectively the velocity projections on the axis r, θ, and φ; p, ρ, and γ are the pressure, density, and ratio of the specific heats. We convert the system (1,1) to a new variable $\psi = \psi(\theta, \varphi)$, satisfying the following

equation

$$\frac{v}{A_1}\frac{\partial\psi}{\partial\theta}+\frac{w}{A_2}\frac{\partial\psi}{\partial\varphi}=0$$

The surface ψ = const represents the current surface, and therefore the variable ψ plays a role analogous to the usual stream function for two-dimensional and axially-symmetrical flow, if all the motion is considered on a sphere of unit radius with the center at the vertex of the body (Fig. 2). Taking into account the connection between the derivatives $\partial/\partial r = -1/r^2\,\partial/\partial\rho$, $r\frac{\partial}{\partial\theta} = -\partial/\partial\theta$, we obtain for the changeover to the changeover to the new variable the following relations

$$\frac{\partial}{\partial\theta}=\frac{1}{\theta_\psi}\frac{\partial}{\partial\psi},\qquad \frac{\partial}{\partial\varphi}=\frac{\partial}{\partial\varphi}\Big|_{\psi=\text{const}}-\frac{\theta_\varphi}{\theta_\psi}\frac{\partial}{\partial\psi}$$

The system (1.1), after transformation, becomes

$$\frac{u}{A_1}\frac{\partial u}{\partial\theta}-v^2-w^2=0,\qquad \frac{w}{A_2}\frac{\partial v}{\partial\varphi}+uv+vw\frac{[(\ln A_1)_\theta]_{\theta=\text{const}}}{A_1}-$$
$$-w^2\frac{(\ln A_2)_\theta}{A_1}=-\frac{1}{\rho A_1\theta_\psi}\frac{\partial p}{\partial\psi} \qquad (1.2)$$

$$\frac{\partial}{\partial\varphi}\left[\frac{\gamma p}{(\gamma-1)\rho}+\frac{u^2+v^2+w^2}{2}\right]=0,\qquad \frac{\partial}{\partial\varphi}\left[\frac{p}{\rho^\gamma}\right]=0$$

$$\frac{\partial}{\partial\varphi}\left[\ln(\rho A_1 w\theta_\psi)\right]+2\frac{u}{w}A_2=0,\qquad \frac{w}{A_2}\theta_\varphi=\frac{v}{A_1}$$

We shall seek the solutions of the equations subject to the following boundary conditions:

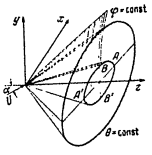

Fig. 1

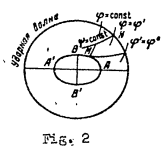

Fig. 2

1. On the shock wave, the equation of whose surface we shall denote by $\theta^*(\varphi)$, the following relation should be satisfied

$$U_n\rho^\circ=U_n^*\rho^*,\qquad U_{\tau_1}=U_{\tau_1}^*,\qquad U_{\tau_2}=U_{\tau_2}^*$$
$$\rho^*=\frac{\gamma+1}{\gamma-1}\rho^\circ\left[1+\frac{2a^2}{(\gamma-1)U_n^{*2}}\right]^{-1},\qquad p^*=p^\circ\left[\frac{2\gamma}{\gamma+1}\frac{U_n^{*2}}{a^2}-\frac{\gamma-1}{\gamma+1}\right] \qquad (1.3)$$

The quantities with indices n, τ_1, and τ_2 are the projections of the velocity and the normal and on two mutually perpendicular tangents to the surface of the shock wave. A superior circle pertains to the parameters in front of the wave, while an asterisk pertains to those behind the wave.

2. On the surface of the body, determined by the equation $\theta = \theta_K = \text{const}$, we have $v = 0$. If the stream velocity at infinity U lies in the plane yOz and makes an angle α with the z axis (Fig. 1), then the velocity components of the undisturbed stream on the surface of the shock wave are determined from the following formulas

$$u^\circ=U\frac{(\sin\alpha r_y+\cos\alpha r_z)}{|\text{grad }r|}\Big|_{\theta=\theta^*},\qquad v^\circ=U\frac{(\sin\alpha\theta_y+\cos\alpha\theta_z)}{|\text{grad }\theta|}\Big|_{\theta=\theta^*}$$
$$w^\circ=U\frac{(\sin\alpha\,\varphi_y+\cos\alpha\varphi_z)}{|\text{grad }\varphi|}\Big|_{\theta=\theta^*} \qquad (1.4)$$

In reference /2/, a small-parameter method was developed for two-dimensional and axially-symmetrical motions of gas with high supersonic velocity and a curving shock wave in front of the body. Following this method, we shall seek a solution of the system (1.2) in the form of a series in powers of the small parameter $\varepsilon = (\gamma-1)/(\gamma+1)$, beginning from Eq. (1.3) the end values of the sought quantities behind the shock wave at $M_\infty^2/\varepsilon^2 \gg 1$, we find that the unknown unknown functions must be determined by power series in the form

$$u=u_0+\varepsilon u_1+\ldots,\qquad v=\varepsilon v_0+\varepsilon^2 v_1+\ldots,\qquad w=w_0+\varepsilon w_1+\ldots$$
$$p=p_0+\varepsilon p_1+\ldots,\qquad \rho=\rho_0/\varepsilon+\rho_1+\ldots,\qquad \theta=\theta_K+\varepsilon\theta_0+\ldots \qquad (1.5)$$

Inserting these series into (1.2), (1.4) and (1.3) and into the conditions on the surface of the body, we find the equations and boundary conditions for the terms of the series with equal indices.

2. Determination of the solution about the first terms of the series. Thus Eq. (1.2) we obtain for the first terms of the series (1.5) the system

$$\frac{\partial u_0}{\partial\varphi}-A_2w_0=0,\qquad w_0^2(\ln A_2)_\theta=\frac{1}{\rho_0\theta_\psi}\frac{\partial p_0}{\partial\psi}$$
$$\frac{\partial}{\partial\varphi}\left[\frac{p_0}{\rho_0}+u_0^2+w_0^2\right]=0,\qquad \frac{\partial}{\partial\varphi}\left[\frac{p_0}{\rho_0}\right]=0 \qquad (2.1)$$
$$\frac{\partial}{\partial\varphi}\left[\ln(\rho_0A_1w_0\theta_\psi)\right]=-2\frac{u_0}{w_0}A_2,\qquad \frac{w_0}{A_2}\frac{\partial\theta_0}{\partial\varphi}=\frac{v_0}{A_1}$$

Here and below the Lame coefficients are calculated for $\theta = \theta_k$ and depend on a single variable φ.

On the shock wave, in the case of $\psi = \psi^*$, we obtain from (1.5) the following boundary conditions:

$$u^* = u_0^\circ, \quad v_0^* = \frac{A_1 w_0^* \theta_{w\varphi}^*}{A_2} + v_0^\circ\left[1 + \frac{2a^2}{(\gamma-1)v_0^{\circ 2}}\right], \quad w_0^* = w_0^\circ$$
$$p_0^* = \rho_0^\circ v_0^{\circ 2}, \quad \rho_0^* = \rho^\circ\left[1 + \frac{2a^2}{(\gamma-1)v_0^{\circ 2}}\right]^{-1} \tag{2.2}$$

here u_0°, v_0°, and w_0° are components of velocity of the incident stream, determined from formulas (1.4) for $\theta^* = \theta_k$. Integrating the first, third, and fourth equations of the system (2.1) along the line $\psi = \text{const}$ from the point M to the point N (Fig. 2), we find

$$u_0 = \Delta_0(\psi)\sin\left[\int_{\varphi^*}^{\varphi} A_2\, d\varphi + \alpha(\psi)\right]$$
$$w_0 = \Delta_0(\psi)\cos\left[\int_{\varphi^*}^{\varphi} A_2\, d\varphi + \alpha(\psi)\right], \quad \frac{p_0}{\rho_0} = \delta_0(\psi) \tag{2.3}$$

The arbitrary functions Δ_0, α, and from conditions (2.2), are equal to the following expressions

$$\Delta_0(\psi) = \pm\sqrt{(u_0^{\circ\prime})^2 + (w_0^{\circ\prime})^2}, \quad \alpha(\psi) = \operatorname{arctg}\frac{u_0^{\circ\prime}}{w_0^{\circ\prime}}$$
$$\delta_0(\psi) = (v_0^{\circ\prime})^2\left[1 + \frac{2a^2}{(\gamma-1)v_0^{\circ\prime 2}}\right] \tag{2.4}$$

The sign in front of the square root should be the same as the sign of w_0'. The primes here and henceforth will denote that the corresponding parameters are calculated on the lines of intersections of the surface of the shock wave with the surface of the stream $\psi = \text{const}$ (the point N on Fig. 2), when $\varphi = \varphi'$. It is obvious that a unique mutual relation exists between the variables ψ and φ' and that the sought functions are best determined in the variables φ' and φ. The fifth equation of the system (2.1) after determination of u_0 and w_0, admits of the following integral:

$$\frac{\rho_0' A_1' \theta_{w\psi}'}{w_0^{\circ\prime}} = \frac{\rho_0 A_1 \theta_{w\psi}}{w_0} \tag{2.5}$$

This relation makes it possible to represent the second equation of the system (2.1) in the integral form:

$$p_0 - p_0^* = \frac{(\ln A_2)_\varphi}{A_1}\int_{\psi^*}^{\psi} \frac{w_0^2 A_1' \rho_0'}{w_0^{\circ\prime}} \theta_{w\psi}'\, d\psi$$

To eliminate the unknown function $\theta_{w\psi}'$ from under the integral, we changeover to an integration variable φ', using the inner quality

$$\theta_{w\psi}'\psi_{\varphi'} = \frac{d\theta_0'}{d\varphi'} - \left(\frac{\partial\theta_0}{\partial\varphi}\right)' = -\frac{A_2' v_0^{\circ\prime}}{A_1' w_0^{\circ\prime}}\left[1 + \frac{2a^2}{(\gamma-1)v_0^{\circ\prime 2}}\right] \tag{2.6}$$

obtained with the aid of the last equation of the system (2.1) and the second condition of (2.2). Inserting the values of θ_0' from (2.2) into expression (2.6) under the integral sign, we find that the pressure at any point of the stream is determined from the formula

$$p_0 = p_0^* - \rho^\circ \frac{(\ln A_2)_\varphi}{A_1}\int_{\varphi^*}^{\varphi'} \frac{w_0^3 v_0^{\circ\prime}}{w_0^{\circ\prime 2}} A_2'\, d\varphi' \tag{2.7}$$

Integrating (2.5) along the line $\varphi' = \text{const}$, starting with the surface of the body, we get

$$\theta_w = \frac{\rho^\circ}{A_1}\int_{\psi^*}^{\psi^0} \frac{\delta_0' w_0 v_0^{\circ\prime}}{\rho_0 w_0^{\circ 2}} A_2'\, d\varphi' \tag{2.8}$$

From this, putting $\varphi' = \varphi^0$, we get the equation of the surface of a shock wave $\mathcal{S}^* (\varphi^0)$. After integration there appears in (2.8) an arbitrary function $\varphi^0(\psi) = \Psi(\varphi^0)$ at $\theta_0 = 0$, which should satisfy, by virtue of the boundary condition on the surface of the body, the following equality

$$\frac{\partial\sigma^*}{\partial\varphi}(w_0)_{\varphi=\sigma^*} = 0$$

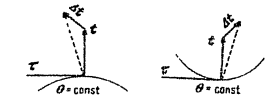

Fig. 3

which admits the following two solutions:

1) Following Ferri /3/, we assume that on the surface of the body $w_0^* \neq 0$. Then φ^0 equals a constant number, the value of which is determined in each specific case.

2) Assume that $\partial\varphi^0/\partial\varphi' \neq 0$. In this case φ^0 is found from the implicit equation

$$\int_{\varphi^0}^{\varphi} A_2\, d\varphi = \operatorname{arctg}\left[\frac{w_0^\circ(\varphi^0)}{w_0^\circ(\varphi^*)}\right] \tag{2.9}$$

An analysis of the integral (2.8) shows that the function can be considered constant only when Eq. (2.9) has no solution, and in the opposite case the first solution leads to negative values of θ_w.

Let us return to formula (2.7). The pressure on the surface of the body is determined from this equation $\varphi' = \varphi^0$. Let us investigate the sign of A_{20}, which determines the sign of the second term in (2.7). We have

$$A_{20} = \tau \frac{dt}{d\xi}, \qquad \tau(x_0 / A_2,\ y_0 / A_2,\ z_0 / A_2)$$

τ is a unit vector directed along the normal to the surface $\varphi = \varphi^0$ with a sphere of unit radius; $\tau(N_0, M_0, P_0)$ is a unit vector normal to Σ and directed along the tangent to the line $\eta = \text{const}$ on the sphere. The sign of the scalar product coincides with the sign of the triple product (τ, ω, τ), which is positive (Fig. 3), if a turn from a convex surface is made, and negative if the turn from a concave surface. Thus, the pressure on the convex parts of the surface is lower than behind the shock wave, and on the concave one it is higher. The increment due to the second term in (2.7) characterizes the influence of the centrifugal forces, due to the transverse flow of the gas.

3. Solution of the problem of flow around a flat triangular wing. As an example of the application of the general method, we can consider the flow about a triangular flat wing with a vertex angle 2α. We choose a system of coordinates satisfying the requirements indicated in section 2. In this problem, we take for this system the axes, r, φ, θ, shown in Fig. 4. The surface of the wing in this system is given by the condition $\theta_K = 0$, and the connection between the old and new coordinates is determined by the following relations

$$x = r\cos\theta\sin\varphi, \qquad y = r\sin\theta, \qquad z = r\cos\theta\cos\varphi \tag{3.1}$$

The Lamé coefficients are $A_1 = 1$, $A_2 = \cos\theta$. Considering that u_0^S, v_0^S, and w_0^S are calculated from (1.4) by substituting (-z) for z, in accordance with Fig. 4, and with $\theta^* = \theta_K = 0$, we find the stream parameters from formulas (2.5), (2.4), (2.7), and (2.8) in the following form

$$u_0 = U\cos\alpha\cos\varphi, \quad w_0 = -U\cos\alpha\sin\varphi, \quad \frac{p_0}{\rho_\infty} = U^2\sin^2\alpha\left[1 + \frac{2}{(\gamma-1)M^2\sin^2\alpha}\right]$$
$$\rho_0 = \rho^0 U^2\sin^2\alpha \qquad \theta_0 = \sin\varphi\,(\operatorname{ctg}\varphi' - \operatorname{ctg}\varphi)\operatorname{tg}\alpha\left[1 + \frac{2}{(\gamma-1)M^2\sin^2\alpha}\right] \tag{3.2}$$

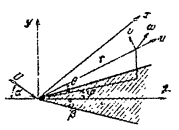

Fig. 4.

By direct substitution we verify that Eq. (2.9) has no solution for the function $\varphi'(\varphi)$ and consequently $\varphi' = \varphi^0$ is a constant, which is found uniquely if the shock wave is not detached (the front edge is supersonic). Actually φ^0 is the coordinate of the surface of the flow, adjacent to the surface of the wind, and since this surface intersects the wave on the front edge (right or left), then $\varphi^0 = \pm\beta$ (Fig. 4). Let us study the flow about the wing in greater exactitude by using the second terms of the series (1.5). The system (1.2) and the boundary conditions for the terms with index 1 are analogous to those considered in section 2. As a result of all the derivations, which we now omit, we get

$$u_1 = -U\frac{\sin\alpha\operatorname{tg}\alpha}{\sin\beta}\left[1 - \frac{2}{(\gamma-1)M^2\sin^2\alpha}\right]\sin(\beta - \varphi),$$
$$w_1 = U\frac{\sin\alpha\operatorname{tg}\alpha}{\sin\beta}\left[1 - \frac{2}{(\gamma-1)M^2\sin^2\alpha}\right]\cos(\beta - \varphi)$$
$$p_1 = 2\rho^0 U^2\sin^2\alpha\left[1 + \frac{2}{(\gamma-1)M^2\sin^2\alpha}\right] - \rho^0 U^2\sin^2\alpha - \rho^0 U^2 / M^2,$$
$$\rho_1 = \frac{4\rho^0}{2 + (\gamma-1)M^2\sin^2\alpha} \tag{3.3}$$
$$\theta_1 = \sin\varphi\operatorname{tg}\alpha\left[1 + \frac{2}{(\gamma-1)M^2\sin^2\alpha}\right]\frac{\sin(\beta - \varphi')}{\sin\beta\sin\varphi'}\left\{1 - \frac{2}{(\gamma-1)M^2\sin^2\alpha} - \right.$$
$$\left. + \operatorname{tg}^2\alpha\left[1 + \frac{2}{(\gamma-1)M^2\sin^2\alpha}\right]\left[\operatorname{cosec}^2\beta - \operatorname{ctg}\beta\frac{\sin(\varphi' - \varphi)}{\sin\varphi\sin\varphi'}\right]\right\}$$

The surface of the shock wave is obtained from the expression $(\xi, \theta_1 + \xi^A \theta_\beta)$ at $\varphi' = \varphi$. Let us consider the intersection of the surface of the wave with the planes $z = 1$. Going to cartesian coordinates by means of formulas (3.1), we find that in the first two approximations the intersection line is the straight line

$$y^* = \frac{\gamma-1}{\gamma+1}\operatorname{tg}\alpha\left[1 + \frac{2}{(\gamma-1)M^2\sin^2\alpha}\right](1 - x\operatorname{ctg}\beta)\times$$
$$\times\left\{1 + \frac{\gamma-1}{\gamma+1}\left(1 - \frac{2}{(\gamma-1)M^2\sin^2\alpha} + \frac{\operatorname{tg}^2\alpha}{\sin^2\beta}\left[1 + \frac{2}{(\gamma-1)M^2\sin^2\alpha}\right]\right)\right\}$$

Consequently, the surface of the shock wave consists of two planes and has a kink at $x = 0$. The flow lines on the surface of the wing, as shown by calculation, are straight lines that converge towards the symmetry axis at an angle $\sim\varepsilon$. We note that the solution obtained contains, in the second approximation, a singularity of the source type ($\omega_z \neq 0$) at the point of the kink of the shock wave ($x = 0$, $y = y^*$). It must be assumed that the kink in the wave and the singularity are due to the approximate nature of the method and will not exist in the exact solution (see Section 4 on this). We have considered flow about one surface of a triangular wave. On the trailing surface at $M \to \infty$ there is formed a base vacuum /4/, and one can assume $p = 0$. As a result of such a flow model, we obtain for the coefficients C_x and C_y, referred to the area of the wing in plan, the following expressions

$$C_x = 2\sin^2\alpha\left\{1+\frac{\gamma-1}{\gamma+1}\left[1+\frac{5-\gamma}{(\gamma-1)M^2\sin^2\alpha}\right]\right\},$$

$$C_y = 2\sin^2\alpha\cos\alpha\left\{1+\frac{\gamma-1}{\gamma+1}\left[1+\frac{5-\gamma}{(\gamma-1)M^2\sin^2\alpha}\right]\right\} \qquad (3.4)$$

It is remarkable that the coefficients C_x and C_y thus obtained with the corresponding coefficients for [illegible], as given in reference /2/. The situation is analogous also in linear theory /5/. Calculated values of the coefficient C_x and C_y as a result of this theory coincide with the Ackeret formulas for a wedge. Fig. 5 shows a comparison of the theory with experiment, carried out on a model of a triangular wing with a rhomboidal profile of 5 percent thickness at $\beta = 30^\circ$, $M = 6.9$, $\gamma = 1.4$, taken from reference /6/. The solid curves plotted from formulas (3.4) go into the dotter curves in that part, where the parameter $\lambda = 1 \sin\alpha < 1$ and the theory is no longer applicable. The dashes show the results of the linear theory, obtained in reference /7/.

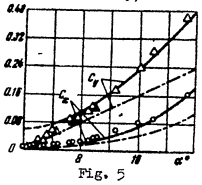

Fig. 5

4. Solution of the problem of flow about an elliptical cone. A second example is the flow about an elliptical cone, the surface of which is given by the equation $x^2/a^2z^2 + y^2/b^2z^2 - 1 = 0$. The case of a round cone was discussed in reference /8/. To plot the system of coordinates we introduce, as indicated in Section 1, the parameter θ. We then obtain a family of surfaces

$$\operatorname{tg}^2\theta = x^2/z^2 + ny^2/z^2 \quad , \qquad (n = a^2/b^2) \qquad (4.1)$$

In the region where $\tan^{-1}\sqrt{n} \leq \theta \leq \pi/2$, the surfaces $\theta = \text{const}$ fill the volume outside the body uniformly and can be taken as a second family. The third family is found by writing down the equation for the orthogonal trajectories to the family of surfaces (4.1). In final form this family is determined by the equation

$$\operatorname{tg}^2\varphi = \frac{(x/z)^{2n}(1+x^2/z^2+y^2/z^2)^{1-n}}{(y^2/z^2)} \qquad (-\pi \leq \varphi \leq \pi) \qquad (4.2)$$

By direct verification it is easy to check that the new system of coordinates x, θ, φ is orthogonal and that when $n = 1$ it goes into the

ordinary spherical system. The coefficients A_1 and A_2 can be calculated from formulas (4.1) and (4.2), using the following relation from vector analysis

$$\sqrt{x_0^2+y_0^2+z_0^2} = 1/\sqrt{\theta_x^2+\theta_y^2+\theta_z^2}$$

After carrying the various calculations, we find

$$A_1 = \frac{\operatorname{tg}\theta}{\cos^{2n}\theta\,[\sec^2\theta+(1-n)\,y_1^2]\,[\operatorname{tg}^2\theta\sec^2\theta-(1-n)\,ny_1^2]^{1/2}},$$

$$A_2 = \frac{2y_1}{\sin 2\varphi}\left(\frac{(\operatorname{tg}^2\theta-ny_1^2)\,[\sec^2\theta+(1-n)\,y_1^2]}{(\operatorname{tg}^4\theta\sec^2\theta+(1-n)\,[\operatorname{tg}^4\theta+\operatorname{tg}^2\theta\,(1-n)-n]\,y_1^2-n\,(1-n)\,y_1^4}\right)^{1/2},$$

$$\operatorname{tg}^2\varphi = [\sec^2\theta+(1-n)\,y_1^2]^{1-n}\,[\operatorname{tg}^2\theta-ny_1^2]^n \qquad (4.3)$$

As can be seen from formulas (4.3), a unique relationship exists between $y_1 = y/z$ and φ, and since y_1 is a geometrical coordinate in the plane $z = 1$, it is more convenient to determine in terms of this quantity all the sought functions. The velocity components of the undisturbed flow are found from (1.4) to equal to

$$u_0^c = U\frac{\cos\alpha+\sin\alpha\,y_1}{[\sec^2\theta_k+(1-n)\,y_1^2]^{1/2}}, \qquad v_0^c = -U\frac{\cos\alpha\operatorname{tg}^2\theta_k-\sin\alpha\,ny_1}{[\operatorname{tg}^2\theta_k\sec^2\theta_k-n(1-n)\,y_1^2]^{1/2}},$$

$$w_0^c = -U\frac{[\sin\alpha\sec^2\theta_k-\cos\alpha\,(1-n)\,y_1]\,[\operatorname{tg}^2\theta_k-ny_1^2]^{1/2}}{[\operatorname{tg}^2\theta_k\sec^2\theta_k+(1-n)\,[\operatorname{tg}^4\theta+\operatorname{tg}^2\theta_k\,(1-n)-n]\,y_1^2-n\,(1-n)\,y_1^4]^{1/2}}, \qquad (4.4)$$

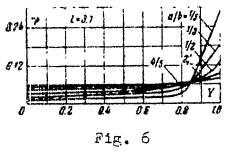

Fig. 6

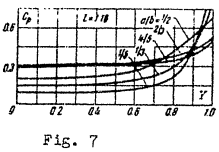

Fig. 7

Figures 6 and 7 show plots of the distribution of the coefficient of pressure C_p over the surface of elliptical cones at $M = \infty$ and $\alpha = 0$.

On these figures

$$Y = y_1\frac{a}{b}\operatorname{tg}\theta_k, \qquad \frac{a}{b} = \frac{4}{3},\ \frac{2}{3},\ \frac{1}{2},\ \frac{1}{3},\ \frac{1}{5},$$

$$l = 1.16,3.1\left(l = \frac{1}{\sqrt{\pi ab}}\right)$$

An investigation of the derivative $(\theta_0^*)_{\varphi}$ of the integral (2.8) shows that the shock wave, no matter how small the value of $a/b \neq 0$, has no kink in the plane of symmetry. Consequently, the singularity that occurs when a plane triangular wing is placed in a stream does not appear in all the cases when the thickness of the wing is not zero.

In conclusion, the author expresses deep gratitude to G. G. Chernyy for great help with the work.

Received 9 June 1958.

BIBLIOGRAPHY

1. Kochin, N. Ye.; Kibel', N. A., and Roze, N. V. Teoreticheskaya gidromekhanika (Theoretical Hydromechanics), vol 1, 1947.
2. Chernyy, G. G. Flow of Gases About Bodies at High Supersonic Speeds, DAN SSSR, vol 107, no 2, p 221, 1956.
3. Ferry, A. Supersonic Flow Around Circular Cones at Angles of Attack, NACA T. R. No 1045, 1951.
4. Goschek, I. Aerodinamika sverkhzvukovykh skorostey (Aerodynamics of High Speeds), Russ. Transl. IL, 1954.
5. Frankel', F. Ye., Karnovich Ye. A. Gazodinamika tonkikh tel (Gas Dynamics of Slender Bodies), 1948.
6. McLellan, C. H. Exploratory Wind-Tunnel Investigations of Winds and Bodies at M-6.9. JAS, No 10, 1951.
7. Gurevich, M. I. Lifting Force of Sweptback Wing in a Supersonic Stream, PMM (Applied Math. and Mechanics) vol 10 no 4, 1946.
8. Conor, A. L. Flow Around a Cone at an Angle of Attack with High Supersonic Speed. Izv. AN SSSR OTN, No 7, 1958.

Calculation of Axisymmetric Jet Nozzle of Least Weight

L. Ye. Sternin

Izvestiya Akademii Nauk SSR, Otdeleniye Tekhnicheskikh Nauk Mekhanika i Mashinostroyeniye, /News of the Academy of Sciences USSR, Department of Technical Sciences, Mechanics and Machine Building/, No 1, Jan-Feb 1959, Moscow, pages 41-45.

The problem of the optimum contour of a jet nozzle was solved only in the last few years. In 1950, A. A. Nikol'skiy /1/ proposed, in solving the variational problem of gas dynamics, to calculate the aerodynamic forces applied to any surface, in terms of the parameters on the characteristic surfaces that bound this surface.

In 1955, G. Guderley and E. Hantsch /2/ gave a solution for the variational problem in a nozzle of least length with an angleentry. The authors of the work have reduced this problem to a numerical integration of a system of ordinary differential equations of first order.

An analogous problem was solved, with a much more rigorous mathematical foundation, by Yu. D. Shmiglevskiy /3/. In this paper, unlike in reference /2/, an effective method was given for integrating the system of differential equations. In reference /3/ the investigation concerned a nozzle with an angle entry and a fixed length and diameter of outlet section. The working fluid was a gas with a constant adiabatic index.

The calculations have shown that the minimum length nozzle is not the best as regards weight characteristics.

It should be noted that in an exact statement of the problem it is very difficult to solve the problem of the maximum-thrust nozzle for a specified weight, since in this case it is impossible to use the aforementioned principle, expounded in reference /1/.

On the other hand, it is natural to assume that when one goes from one extremal* nozzle to another, close to it, the weight depends principally on the change of the end dimensions and depends little on the specific nature of the change in the intermediate points. In the present paper, the weight is approximated by an arbitrary function of the end dimensions of the nozzle. In the case when the nozzle is stamped out from a conical blank, we obtain the exact solution of the problem.

When solving the variational problem, it is not logical to consider a nozzle with an angle entry, since in real engines it is necessary to round off the point because of the presence of technological difficulties and dangers of burning.

The formulas given below are correct for nozzles with rounding off in the critical section. Nozzles with angle entry are a particular case of rounded off nozzles (the radius of round-off equal to zero).

Using calculations performed with the formulas given below, it is possible to conclude the advisability of any particular degree of rounding off.

The symbols are as follows: x, y -- rectangular system of coordinates, the origin of which is in the center of the critical section of the nozzle; p -- pressure in the stream; ρ -- density; p^0 -- counter pressure; w -- velocity; θ -- angle of inclination of the velocity to the x axis; α -- angle between the velocity and the characteristic, a* -- critical speed.

$$I=\int_{a_*}^{w}\operatorname{ctg}\alpha\frac{dw}{w},\qquad \lambda=\frac{90}{\pi}(\theta-I),\qquad \mu=-\frac{90}{\pi}(\theta+I)$$

$$f_1=y\left[p-p^0+\rho w^2\frac{\sin\alpha\cos\theta}{\sin(\alpha+\theta)}\right],\qquad f_2=y\rho w\frac{\sin\alpha}{\sin(\alpha+\theta)},\qquad f_3=\operatorname{ctg}(\alpha+\theta)$$

$$\Phi_1=y\left[p-p^0+\rho w^2\frac{\sin\alpha\cos\theta}{\sin(\alpha-\theta)}\right],\qquad \Phi_2=y\rho w\frac{\sin\alpha}{\sin(\alpha-\theta)},\qquad \Phi_3=-\operatorname{ctg}(\alpha-\theta)$$

*By extremal nozzle, we understand here a nozzle having the maximum thrust, constructed to specified diameters, and lengths, (the statement of the problem of reference /3/).

1. Variational Problem. Let us turn to Fig. 1. To the left of the characteristic AM, the flow may be arbitrarily vortex free, but must be known beforehand. The characteristic AM does not change during the variations. In view of the fact that the variational problem has a degenerate character, the number of equations for an arbitrary characteristic AM and for a specified weight exceeds the number of unknowns, and there is no solution. As will be seen from the following, the solution is found only for one of the characteristics of the family AM, A_1M_1, etc., which for a special weight we shall call the characteristic AM.

The thrust of the post-critical portion of the nozzle is

$$P=R+2\pi\left(\int_C^B f_1\,dy-\int_C^A\Phi_1\,dy\right) \tag{1.1}$$

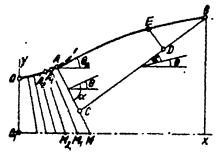

where R is the thrust of Sn.OA. From the condition of equality of the flow through the characteri tics AC & CB we have

$$Q=\int_C^B f_2\,dy-\int_C^A\Phi_2\,dy=0 \tag{1.2}$$

Fig. 1. Diagram showing arrangement of characteristics.

the weight of the nozzle is

$$G=S_0+S[y(A),y(B),x(B)-x(A),\theta_A] \tag{1.3}$$

Here S_0 is the weight of the portion of the nozzle AB, S is any continuous function that determines the dependence* of the surface of the nozzle and thickness of the wall on the end dimensions.

Furthermore

$$L=x(B)-x(A)=\int_C^B f_3\,dy-\int_C^A\Phi_3\,dy \tag{1.4}$$

Along AC and CB, the following equations are satisfied (see, for example, reference /2/):

$$g_1\left(\lambda,\mu,\frac{d\lambda}{dy},y\right)\equiv-\frac{\operatorname{ctg}\alpha}{w}\frac{dw}{dy}+\frac{d\theta}{dy}+\frac{\sin\alpha\sin\theta}{y\sin(\alpha+\theta)}\equiv\frac{d\lambda}{dy}+\frac{90}{\pi}\frac{\sin\alpha\sin\theta}{y\sin(\alpha+\theta)}=0 \tag{1.5}$$

*The paremeters S_0 and S may include a friction factor, proportional to the surface of the nozzle.

on CB, and analogously on AC

$$g_2\left(\lambda, \rho, \frac{d\psi}{dy}, y\right) = 0 \qquad (1.6)$$

The functional is represented in the following form

$$I_1 = P + m_1 Q_1 + \frac{m_2}{S_L'} G + \int_C^B b_1(y)\, \rho\, dy + \int_C^A b_2(y)\, g_2\, dy \qquad (1.7)$$

where m_1 and m_2 are constant Lagrange factors, and $b_1(y)$ and $b_2(y)$ are variable factors.

We note for what is to follow that

$$\delta \int_C^A b_2(y)\, g_2\, dy = 0$$

At the point C, the variations are connected by the relation

$$\delta\lambda_C = \left(\frac{d\lambda}{dy}\Big|_{AC} - \frac{d\lambda}{dy}\Big|_{CB}\right)\delta y_C, \quad \text{or} \quad \delta\lambda_C = B(y)\,\delta y_C$$

where

$$B(y) = \frac{d\lambda}{dy}\Big|_{AC} - \frac{d\lambda}{dy}\Big|_{CB}$$

We arrive at the following equations

$$\left.\begin{aligned} &2\pi f_{1\lambda}' + m_1 f_{2\lambda}' + m_2 f_{3\lambda}' + b_1 g_{1\lambda}' - b_1' = 0 \\ &2\pi f_{1\mu}' + m_1 f_{2\mu}' + m_2 f_{3\mu}' + b_1 g_{1\mu}' = 0 \\ &\frac{d\lambda}{dy} + \frac{90}{\pi}\frac{\sin\alpha\sin\theta}{y\sin(\alpha+\theta)} = 0 \end{aligned}\right\} \text{on } BC \qquad \begin{matrix}(1.8)\\(1.9)\\(1.10)\end{matrix}$$

$$\left.\begin{aligned} &2\pi f_1 + m_1 f_2 + m_2 f_3 + m_2 \frac{S_{y(B)}'}{S_L'} = 0 \\ &b_1 = 0 \end{aligned}\right\} \text{at point B} \qquad \begin{matrix}(1.11)\\(1.12)\end{matrix}$$

$$2\pi f_{1\lambda}' + m_1 f_{2\lambda}' + m_2 f_{3\lambda}' + b_1 B_1(y) = 0 \text{ at point C} \qquad (1.13)$$

where $B_1(y)$ is a certain definite function of y.

We note that the Eqs. (1.8), (1.9), and (1.12) fully agree with Eqs. (16a), (16b), and (16f) of reference /2/, while Eq. (1.11) is an analogue of Eq. (16d).

It was noted in reference /3/ that a solution of the system is the value

$$b_1(y) \equiv 0 \qquad (1.14)$$

Actually, if one assumes the condition (1.14), the expressions obtained from Eqs. (1.8) and (1.9) for $\alpha(y)$ and $\theta(y)$ satisfy the Eqs. (1.10) and (1.13) for all m_1 and m_2.

To simplify the system (1.8) ÷ (1.13), it is necessary to substitute the values of the derivatives $f'_{1\lambda}$, $f'_{1\mu}$, $f'_{2\lambda}$, $f'_{2\mu}$, etc.*

After performing the transformations, we arrive at the following formulas

$$m_1 \cos\alpha + 2\pi w \cos(\alpha - \theta) = 0 \quad \text{along BC} \qquad (1.15)$$

$$m_2 + 2\pi y \rho w^2 \operatorname{tg}\alpha \sin^2\theta = 0 \qquad (1.16)$$

$$\frac{p - p^0}{\rho w^2} \operatorname{ctg}\alpha - \sin\theta\cos\theta = \frac{S_{y(B)}'}{S_L'}\sin^2\theta \text{ at point B} \qquad (1.17)$$

Before we calculate the parameters in BC, we must find x, and y at the points BC and the Lagrange multipliers m_1 and m_2.

To find these ten unknowns we have the following system of 11 independent equations (Eqs. 1.15) and (1.16) at points B and C, four equations (Eqs. 1.17), the coupling (Eqs. 1.2 and (1.3), the condition (1.4), and three equations at the point C of the type

$$y(C) = y_C[x(C)], \quad \theta(C) = \theta_C[x(C)], \quad \alpha(C) = \alpha_C[x(C)] \qquad (1.18)$$

which express the fact that the parameters at the point C must satisfy the equations of the characteristic AM.

It is obvious, thus, that for a given weight the solution can occur on some one characteristic. This fact is a consequence of the fact that the system of differential equations (1.10), (1.8), and (1.9) obtained was of the first order.

Since x does not enter into the equations, then in practical solutions one must deal with a system of eight equations, which can be readily solved by the method of successive approximations.

We note that in the arguments given above we did not

*The values of these derivatives are given in reference /2/: formulas (19a) -- (19f). It must be borne in mind that in formulas (19a) and (19b) of reference 2 the values sin θ cos θ are erroneously marked sinα cos θ.

use quations that relate the velocity with the density and pres ure. Therefore, the system (1.15) -- (1.18) gives a solu ion of the problem not only for gases with a constant adia atic index, but also for gases with any connection between the pressure, density and velocity.

2. Concerning the Condition of Transversality on the Free End. Eq. (1.17), found by variational methods, can be obta ned by another method, the idea of which, as applied to the optimal nozzles of specified length, belongs to Busemann /2/.

Let us imagine that the contour of the nozzle is made in t e best possible manner everywhere with the exception of the ast element dS. We shall vary this element, postulating a ma imum thrust. The thrust of this element is

$$dP = 2\pi y\,(p - p^0)\,dy$$

According to Fig. 2, we have

$$dS = S'_{y(B)}\,dy + S'_L\,dL, \qquad dL = dx = dy\,\mathrm{ctg}\,\theta$$

Hence

$$dP = 2\pi y\,dS\,\frac{p - p^0}{S'_{y(B)} + S'_L \mathrm{ctg}\,\theta} \tag{2.1}$$

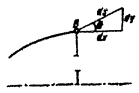

Fig. 2. For use in the derivation of the condition of transversality on the free end.

In the variations of θ, the factor in front of the fraction is constant; furthermore, when the Mayer flow is formed, λ = const. It is therefore enough to differentiate the index (2.1) the fraction with respect to μ and to set the derivative equal to 0.

Considering that

$$\frac{180}{\pi}\frac{dp}{d\mu} = \rho w^2 \lg \alpha, \qquad \frac{180}{\pi}\frac{d\theta}{d\mu} = -1 \tag{2.2}$$

we obtain after differentiation exactly Eq. (1.17).

3. Particular Cases. Nozzle of specified length. In this case

$$G = \gamma (S_0 + L)$$

where γ is a dimensional factor. Let us assume $\gamma = 1$, and we obtain

$$S'_{y(B)} = 0, \qquad S'_L = 1$$

By virtue of this, Eq. (1.17) becomes

$$2\frac{p - p^0}{\rho w^2}\,\mathrm{ctg}\,\alpha = \sin 2\theta$$

and this equation is given in reference /2/.

Nozzle is stamped out of a conical blank. Here

$$G = \gamma (S_0 + \pi [y(B) + y(A)] \sqrt{L^2 + [y(B) - y(A)]^2})$$

Hence

$$S'_{y(B)} = \gamma\pi \frac{L^2 + 2y(B)[y(B) - y(A)]}{\sqrt{L^2 + [y(B) - y(A)]^2}}$$

$$S'_L = \gamma\pi \frac{L[y(B) + y(A)]}{\sqrt{L^2 + [y(B) - y(A)]^2}}$$

or

$$\frac{S'_{y(B)}}{S'_L} = \frac{L^2 + 2y(B)[y(B) - y(A)]}{L[y(B) + y(A)]}$$

The transversality equation (1.17) becomes

$$\frac{p - p^0}{\rho w^2}\,\mathrm{ctg}\,\alpha - \sin\theta\cos\theta = \sin^2\theta\,\frac{L^2 + 2y(B)[y(B) - y(A)]}{L[y(B) + y(A)]}$$

4. Problem with Weight Equivalent. In most practical cases along with determining the optimum nozzles of a given weight it is necessary to choose the degree of expansion of the nozzle. In many cases, one is guided here only by the weight equivalent, i.e., by the number ζ, which shows how many kilograms of nozzle thrust are offset by one kilogram of weight.

If ζ is specified, it is advisable to solve the variational problem concerning the minimum-wave nozzle in such a way as to obtain simultaneously the degree of expansion of the nozzle.

In this case, the expression for the functional beco-

$$I = P - \xi G + m_1 Q + \int_C^B b_1 g_1 dy + \int_B^A b_2 g_2 dy$$

Naturally, the system of equations that express the solution of the problem remains the same as in Section 1, with the exception of Eq. (1.16). This is replaced by the following equation

$$2\pi y \rho w^2 \operatorname{tg} \alpha \sin^2\theta = S_L' \xi \tag{4.1}$$

The number of unknowns is reduced by one, since the Lagrange multiplier m2 drops out. Simultaneously the condition Eq. (1.3) drops out of the system of equations. There remain seven unknowns α, ξ and y at points O and B, as well as the unknown m1.

Remark. When making the variation, the form of the initial portion of the nozzle was assumed arbitrary. However, by virtue of the fact that the characteristic AC is fixed, the geometrical characteristics of the section OA did not enter into Eq. (1.15), (1.16), and (1.17).

Nevertheless, in a numerical solution of the problem, using for example, Eqs. (1.2) and (1.3), it becomes necessary to take into account the parameters on the line OA.

Let us formulate the solution for a nozzle with angle entry.

Let the line OAB be an intermediate stream line of the solution. The line CB will be a section of an extremal. The flow through AC will equal the flow through CB, etc., i.e., all the equations will be satisfied for the contour of the nozzle, with the exception of (1.17).

Thus, by solving the problem of optimum nozzle of minimum weight for a contour with an angle point, we thereby solve the variational problems for each intermediate stream line, thereby determining the extremal contours for the point B, located on the extremal. Analogous results for the external problem of gas dynamics were obtained in reference /3/. Naturally, these extremal contours will not have the minimum weight.

Received 4 June 1958.

BIBLIOGRAPHY

1. Nikol'skiy, A. A. On Bodies of Revolution with Channels, Having a Minimum Wave Resistance in Supersonic Flow, Tr. TsAGI (Works of the Central Aero-Dynamic Institute), 1950.
2. Guderley, and Hantsch, Best Shapes of Axisymmetric Supersonic Jet Nozzles (Russ. Transl.) Mekhanika (Mechanics) 4, 38, 1956.
3. Shmyglevskiy, Yu. D. Certain Variation Problems in Gasdynamics of Axisymmetric Supersonic Flows, PMM (Applied Mechanics and Mathematics) vol XXI no 2, 1957.

Experimental Investigation of Self-Oscillations of Square Plates in Supersonic Flow

G. N. Mikishev

Izvestiya Akademii Nauk SSR, Otdeleniye Tekhnicheskikh Nauk Mekhanika i Mashinostroyeniye, /News of the Academy of Sciences USSR, Department of Technical Sciences, Mechanics and Machine Building/, No. 1, Jan-Feb 1959, Moscow, pages 154-157

We investigate the self-oscillations (flutter) of a square flat plate in a supersonic stream at Mach number values M = 1.7, 2.3, and 3 for the case when two edges of the plate, perpendicularto the stream, are clamped, while the other two edges, parallel to the stream, are supported.

The results of the experiment are compared with the theoretical solution /1/.

1. Experimental Procedure. The specimens were made of steel 1 Kh18N9 (σ_s = 80 --120 kg/mm^2) and of duraluminum D16AT (σ = 40 kg/mm^2) measuring 300 x 300 mm and 250 x 250 mm, of different thickness. For the steel the thickness of the plates varied from 0.3 to 0.8 mm, for duraluminum from 0.5 to 1.0 mm.

The fixture for clamping the specimens in the wind tunnel is shown in Figs. 1 and 2. It comprises a plate which is attached with two edges to the walls of the tunnel, while the other two edges are wedge-like, for streamlining. The plate has a square cavity in the center. In the bottom of the cavity are drainage holes for rapid equalization of the pressures and to reduce the damping of the air in the cavity. The tested specimen is secured from the top of the cavity. The method of attachment of the specimen to the plate is seen in the included photographs.

The front edge of the plate is bent at a right angle and is clamped by two steel strips, with the aid of which the plate is attached to the base plate. The side edges of the plate bear, both on the inside and the outside, against steel triangular prisms. The prisms are attached to the base plate by screws. The rear edge of the plate is clamped by means of a steel cover plate. By adjusting the screws with which the rear cover plate and the front bearing prisms are secured it is possible to choose such a position, at which the edges of the place can come closer quite freely

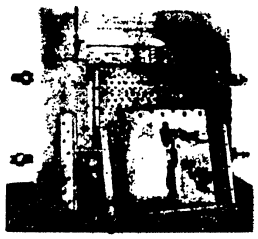

Fig. 1

Fig. 2

The fixture is leveled (horizontally) in the working portion of the wind tunnel.

Thus, the plate is exposed to the stream at a zero angle of attack, from the upper side. On the lower side, in the cavity of the fixture, there is stationary air.

The pressure in the cavity is practically equal to the pressure in the stream.

The pressure was measured at several points both in the stream and inside the cavity, by means of mercury manometers and also by pressure transducers of the rheochord type.

To determine the instant when flutter occurs, and also to determine the frequency and the wave form of the oscillations, resistance tension gauges were used. The tension gauges were fastened to the lower side of the plate. The wires from the tension gauges passed through the body of the base plate outside the wall of the tunnel.

Before each exposure to the air blast, frequency tests were made on the plate by resonance method. For this purpose the fixture was suspended on rubber shock absorbers. The oscillations were excited by a directional mechanical vibrator, which was fastened to the fixture. The resonant frequency was determined by means of a tachometer and from the oscillogram of the recording produced by tne tension-gauge trans-

ducers. The wave form of the oscillations was determined by means of sand. The only plates selected for tests in the wind tunnels were those in which the natural frequencies deviated not more than 10% from the calculated values.

During the time of the blast, the process of the oscillations was also investigated with the aid of high speed motion picture photography.

The plate was made to flutter by selecting the thickness of the plate and by continuously varying the pressure in the stream at a constant Mach number.

2. Certain Results of the Tests. Observations have shown that long before the plate begins to flutter intensely, the spectrum of the natural frequencies is strongly deformed. For example, the fundamental natural frequency of the plate at the instant of occurrence of flutter increases by more than 1.5 times compared with the frequency in still air.

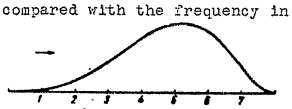

Fig. 3

At the same time a change occurs also in the wave form of the oscillations. For example, the profile of the pre-flutter wave form of the oscillations of the fundamental tone, unlike the profile in still air, is not symmetrical, and the peak of the profile is shifted towards the rear edge. Fig. 3 shows the theoretical pre-flutter profile of the wave form of the fundamental-tone oscillations.

The actual profile, as shown by measurements, was sufficiently close to the profile shown in the figure.

In the stability region, there are observed weak oscillations of the plate in the stream. These oscillations occur at the natural frequency, have a random character, and are rapidly damped. When going during the boundary of the stability region, the randomly occurring oscillations are replaced by intense flutter.

Fig. 4 shows curves of the process of the currents of flutter, recorded with the aid of strain-gauge transducers at the points 2, 3, and 4 (see Fig. 3). First the oscillations that occur because of various random disturbances in the stream are rapidly damped (Fig. 4a, b). Then, as the pressure in the stream is increased, they are gradually changed

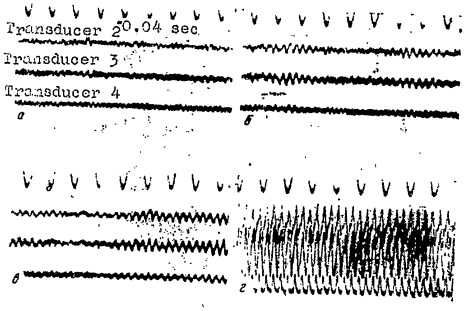

Fig. 4

into intense undamped oscillations (Fig. 4c, d).

In the case of natural oscillations of the plates, the wave-forms of the oscillations are standing waves, and in the flutter mode the oscillations of the plate recall traveling waves. This is seen from a review of the film, obtained with the aid of high speed motion picture photography. Fig. 5 shows certain frames of this film for a steel plate 0.3 mm thick.

The photographs show approximately 4/5 of the length of the plate on the rear edge. The front portion of the plate is covered by the wall of the tunnel (upper dark corner). The direction of the stream is from left to right. A square grid with a pitch of 1/5 of the length was drawn on the plate, and only the transverse lines of the grid are shown in the photograph.

The first photograph corresponds to supersonic flow over the plate before the occurrence of self-oscillations. The subsequent seven photographs fix the positions of the plates also during the time of one cycle of strongly developed flutter. The photographs display clearly the motion of the hump in the plane of the plate. Consequently, the flutter of the plate represents traveling waves.

During a certain time the plate oscillates with a constant amplitude. Then a fatigue crack is formed at the

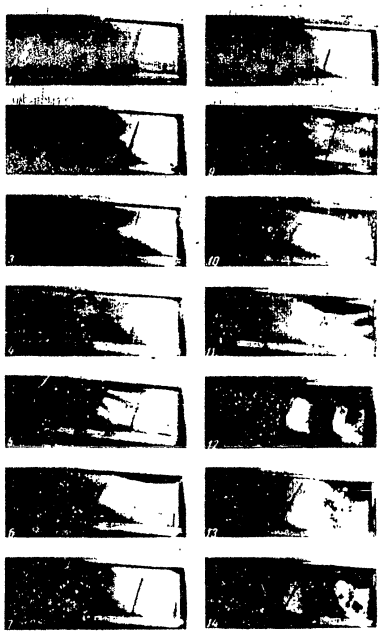

Fig. 5

Fig. 6

edge and the plate begins to disintegrate.

The disintegration of the plate proceeds opposite to the stream. In photographs 9 -- 14, Fig. 5, is shown the development of the fatigue crack and the disintegration of the plate during the blasting process. Fig. 6 shows also a photograph of the disintegration of a still plate 0.5 mm thick, taken after the blast.

The greatest amplitudes and the fastest disintegration occur in those plates in which the edge can come closer during the time of oscillations. For example, steel plates were destroyed in this case within three or four seconds after the occurrence of intense oscillations. The maximum amplitude of oscillations in this case reached approximately 5 -- 8 mm. The limitations imposed on the coming together of the edges decreased the amplitude of the oscillations and increased considerably the time necessary to disintegrate the plate.

The disintegration always begins in the most highly stressed rear edge of the plate.

Various tested methods of fastening the edges of the plate (particularly fastening of the front and rear edges of the plate directly by screws to the fixture) did not change the character of the disintegration.

The theoretical limit of the stability region is determined by the expression

$$\lambda = \frac{a^3 p_{\infty}}{D} \beta_{1,2}$$

$$\left(\beta_1 = M,\ \beta_2 = \frac{M^2}{\sqrt{M^2-1}},\ M = \frac{c}{c_0}\right)$$

where a is the length of the plate, D the cylindrical stiffness, p the pressure in the undisturbed stream, $\varkappa$ the polytropic index, c. c_0 the speed of the stream and the speed of sound in the undisturbed stream. The value of the parameter λ for the principal region of stability, calculated for a quadratic plate and reported to the author by A. A. Movchan, is 814. Figures 7 and 8 show a comparison with experiment of the calculated limits of the principal region of stability (the dotted curves correspond to the value β_1, while the solid curve to β_2). Fig. 7 shows the comparison for a Mach number of 1.7.

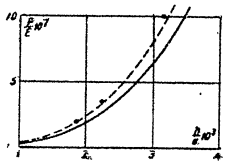

Fig. 7

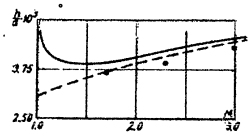

Fig. 8

The abscissas represent the ratio of the thickness of the plate to the length, while the ordinates represent the ratio to Young's modulus of the material of the plate. The experimental points correspond to the moment of occurrence of self-oscillations. Each experimental point is obtained as a mean of several tests. The first two points correspond to steel plates, the third point to duraluminum plates.

Fig. 8 shows a comparison with experiment of the calculated limits of the stability region as a function of the Mach number. The curves are plotted for duraluminum plates and pressures corresponding to sea level.

The experimental points were also reduced by recalculating to those conditions. Each experimental point corresponds to a plate of such thickness, at which the flutter still occurs. In thicker plates, no flutter was observed.

As can be seen from the foregoing comparison, the

calculated curves are in satisfactory agreement with experiment.

Received 9 June 1958.

BIBLIOGRAPHY.

Movchan, A. A. On the Stability of a Panel Moving in a Gas, PMM (Applied Mathematics and Mechanics), Vol. XXI, No. 2, 1957.

Self-Oscillating Systems in the Presence of Slowly Changing External Influences

A. A. Pervozvanskiy

Izvestiya Akademii Nauk SSR, Otdeleniye Tekhnicheskikh Nauk Mekhanika i Mashinostroyeniye, /News of the Academy of Sciences USSR, Department of Technical Sciences, Mechanics and Machine Building/, No 1, Jan-Feb 1959, Moscow, pages 158-161.

The assumption of slowness of the variation of the external disturbances that act on the system which enters into a self-oscillating mode has made it possible to develop a sufficiently effective procedure of dynamic calculation /1/.

However, it was assumed here that the influences themselves are specified functions of time. Therefore, it is of certain interest to develop a procedure for the case when the external influence is a stationary random process, specified in terms of its probability characteristics*

Let us consider for simplicity the dynamics of a system, containing one nonlinear inertialess element

$$Q(p)x + P(p)y = N(p)z, \qquad y = f(x) \tag{1}$$

where Q(p), P(p), and N(p) are linear differential operators, f(x) is a single-valued odd function and z is a stationary normal random process.

We assume that in system (1) there can be realized at z = 0 a self-oscillation mode, and we assume that z(t) represents a process with zero mathematical expectation, while the variations of z(t) within the limit of the self-oscillation period are insignificant, i.e., with a probability close to unity

$$\left|\frac{dz}{dt}\right| T \ll |z| \qquad \left(T = \frac{2\pi}{\omega}\right) \tag{2}$$

where T is the period of the self-oscillations.

We shall seek a solution of (1) in the form of a sum of periodic component x_1, y_1 and a slowly-varying (in the sense indicated above) component x_2, y_2.

$$x = x_1 + x_2, \qquad y = y_1 + y_2 \tag{3}$$

with both components being generally speaking random functions of time. If we assume furthermore that the system (1) satisfies certain conditions of applicability of the method of harmonic linearization, then

$$x_1 = A\sin\omega t \tag{4}$$

and when y is expanded into a Fourier series we can retain only the first terms

$$y = \varphi_0(A, x_2) + \varphi_1(A, x_2)x_1$$

where

$$\varphi_0 = \frac{1}{2\pi}\int_0^{2\pi} f(A\sin u + x_2)\,du$$

$$\varphi_1 = \frac{1}{\pi A}\int_0^{2\pi} f(A\sin u + x_2)\sin u\,du$$

We now separate from Eqs. (1) the equations for the periodic components

$$Q(p)x_1 + P(p)y_1 = 0, \qquad y_1 = \varphi_1(A, x_2)x_1 \tag{5}$$

and for the slowly varying components

$$Q(p)x_2 + P(p)y_2 = z, \qquad y_2 = \varphi_0(A, x_2) \tag{6}$$

Assuming that the amplitude A is also a slowly varying function in the sense of (2), we obtain from the system (5) the following conditions

$$\mathrm{Re}\frac{Q(j\omega)}{P(j\omega)} + \varphi_1(A, x_2) = 0, \qquad \mathrm{Im}\frac{Q(j\omega)}{P(j\omega)} = 0 \tag{7}$$

The second condition, as usual, determines the frequency of the self-oscillation, which in this approximation is found to be constant, and the "phase advance" effect is not detected; see for example reference /3/.

The first condition of (7) can be considered as an equation for the dependence of the amplitude A on the slowly-varying component x_2

$$\Phi(A, x_2) = 0 \tag{8}$$

Let us assume that this dependence can be solved in explicit form

*The principal idea of the procedure detailed below is pointed out in reference /2c/).

$$A = A(x_2) \qquad (9)$$

Then the transfer function $q_0(A, x_2)$ is expressed only in terms of x_2, and the system (6) reduces to the form

$$Q(p)x_2 + P(p)y_2 = z, \qquad y_2 = q_0^*(x_2) \qquad (10)$$

where

$$q_0^*(x_2) = q_0[A(x_2), x_2]$$

An approximate solution of the system (10) can be obtained either by direct linearization, or else by using the method of statistic linearization. We note that in the case of direct linearization (10) there is no need for resolving the implicit dependence (8). In fact, we have

$$q_0^*(x_2) \approx \frac{dq_0^*}{dx_2}\Big|_{x_2=0} x_2 = \left[\frac{\partial q_0}{\partial x_2} - \frac{\partial q_0}{\partial A}\frac{\partial \Phi}{\partial x_2}\left(\frac{\partial \Phi}{\partial A}\right)^{-1}\right]_{x_2=0} x_2$$

However, for an arbitrary piecewise-differentiable non-linear characteristic f(x), it is possible to show that $\partial q_0/\partial A \equiv 0$ when $x_2 = 0$.

Hence

$$q_0^*(x_2) \approx \frac{\partial q_0}{\partial A}\Big|_{x_2=0} x_2 \qquad (11)$$

and in the expression for the derivative, naturally, it is necessary to put $A = A_0$, where A_0 is the amplitude of the self-oscillations, calculated in the presence of external disturbances.

The statistical linearization (in the simplest, most convenient form) is based on the assumption of normal distribution of slowly-varying components of the input signal.

$$\psi(x_2) = \frac{1}{\sqrt{2\pi}\sigma_x} \exp\left(-\frac{x_2^2}{2\sigma_x^2}\right)$$

where σ_x is the mean-squared deviation of x_2. Then

$$q_0^*(x_2) \approx q^*(\sigma_x)x_2, \qquad (12)$$

where*

$$q^*(\sigma_x) = \frac{1}{\sigma_x^2}\int_{-\infty}^{\infty} q_0^*(x)x\psi(x)\,dx \qquad (13)$$

It is easy to show that upon a small change in dq^*/dx_2 in the probable range x_2 both methods give identical results.

*It follows from an examination of the system (10), that the mathematical expectation x_2 vanishes.

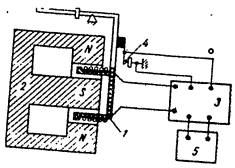

Fig. 1. Vibration accelerometer. 1) sensitive coil, 2) magnet, 3) electronic commutator, 4) contacts, 5) power supply.

For a more detailed acquaintance with the proposed procedure, let us consider by way of an example a calculation of an accelerometric system (Fig. 1). It is proposed that the system measures the acceleration of an aircraft, occurring during turbulence of the atmosphere. The dynamic properties of such a system can be described by the equation

$$(ap^3 + bp^2 + cp + d)x + k_1 f(x) = k_2(T_k p + 1); \qquad (14)$$

$$[a = T_2^2 T_k,\ c = T_1 + T_k(1 + k_3),\ b = T_2^2 + T_1 T_k,\ d = 1 + k_3]$$

Here x is the angle of deviation of the sensitive coil, z the acting acceleration, T_1 the damping constant of the sensitive coil, T_k the electric constant of the sensitive coil, T_2^2 its inertia constant, and k_1, k_2, k_3 the transfer functions.

The nonlinear characteristic f(x) of an electronic commutator is shown in Fig. 2 in the absence of external actions (z = 0) we have

$$\omega = \omega_0 = \sqrt{\frac{c}{a}}, \qquad A = A_0 = \frac{4k_1}{\pi}\frac{a}{bc - ad}.$$

The measured acceleration is proportional to the lateral wind component

$$z(t) = kv(t)$$

In reference /4/, the velocity v(t) was assumed to be a random stationary function, the correlation function of which was determined experimentally. For $\tau \ll 15$ seconds, this experimental curve can be approximated with sufficient accuracy by the expression of Fig. 3.

$$R_v(\tau) = Be^{-\alpha_1|\tau|}\cos\omega_1\tau$$

We seek the solution of system (14) in the form

$$x = x_2 + A \sin \omega t$$

For the characteristic (Fig. 2) we have

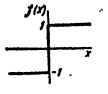

Fig. 2

$$q_1 = \begin{cases} -1 & x_2 < -A \\ \frac{2}{\pi} \arcsin \frac{x_2}{A} & |x_2| \leqslant A \\ 1 & x_2 > A \end{cases} \qquad q_1 = \frac{4}{\pi A} \sqrt{1 - \left(\frac{x_2}{A}\right)^2}$$

Conditions (8) for this system will have the form

$$a\omega^2 - c = 0, \qquad -b\omega^2 + d + k_1 q_1 (A, x_2) = 0$$

Hence

$$\Phi(A, x_2) = \frac{1}{A_0^2} A^4 - A^2 + x_2^2 = 0 \tag{15}$$

It follows from (15) that

$$x_2 \leqslant A \tag{16}$$

Linearization in accordance with (11) yields

$$q_0^* \simeq \frac{2}{\pi} \frac{1}{A_0} x_2 = \frac{bc - ad}{2ak_1} x_2 \tag{17}$$

It is now possible to determine the mean-square deviation $\sigma_{\dot{x}}$ in the usual manner

$$\sigma_{\dot{x}}^2 = \frac{1}{2\pi} \int_{-\infty}^{\infty} \frac{k_2^2 [T_k^2 \omega^2 + 1] S_z(\omega) d\omega}{\left[-b\omega^2 + \frac{bc + ad}{2a}\right]^2 + \omega^2 [-a\omega^2 + c]^2}$$

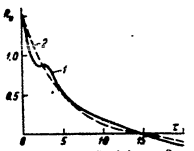

Fig. 3. Correlation function of turbulent disturbances (1) and its approximation (2).

where $S_z(\omega)$ is the spectral density of z(t).

Let us describe a procedure for calculating by the method of statistical linearization. It follows from (15) that

$$A = \sqrt{\frac{1}{2}(A_0^2 + A_0 \sqrt{A_0^2 - 4x_2^2})} \tag{18}$$

and the limits of variation of the quantities are as follows

$$|x_2| \leqslant \frac{1}{2} A_0, \qquad \frac{1}{\sqrt{2}} A_0 \leqslant A \leqslant A_0 \tag{19}$$

Let us furthermore find

$$q_0^* = \frac{2}{\pi} \arcsin \frac{x_2 \sqrt{2}}{\sqrt{A_0^2 + A_0 \sqrt{A_0^2 - 4x_2^2}}} = \frac{1}{\pi} \arcsin \frac{2x_2^2}{A_0}$$

which, in particular, directly confirms (17). We now employ the method of statistical linearization.

We assume, as already indicated above, the distribution of x_2 to be normal, although the limitation (19) should be taken into account. Then, by virtue of (13), we have

$$q^*(\sigma_x) = \frac{1}{\sigma_x \sqrt{2}} \int_{-A/2}^{A/2} \frac{x}{\pi} \arcsin \frac{2x}{A_0} \psi(x)\, dx = \frac{2\sqrt{2}}{\sigma_x \sqrt{\pi}} a^2 J_1(a)$$

where

$$J_1(a) = \int_0^1 x \arcsin x e^{-a^2 x^2} dx, \qquad a = \frac{A_0}{2\sqrt{2}\sigma_x}$$

A curve of $J_1(\alpha)$ is shown in Fig. 4. Inserting into (14) we get

$$\sigma_x^2 = \frac{1}{2\pi} \int_{-\infty}^{\infty} \frac{k_2^2 [T_k^2 \omega^2 + 1] S_z(\omega) d\omega}{[-b\omega^2 + d + k_1 q_{cr}(\sigma_x)]^2 + \omega^2 [-a\omega^2 + c]^2}$$

which can be considered as an implicit expression for σ. Thus, the quantity $\sigma_{\dot{x}}$ can be obtained by some approximate method. Then, for the mean value and the dispersion of the amplitude we have the following formulas

$$A_\Phi = \frac{4\sigma_x}{\sqrt{\pi}} a^2 J_2(a),$$

$$\sigma_A^2 = \frac{8\sigma_x^2}{\sqrt{\pi}} a^2 J_3(a) - \frac{8\sigma_x d^2}{\sqrt{\pi}} A_{cp} J_2(a) + \frac{2a}{\sqrt{\pi}} m_A^2 J_4(a)$$

where

$$J_2(a) = \int_0^1 \sqrt{1 + \sqrt{1 - x^2}}\, e^{-a^2 x^2} dx, \qquad J_4(a) = \int_0^1 e^{-a^2 x^2} dx$$

$$J_3(a) = \int_0^1 (1 + \sqrt{1 - x^2})\, e^{-a^2 x^2} dx$$

have been calculated and presented in the form of graphs in Fig. 5.

The description of the accelerometric system was graciously presented to us by I. P. Pal'tov, and the principal calculations for the system were performed by V. S. Baranova.

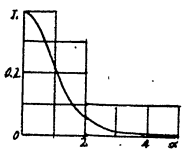

Fig. 4

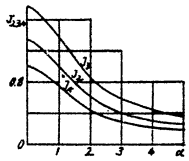

Fig. 5

The author expresses his deep gratitude to them.

Received 4 July 1958.

BIBLIOGRAPHY

1. Popov, Ye. P. Dinamika sistem avtomaticheskovo regulirovaniya (Dynamics of Automatic Control Systems), GITTL, 1954.

2. Pervozvanskiy, A. A. Approximate Method for the Investigation of Self-Oscillating Systems in the Presence of Random Influences, Izv. AN SSSR OTN (News of the Academy of Sciences USSR, Dept. of Tech. Sciences) No 3, 1958/

3. Bershteyn, I. L. On Fluctuations Near Periodic Motions of Self-Oscillating Systems. DAN SSSR (Transactions, Academy of Sciences USSR) vol XLVI, 1939.

4. Pelegrin, M. Statisticheskiy raschet sledyashchikh sistem (Statistical Design of Servomechanisms), Russ. Transl. IL, 1957.

One Approximation Method of Investigating Self-Oscillating Systems in the Presence of Slowly Changing External Influences

V. I. Sergeyev

Izvestiya Akademii Nauk SSR, Otdeleniye Tekhnicheskikh Nauk, Mekhanika i Mashinostroyeniye, [News of the Academy of Sciences USSR, Department of Technical Sciences, Mechanics and Machine Building], No. 1, Jan-Feb 1959, Moscow, pages 162-164

In the present investigation we studied self-oscillations on the basis of the method of the equivalent linearization of nonlinear oscillating system /1/, and its further development as applied to non-linear systems of high order /2/.

By way of an example, illustrating the application of the discussed method, of the investigation of self-oscillating systems, we consider the servomechanism shown in Fig. 1, the principal elements of which are the setting shaft 1, the output shaft 2, the amplifier 3, the dc motor with separate excitation 4, and the step-down reduction gear 5. We choose for the nonlinear element a link with "saturation zone" and arbitrarily lump in the characteristic of the motor (Fig. 1). We write the dynamic equations for the linear portion of the servo system in the following form:

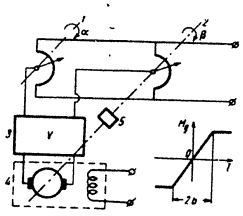

Fig. 1

$$(T_1 p + 1) p\beta = k_1 I \qquad (1)$$

$$\left(p = \frac{d}{dt}\right)$$

$$(T_2 p + 1) I = k_2 \alpha - (k_2 + k_3 p)\beta \qquad (2)$$

where T_1 and T_2 are the mechanic and electromagnetic time constants respectively, k_1, k_2 and k_3 are constant coefficients, determined by the parameters of the servo system, I the current in the armature circuit and $\alpha(t)$ slowly varying external signal.

We shall assume that the stability conditions for the characteristic equation, corresponding to (1) and (2), are not satisfied. In this case, in the presence of substantial nonlinearities, and particularly of a "saturation zone" self-oscillations can occur in the system. The characteristics of the chosen type of non-linear element is an odd function, and consequently by using the method of equivalent linearization, it can be represented by the following approximate expression

$$F(I) = q^*(a, I'') + q(a, I'')I' \tag{3}$$

Here a is the amplitude of the self-oscillations, I'' and I' are the corresponding aperiodic (constant) and periodic components of the current I.

Let us assume, for example, the amplitude of the self-oscillations to be limited by the values $b - I'' < a < b + I''$. We can then obtain the following expressions for the terms in the right half of (3).

$$q^*(a, I'') = -\frac{k_1 a}{\pi}\left[\frac{b-I''}{a}\left(\frac{\pi}{2} + \arcsin\frac{b-I''}{a}\right) + \sqrt{1-\left(\frac{b-I''}{a}\right)^2}\right] + bk_1 \tag{4}$$

$$q(a, I'') = k_1\left[\frac{1}{2} + \frac{1}{\pi}\left(\arcsin\frac{b-I''}{a} + \frac{b-I''}{a}\sqrt{1-\left(\frac{b-I''}{a}\right)^2}\right)\right] \tag{5}$$

Let $\alpha(t)$ be a certain slowly-varying function, which can be replaced with sufficient accuracy for practical calculations by a broken straight line (Fig. 2). Let us impose certain limitations on the time segments Δt_s ($s = 1, 2, \ldots, n$), a limitation that is obvious, the minimum value is determined by the period of the self-oscillations, i.e., $\Delta t_s \geqslant 2\pi/\omega_s$, where ω_s is the frequency of the self-oscillations. On the basis of the foregoing, we replace $\alpha(t)$ by the following approximate expression

$$\alpha(t) \approx \alpha(\Delta t_1) + \alpha(\Delta t_2) + \ldots + \alpha(\Delta t_s) + \ldots \tag{6}$$

where

$$\alpha(\Delta t_s) = A_s + B_s \Delta t_s \qquad (\Delta t_s = t_s - t^*_{s-1},\ t^*_{s-1} \leqslant t_s \leqslant t^*_s)$$

In this case, the function $p\alpha(t)$ is piecewise-continuous (Fig. 2). We write Eqs. (1) and (2) for the aperiodic components of the self-oscillations on the s-th segment of time (Δt_s)

$$(T_1 p + 1)\, p\beta''_s = k_1 I''_s \tag{7}$$

$$(T_2 p + 1)\, I''_s = k_1 \alpha_s - k_2 \beta''_s - k_2 p\beta''_s \tag{8}$$

and have on the basis of (6)

$$\alpha_s = A_s + B_s \Delta t_s, \qquad p\alpha_s = B_s, \qquad p^2\alpha_s = 0 \tag{9}$$

Inasmuch as $\beta''(t)$ is also a slowly varying function, we have by analogy

$$\beta''_s = A^*_s + B^*_s \Delta t_s, \qquad p\beta''_s = B^*_s, \qquad p^2\beta''_s = 0 \tag{10}$$

Differentiating (7) and (8) and taking (9) and (10) into account, it is easy to show that the following equality holds

$$p\beta''_s = p\alpha_s \tag{11}$$

and this means that the error in the displacement of the brush of the responding potentiometer will be a constant quantity inside each s-th segment of time.

$$\Delta\beta''_s = A_s - A^*_s = \text{const} \tag{12}$$

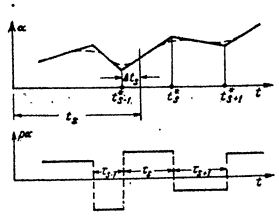

Fig. 2.

Consequently, the replacement of the curve $\alpha(t)$ by a broken line leads, inside of each s-th time interval, to the equality of the mean values of the angular velocities of the input and output brushes of the potentiometer (11) if their error angle (12) is constant.

The choice of the magnitude of the interval Δt_s is determined by the character of variation of $\alpha(t)$: corresponding to a smoother variation of $\alpha(t)$ are greater values of Δt_s, and vice versa. The following is obvious -- as Δt_s decreases (in the limit $\Delta t_s = 2\pi/\omega_s$) the accuracy of the calculation of the parameters of self-oscillations increases.

Thus, when the external signal is replaced by a function of type (6), the self-oscillation process in the considered time interval can be approximately represented in the form of a sequence of quasi-stationary processes the duration of each of which is determined by the choice of the value of Δt_s. Here the transition from one quasi-stationary mode to another is realized so to speak "instantaneously" on the boundary of the sections (Δt_{s-1} and Δt_s, Δt_s and Δt_{s+1}, etc). Inside each quasi-stationary process the values of a_s and ω_s are assume constant.

Let us determine β'' for the problem under consideration. Inserting (11) into (8), we find

$$\beta''_s = \alpha_s - \frac{k_2 I \alpha_s + I''_s}{k_2} \tag{13}$$

where the quantity I_s' is still unknown. From (13) we determine the "constant" component of the error of the system

$$\Delta\beta_s'' = -\frac{k_3 p\alpha_s + I_s'}{k_2} \tag{14}$$

Usually the error $\Delta\beta_s''$ is small, since k_2 is a value of the same order of magnitude as the gain of the amplifier 3.

Let us determine a_s. For this purpose we write (1) and (2) for the aperiodic components, inserting into (1) the value $F_2(1) = q(a, I'')$ I' from (3) instead of the right-hand half, putting $\alpha = 0$ in (2), and performing several transformations. We finally obtain the following differential equation

$$\{T_1T_2p^3 + (T_1 + T_2)p^2 + [1 + k_3q(a_s, I_s'')]p + k_2q(a_s, I_s'')\}\beta_s' = 0 \tag{15}$$

Writing down the characteristic equation ($p \equiv z$) for (15) and putting in it $z = j\omega$, we solve this equation with respect to the function $q(a, I_s'')$, which we insert in the left half of (5).

We then obtain after t ansformations

$$\arcsin\frac{b - I_s''}{a_s} + \frac{b - I_s''}{a_s}\sqrt{1 - \left(\frac{b - I_s''}{a_s}\right)^2} = \pi\left\{\frac{2(T_1 + T_2)}{k_1[T_1T_2k_2 - (T_1 + T_2)k_3]} - 1\right\}_{II^*} \tag{16}$$

Inasmuch as the parameters of the dynamic system are specified, the right half of (16) is a known quantity. Using the graph given in reference /3/, we can find the value of the ratio

$$\frac{b - I_s''}{a_s} = \text{const} \tag{17}$$

which is independent of $\alpha(\Delta t_s)$ and is consequently independent of the form of $\alpha(t)$. The foregoing follows directly from (16). We can now proceed to determine a_s and I_s''. We insert $F_1(I) = q''(a_s, I_s'')$ from (5) into (7). Then, taking (10) and (11) into account, we have

$$q''(a_s, I_s'') = p\alpha_s \tag{18}$$

From a simultaneous solution of (4) and (18) we get

$$a_s = \frac{bk_1}{\pi}\left[\frac{b - I_s''}{a_s}\left(\frac{\pi}{2} + \arcsin\frac{b - I_s''}{a_s}\right) + \sqrt{1 - \left(\frac{b - I_s''}{a_s}\right)^2}\right] - \frac{p\alpha_s}{E} \tag{19}$$

From (19) we can determine a_s for all sequences of quasi-stationary processes over a given time interval. From the found values of a_s we readily determine from (17) the values of I_s, and then use (14) to determine the aperiodic ("dc") components of the errors of the system $\Delta\beta_s''$. In order to go from the amplitude of the self-oscillations of the current I, calculated from (19) to the amplitude of self-oscillations of the coordinate β, it is necessary to make use of (1).

In the foregoing calculations, the external signal was assumed not to be random. Let us now proceed to calculate a self-oscillating system under the influence of a random function, one of the realizations of which is shown in Fig.2 in the form of $\alpha(t)$. By way of an example of a random function as a typical input signal of a servomechanism with definite probability-theory characteristics, we use the data given in reference /4/, according to which no limitations whatever are imposed on $\alpha(t)$, while the function $p\alpha(t)$ is assumed to be stationary with a characteristic specified in the form of a correlation function and a mathematical expectation of the following type:

$$K_{p\alpha}(\tau) = \sigma^2[p\alpha]e^{-\lambda|\tau|}\cos\beta\tau, \qquad M[p\alpha] = \text{const} \tag{20}$$

where $\sigma[p\alpha]$ is the mean squared deviation, τ the interval of variation of the independent variable, and $M[p\alpha]$ is the mathematical expectation. From (20) we get

$$K_{p\alpha}(0) = \sigma^2[p\alpha] \tag{21}$$

Then the dispersion and the mathematical expectation of the amplitude of the self oscillations are determined respectively by the following; relations:

$$\sigma^2[a] = \frac{\sigma^2[p\alpha]}{E^2}, \qquad M[a] = \frac{bk_1 - M[p\alpha]}{E} \tag{22}$$

where E denotes the expression in the denominator of (19). Using (22), we can readily find the corresponding probability-theory characteristics of the aperiodic component of the self-oscillations.

The quantity $\sigma^2[p\alpha]$ can also be calculated from the formula for the dispersion, without resorting to the calculation of the correlation function.

As is known, a stationary random function $\alpha(t)$ will be differentiable for all t, if its correlation function $K_\alpha(\tau)$ as a continuous secondary derivative with respect to τ. In this case, the random function $p\alpha(t)$ will also be a continuous stationary random function, with

$$K_{p\alpha}(\tau) = -\frac{d^2K_\alpha(\tau)}{d\tau^2} \tag{23}$$

When $K_{p\alpha}(\tau)$ is determined from (23), the value of $\sigma^2[p\alpha]$ can also be calculated as before from formula (22) with a count of the equality (21).

Received 14 June 1958.

BIBLIOGRAPHY

1. Bogolyubov, N. N. and Mitropol'skiy, Yu. A. Asimptoticheskiye metody v teorii nelineynykh kolebaniy (Asymptotic Methods in the Theory of Nonlinear Oscillations), GITTL, 1955.

2. Popov, Ye. P. Self-Oscillations of Nonlinear Systems of High Order under Slowly Varying External Influences. DAN SSSR vol 98, no 4, 1954.

3. Sergeyev, V. I. On One Method of Calculating the Amplitudes of Self-Oscillations. Izv. AN SSSR, OTN, No 7, 1958.

4. Teoriya slydyashchikh sistem (Theory of Servomechanisms), Russ. Transl. IL, 1953.

On the Motion of a Slender Solid Body under the Action of a Strong Shock Wave

S. S. Grigoryan

Izvestiya Akademii Nauk SSR, Otdeleniye Tekhnicheskikh Nauk, Mekhanika i Mashinostroyeniye [News of the Academy of Sciences USSR, Department of Technical Sciences, Mechanics and Machine Building], No 1, Jan-Feb, 1959, pages 165-166.

If a shock wave is incident on a solid moving in air, then, because of the change in the distribution of pressures on the surface of the body, the law of motion of the latter changes. To find the changed law of motion of the body, it is necessary to know the pressure field, produced by the wave moving past the body, and to find this pressure field it is necessary to know the law of motion of the body, and therefore the solution of the problem involves in general very great difficulties. If, however, the body is "slender" and the wave strikes it in such a way that the additional disturbances behind the waves caused by reflection and diffraction are small, then, neglecting these perturbances* the problem concerning the motion of the body under the action of a shock wave can be solved.

Let a plane, cylindrical, or spherical shock wave propagate along the x axis in accordance with the law

$$x = R_0(t)$$

and let the pressure distribution behind its front be

$$p = p_0 P(x, t)$$

At a certain instant of time the wave reaches the nose of the sharp slender body, moving along the x axis. In this case, the surface of the body is projected on the plane perpendicular to the x axis, makes a figure with a small area (the body is "slender"). During the next instant, the body is submerged by the shock wave, and is acted upon by a pressure equal to

$$F_x = p_0 \int_0^{R_0 - X_0} P(X_0 + u, t) \frac{dS}{du} du \qquad (1)$$

*This assumption is analogous to the principal assumption used by A. N. Krylov when he formulated his famous theory of roll of a ship [1].

Here $x = X_0(t)$ is the known law of motion of the body, S is the area of the transverse cross section of the body, u is the coordinate measured from the nose of the body along the x axis inside the body. We assume here that in view of the thinness of the body, pressure at the points of the parameter of transverse cross section is the same. Taking into account the slenderness of the body, we assume that

$$S(u) = \varepsilon^2 L^2 \sigma\left(\frac{u}{L}\right) \qquad (\varepsilon \ll 1)$$

where L is the length of the body. Then the expression (1) can be represented in the following form

$$F_w = \varepsilon^2 L^2 p_0 \int_0^{R(\tau)-X(\tau)} \sigma'(v) P[X(\tau)+v,\ \tau]\, dv \qquad (2)$$

Here

$$R_0(t) = LR(\tau), \quad X_0(t) = LX(\tau), \quad t = T\tau$$

T is a constant with the dimension of time, for example, $T = L/a_0$, where a_0 is the velocity of sound in the undisturbed air in front of the wave.

The translational motion of the body will then be described by the following equation

$$\frac{mL}{T^2}\frac{d^2X}{d\tau^2} = \varepsilon^2 L^2 p_0 \int_0^{R(\tau)-X(\tau)} \sigma'(v) P[X(\tau)+v,\ \tau]\, dv + NF(\tau) \qquad (3)$$

where $NF(\tau)$ is the known force acting on the body, for example the thrust of the engine. Rewriting (3) in dimensionless form, we obtain

$$\frac{d^2X}{d\tau^2} = \mu \int_0^{R(\tau)-X(\tau)} \sigma'(v) P[X(\tau)+v,\ \tau]\, dv + \nu F(\tau) \qquad (4)$$

which is an integro-differential equation for $X(\tau)$. Integrating Eq. (4) twice we reduce it to the integral equation

$$X(\tau) = \mu \int_0^{\tau} (\tau - \xi)\left(\int_0^{R(\xi)-X(\xi)} \sigma'(v) P[X(\xi)+v,\ \xi]\, dv\right) d\xi + f(\tau) \qquad (5)$$

$$f(\tau) = a + b\tau + \nu \int_0^{\tau} (\tau - \xi) F(\xi)\, d\xi \qquad (6)$$

where a and b are dimensionless initial positions and velocity of the body. The problem thus reduces to solving Eq. (5). This equation can be solved by the classical method of successive approximation.

Denoting by letter A the operator that appears in the right half of Eq. (5), let us write the latter in the form

$$X(\tau) = AX(\tau) \qquad (5')$$

If the solution $X(\tau)$ at a certain instant of time τ_0 changes into R, i.e., $X(\tau_0) = R(\tau_0)$, this means that the body leaves the shock wave in its entirety, but after this instant its motion is no longer determined by Eq. (5), and it is known that

$$X(\tau) = X(\tau_0) + X'(\tau_0)(\tau - \tau_0) + \nu \int_{\tau_0}^{\tau} (\tau - \xi) F(\xi)\, d\xi \qquad (7)$$

Therefore, the problem consists of setting up the solution (5) in the interval $0 \leq \tau \leq \tau_0$ (if there exists a $\tau_0 < \infty$).

Let us define operator A* in the following manner

$$A^*V = \begin{cases} AV & \text{if } AV \leq R(\tau) \\ R(\tau) & \text{if } AV > R(\tau) \end{cases} \qquad (8)$$

Then, obviously, the operator A* transforms any continuous function $V(\tau) \leq R(\tau)$ into a function with the same properties. Consequently, by solving the equation

$$X^* = A^*X^* \qquad (9)$$

by the method of successive approximation, i.e., by putting $X^*_{n+1} = A^*X^*_n$, we have

$$X^*_n(\tau) \leq R(\tau) \qquad (10)$$

Considering σ' and P to be bounded, and $R(\tau)$ to be monotonically increasing, something that always is satisfied in practice, we obtain for any continuous function $V_1 < R$ or $V_2 < R$ the following inequality

$$|A^*v_1 - A^*v_2| < \mu q \tau \left[1 + R(\tau) \max_{0 \leq \xi \leq \tau} k(\xi)\right] \int_0^{\tau} |v_1(\xi) - v_2(\xi)|\, d\xi \qquad (11)$$

where $k(\xi)$ is the function from the Lifschitz inequality

$$|P(v_1, \xi) - P(v_2, \xi)| < k(\xi)|v_1 - v_2| \qquad (12)$$

which is assumed to be satisfied, and $q = (\max \sigma')(\max P)$.

Using (11), it is easy to establish that the sequence $\{X^*_n(\tau)\}$ converges uniformly for all values of τ to the solution $X^*(\tau)$ of Eq. (9). In the inverval, $0 < \tau < \tau_0$, where τ_0 is the root of the equation $X'(\tau_0) = R(\tau_0)$, the quantity $X^*(\tau)$ is the solution of Eq. (5), i.e., the solution $X(\tau)$ of our problem.

The solution constructed corresponds to the case when the area of the transverse cross section of the body is a

continuous function of the variable v, or more accurately, when $\sigma'(v)$ is a bounded, piecewise-continuous function, and σ' differs from 0 only at $0 < v < 1$. If, however, the area of the transverse cross section of the body experiences a discontinuity in certain cross sections (for example, when the tail section of the body has an area different from 0), additional terms appear in Eq. (5). These terms can be obtained automatically from the presentation of (5), if it is considered that

$$\sigma(v) = \sigma_1'(v) + \sum_{i=1}^{k} a_i \delta(v - v_i)$$

where $\sigma_1'(v)$ is a piecewise continuous function, $\delta(v)$ is a δ-function, and a_i are numbers that determine the jumps in the area of the transverse cross section at the sections $v = v_i$. The resultant equation also admits of setting up a solution by the method of successive approximations.

Received 13 October 1958.

BIBLIOGRAPHY

1. Krylov, A. N. Theory of Pitching of Ships in Waves, Sobrannyye trudy (Collected Works), Vol XI, pages 136-182, 1951.

Useful Interference of an Airfoil and Fuselage in Hypersonic Velocities

G. L. Grodzovskiy

Izvestiya Akademii Nauk SSR, Otdeleniye Tekhnicheskikh Nauk, Mekhanika i Mashinostroyeniye /News of the Academy of Sciences USSR, Department of Technical Sciences, Mechanics and Machine Building/, No. 1, Jan-Feb., 1959, pages 170-173

The biplane of Busemann /1/ is the first model of a system which makes it possible to transport a certain volume at supersonic speed without giving rise to further wave resistance.

Three dimensional systems that make use of the useful interference of the pressure field of the transported body and the carrier surface were considered by A. Ferri /2/. The results of calculations of such systems by linear theory of supersonic flow /2, 4/ have shown that the application of the useful interference may improve the quality of the system*. Thus, for example, at a spe ified value of the lift coefficient C_y, the fineness ratio $K = C_y/C_x$ of a system consisting of a wing (triangular plate with sonic forward and straight rear edges), bearing against a wedge-like fuselage, is 34% higher than in the case of an isolated wing and fuselage. In the case of a triangular wind, bearing against a fuselage in the form of half of a cone, the fineness ratio of the system is obtained by linear theory 12% higher than in the case of an isolated wing and conical fuselage of the same volume.

In the present work, we consider analogous systems at high supersonic velocities where the results of the linear theory cannot be applied. We investigate combinations of a wedge-shaped fuselage and a triangular or arrow-shaped wing (Fig. 1a), a half-conical fuselage and a triangular wing (Fig. 1b) and a fuselage in the form of a half-body with power-law shape and a corresponding wing at zero angle of attack of the wing (Fig. 1c).

The systems are considered at $M \to \infty$ for the case of slender bodies.

*Analogous systems were considered independently in 1954 by Yu. A. Grebnev, N. T. Dan'kov, and S. S. Semenov.

On the basis of the law of similarity for large supersonic velocities and stabilization of aerodynamic coefficients /5 -- 8/, the results obtained can be used for bodies of similar form at large supersonic speeds.*

The geometric relations of a combination of a wedge-like fuselage (with an angle of wedge 2ω) and a triangular or arrow-shaped wing are shown in Fig. 1a, where

$$\varkappa = \frac{\varkappa+1}{2}\omega, \qquad \alpha = \omega\sqrt{\varkappa\frac{\varkappa-1}{2}}$$

ε is the angle of thefront of the jump from the wedge, and α is the Mach angle.

In this system, there acts on the lateral surface of the wedge and on the lower surface of the wing a constant relative pressure

$$\bar{p} = \frac{p-p_2}{\frac{1}{2}\varkappa M^2 p} = (\varkappa+1)\omega^2$$

In the remaining surfaces of the system the relative pressure is 0 (the lower surface of the wing is cut at the Mach angle, Fig. 1). Correspondingly, in the case of a triangular wing OAB (Fig. 1a), the coefficient of lift referred to the carrying area of the wing OAB is

$$C_y = (\varkappa+1)\omega^2$$

at a fineness ratio

$$K = \frac{C_y}{C_x} = \sqrt{\frac{(\varkappa+1)(\varkappa-1)}{2\omega C_y}}$$

In the case of a sweptback wing OACB (Fig. 1a), if the rear edge of the wing AC is made along the line of intersection with the Mach cone and a vertex at the point O, then the entire increased lower surface of the wing is acted upon by a constant relative pressure $\bar{p} = C_y = (\varkappa+1)\omega^2$ (at a constant wedge resistance). Consequently, the quality will also increase somewhat by 4.4% at $\varkappa = 1.4$.

*Thus, for example, at large supersonic speeds the product of the coefficient of wave resistance and the square of the elongation is a constant quantity, $C_x L^2 = C^* = \text{const}$. The value of the constant C^* (which is independent of the Mach number) is best calculated from a calculation of the flow around a slender body at $M \to \infty$)see, for example, /9/).

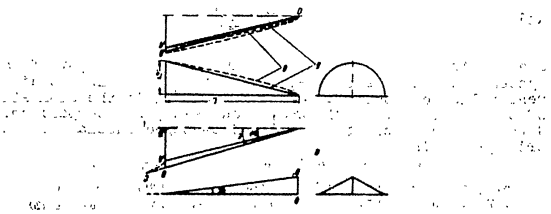

Fig. 1. Three-dimensional systems that make use of the useful interference of the pressure field of fuselage and wing; a -- wedge-shaped fuselage and triangular or sweptback wing; b -- semi-conical fuselage and triangular wing; c -- fuselage in the form of a half-body with power-law shape and corresponding wing.

To investigate a combination of a semi-conical fuselage and a triangular wing (Fig. 1b) or a fuselage in the form of half-body of power-law form and a corresponding wing (Fig. 1c), we use the results of the calculation of the flow parameters at hypersonic velocities around bodies of revolution of power-law form /9/ (see also /10/, /11/), based on the theory of non-stationary one-dimensional self-similar flow of L. I. Sedov /12, 13/. (The tables of the parameters of the flow of bodies of revolution of power-law form $r = cx^m$ at values of m from 1.0 to 0.65 were calculated by 1956 by A. G. Velesko, G. L. Grodzovskiy, and N. L. Krashennikova).

In the systems under consideration (Figs. 1b and c), the forward edge of the wing OB -- $r_2 = cx^m$ coincides with the shock wave from the half-body OA -- $r_T = r_T c x^m$, and therefore the flow around the half-body coincides with the flow around the entire body. The characteristic feature of this flow is the similarity between the profiles of the relative values of the pressure $p_2 = p/p_2$, density $\bar{\rho} = \rho/\rho_2$, etc., as functions of the relative radius $\bar{r}_2 = r/r_2$ (p_2, ρ_2 and r_2 are the parameters on the shock wave, $\bar{r}_T = r_T/r_2$ is the ratio of the radius of the body to the radius of the shock wave). The results of the calculation of the profiles of the pressure and density at $\varkappa = 1.4$ are shown in Fig. 2. The data of Fig. 2a make it possible to determine the distribution of the relative pressure over the lower surface of the half-body with with from the relation

and to $$\bar{p} = \frac{4\bar{p}_2}{\varkappa+1}\left(\frac{dr_1}{dx}\right)^2$$

and to find the corresponding value of the equality of the system. We give below the values of K/c_y and K/L at different values of power exponents $m(\bar{L} = L/r_0$ is the elongation of the shell of the half-body), and also, for comparison, data for the combination of a wedge-shaped fuselage and a triangular wing

m =	1.0	0.9	0.85	0.80	0.75	0.70	0.65	wedge
$K\sqrt{c_y}$ =	1.000	0.995	0.980	0.965	0.945	0.915	0.875	0.250
K/L =	0.695	0.735	0.755	0.775	0.785	0.785	0.765	0.220

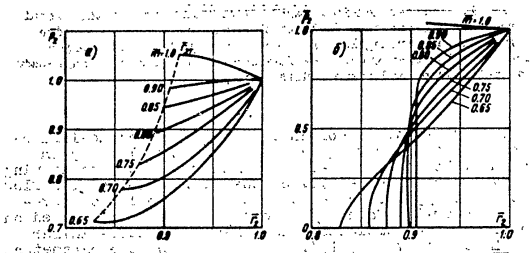

Fig. 2. Profile of relative pressure $\bar{p}_2$ and density $\bar{\rho}_2$ in the sweeping of a body of power-law shape, $\bar{r} = \bar{c}\bar{x}^m$, by a supersonic stream ($\varkappa = 1.4$).

The last column contains the parameters for a wedge-shaped fuselage and triangular wing. The value of C_y pertains to the total area of the triangular wing ABD (Fig. 1a); the situation is the same for the case of a wing with a half-body of revolution (Fig. 1b and 1c). In the case of a wedge-shaped fuselage, the elongation $\bar{L}$ is referred to the radius of the semi-circle that is equivalent to the area of the middle section.

The data of the table shows that hypersonic velocities (unlike the results of the linear theory [2 — 4]) at a specified value of C_y, a combination of a wedge-shaped fuselage and wing has a considerably larger wave resistance than in the case of a half-round fuselage. This is connected with

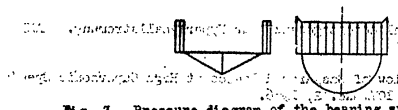

Fig. 3. Pressure diagram of the bearing system in the case a — of a wedge-shaped fuselage and b — of a half-round fuselage, for hypersonic velocities.

the character of the distribution of pressure over the considered systems (Fig. 3), for at a wedge-shaped fuselage the lift is realized only on a small portion of the span.

The transition from the half-conical fuselage to a half-body of power-law form ($m < 1$) reduces somewhat the fineness ratio of the system for a specified C_y and increases the quality for a specified elongation of the hull. It is important here to increase the relative volume of the hull, and the distribution of the density and pressure around the system (Fig. 2) is more favorable with respect to heat protection.

Received 28 May 1958.

BIBLIOGRAPHY

1. Busemann, A. Atti del V Convegno "Volta", Rome, Reale Academia d'Italia, 1935
2. Ferri, A. Recent Theoretical Work in Supersonic Aerodynamics at the Polytechnic Institute of Brooklyn. Proc. of the Conference on High-Speed Aeronautics Polytechnic Inst. of Brooklyn, New York, 1955.
3. Ferri, A., Clarke, J. Lu Ting. Favorable Interference in Lifting Systems in Supersonic Flow. IAS Preprint, No. 664, 1957.
4. Reyn, I. W., Clarke, I. H. An Assesment of Body Lift Contributions and of Linearized Theory for Some Particular Wing-Body Configuration, Rep., No. 305, Polytechnic Inst. of Brooklyn, 1956.
5. Tsien, H. Similarity of Hypersonic Flows. J. Math. a. Phys. v. XXV, 3, 1946.
6. Bam-Zelikovich, G. M., Bunimovich, A. I., Mikhaylova, M. P. Motion of Slender Bodies with Large Supersonic Speeds, Teoreticheskaya gidromekhanika (Theoretical Hydromechanics), Coll. of articles, No. 4, Oborongiz, 1949.

7. Oswatitsch, K. Annlichkeitsgesetze für Hyperschallstromung. ZAMP, 11, No. 4, 1951

8. Chernyy, G. G. Flow of Gas Around Bodies at High Supersonic Speeds, DAN SSSR, Vol. 107, No. 2, 1956.

9. Gonzdovskiy, G. L. Certain Features of Flow Around Bodies at High Supersonic Speeds, Izv. AN SSSR, OTN, No. 6, (1957).

10. Lees, L.; Kubota, T. Inviscid Hypersonic Flow Over Blunt-Nosed Slender Bodies, IAS, III, V. 24, No. 3, 1957.

11. Kubota, T. Inviscid Hypersonic Flow over Blunt-Nosed Slender Bodies, Heat Transfer and Fluid Mech. Inst. Reprints of Papers, Stanford, 1957.

12. Sedov, L. I. Metody podobiya i razmernosti v mekhanike (Methods of Similarity and Dimensionality in Mechanics), 4th ed., M. 1957.

13. Krashenninikova, N. L. On Unsteady Flow of a Gas Displaced by a Piston. Izv. AN SSSR, OTN, No. 8, 1955.

Flow Around Bodies by a Non-Ideal Flow with High Supersonic Velocities

G. A. Lyubimov

Izvestiya Akademii Nauk SSR, Otdeleniye Tekhnicheskikh Nau, Mekhanika i Mashinostroyeniye /News of the Academy of Sciences USSR, Department of Technical Sciences, Mechanics and Machine Building/, No. 1, Jan-Feb., 1959, pages 173-175.

A method was recently proposed for solving the problem of the flow around flat contours and bodies of revolution by a gas stream with large supersonic velocities by expanding the solution in a series with respect to a parameter that characterizes the ratio of the densities in front of the shock and behind it /1 -- 3/.

For a perfect gas with constant specific heat, such a parameter can be the quantity $\varepsilon = (\gamma-1)/(\gamma+1)$ (where γ is the ratio of the specific heats).

The solutions obtained by this method, in which only the first terms of the expansions are retained, are in good agreement with the available exact solutions, and also with the experimental data given at Mach numbers of the incident stream on the order of 3 or 4 and above.

The solution is built up in the expansion in terms of the parameter ε basically by bearing in mind that the gas is considered ideal with a constant ratio of specific heat γ. In reference /3/, it is indicated that the method can be extended to include the flow of non-ideal gases at $M = \infty$.

In the present article, the method of reference /1/ is extended to the case of flow about bodies of revolution and flat contours by a stream of gas with arbitrary dependence of the internal energy on the pressure and temperature.

1. The Fundamental Equations and their Solutions. We choose a system of coordinates, connected with the contour in the stream in such a way that the position of the point M is determined by its distance y along the normal to the surface of the body and by the length x along the arc of the contour, reckoned from a certain fixed point 0 to the base of the perpendicular, dropped from M on the surface of the contour (Fig. 1).

Let us also introduce the stream function ψ defined by the relation

$$d\psi = \rho u r^{\nu-1}\,dy - \rho v r^{\nu-1}\left(1+\frac{y}{R}\right)dx$$

Then the equation of motion of the gas in coordinates x and ψ will be of the form [1]

$$\frac{\partial y}{\partial \psi} = \frac{1}{\rho u r^{\nu-1}}, \qquad \frac{\partial y}{\partial x} = \left(1+\frac{y}{R}\right)\frac{v}{u}, \qquad \frac{\partial S}{\partial x} = 0$$
$$\rho u \frac{\partial u}{\partial x} + \rho v \frac{\partial v}{\partial x} + \frac{\partial p}{\partial x} = 0 \qquad (r = r^{\circ} + y\cos\alpha) \tag{1}$$
$$\frac{1}{1+y/R}\frac{\partial v}{\partial x} - \frac{u}{R+y} = -\rho^{\nu-1}\frac{\partial p}{\partial \psi}$$

where u and v are the velocity components along the directions x and y; p, ρ, and S are the pressure, density, and entropy of the gas, R is the radius of the curvature of the contour, and ν has values of one or two respectively for flat bodies or bodies of revolution, r is the distance of the points from the axis of symmetry, and α is the angle between the tangent to the contour of the body and the direction of the incident stream.

The solution of these equations in the case of flow around bodies with production of a frontal shock wave should satisfy the conditions on the surface of the shock wave, which in the variables adopted have the form

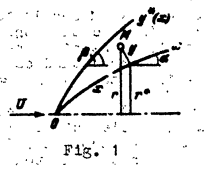

Fig. 1

$$\frac{p_1^{\circ}}{\rho} = \varepsilon \tag{2}$$
$$u + \varepsilon y^{*\prime}\frac{1}{1+y^{*}/R} = U\left(\cos\alpha - \sin\alpha\,\frac{y^{*\prime}}{1+y^{*}/R}\right)$$
$$p = p_1^{\circ} - \rho_1^{\circ}(1-\varepsilon^2)U^2\sin^2\beta$$
$$v - \varepsilon u\frac{y^{*\prime}}{1+y^{*}/R} = \varepsilon U\left(\sin\alpha + \cos\alpha\,\frac{y^{*\prime}}{1+y^{*}/R}\right)$$
$$i(p,\rho) = i(p_1^{\circ},\rho_1^{\circ}) + \frac{1}{2}(1-\varepsilon^2)U^2\sin^2\beta$$

Here, p_1°, ρ_1, and U are the values of the parameters of the gas in the incoming stream, i is the heat content, $y^*(x)$ is the equation of the surface of the shock wave, β is the angle between the tangent to the surface of the shock wave and the direction of the incident stream, ε is the ratio of the densities in front and behind the shock wave which, in the case of a curvilinear wave, is a function of x.

The solutions of the system (1) will be sought in the form of series in powers of ε

$$p = p_0 + \varepsilon p_1 + \ldots, \quad u = u_0 + \varepsilon u_1 + \ldots, \quad \rho = \frac{\rho_0}{\varepsilon} + \rho_1 + \ldots,$$
$$v = \varepsilon v_0 + \ldots, \quad y = \varepsilon y_0 + \ldots.$$

Inserting these series into the system (1), collecting terms of equal order of magnitude, and integrating the resultant equations, we obtain the following expressions for the written terms

$$u_0 = u_0^{\circ}(\psi), \qquad p_0 = \frac{1}{R r^{\nu-1}}\int_0^{\psi} u_0\,d\psi + p_0^{\circ}(x), \qquad S = \theta_0^{\circ}(\psi) = S\left(p_0, \frac{\rho_0}{\varepsilon}\right)$$
$$y_0 = \frac{1}{r^{\nu-1}}\int_0^{\psi}\frac{d\psi}{\rho_0 u_0}, \qquad v_0 = u_0\left(\frac{\partial y_0}{\partial x} + \frac{1}{\varepsilon}\frac{\partial \varepsilon}{\partial x}y_0\right), \qquad \frac{\partial u_0 u_1 \varepsilon}{\partial x} + \frac{\varepsilon}{\rho_0}\frac{\partial p_0}{\partial x} = 0 \tag{3}$$
$$p_1 = \frac{1}{r^{\nu-1}}\int_{\psi_0^{*}}^{\psi}\left\{\frac{u_1}{R} - \frac{1}{\varepsilon}\frac{\partial r_0 \varepsilon}{\partial x} - \frac{u_0}{H}\left[\frac{y_0}{R} + (\nu-1)\frac{y_0}{r^{\circ}}\cos\alpha\right]\right\}d\psi + p_1^{\circ}(x)$$
$$S_0 = \theta_1^{\circ}(\psi) = S\left(p_0 + \varepsilon p_1, \frac{\rho}{\varepsilon}\right)$$

Here, $p_0^*(x)$, $\theta_0^*(\psi)$, $u_0^*(\psi)$, $p_1^*(x)$, and $\theta_1^*(\psi)$ are arbitrary functions of their arguments, which should be determined from the boundary conditions. ψ_0^* will be determined later on.

The boundary conditions should be satisfied on the line $\psi = \psi^*(x)$, which is the equation of the shock wave in the coordinates x, ψ. If we use a suitable numbering of the stream lines, then

$$\psi^{\circ}(x) = \frac{\rho_1^{\circ} U r^{\circ\nu}}{\nu} = \psi_0^{\circ} + \varepsilon\psi_1^{\circ} + \ldots = \frac{\rho_1^{\circ} U}{\nu} r^{\circ\nu}\left(1 + \nu y_0^{\circ}\frac{\cos\alpha}{r^{\circ}} + \ldots\right)$$

where $y_0^* = y_0(x, \psi_0^*)$. Using this, we obtain the following conditions, which should be satisfied by the functions that enter into the solutions at $\psi = \psi^*$

$$\rho_1 = \rho_1^{\circ}, \qquad p_1 = \frac{\partial p_0}{\partial \psi}\Big|_{\psi=\psi_0^{*}}\psi_1^{\circ}, \qquad u_0 = U\cos\alpha, \qquad p_0 = p_1^{\circ} + \rho_1^{\circ}U^2\sin^2\alpha$$
$$p_1 = -\frac{\partial p_0}{\partial \psi}\Big|_{\psi=\psi_0^{*}}\psi_1^{\circ} = \rho_1^{\circ}U^2\sin^2\alpha + \rho_1^{\circ}U^2 2\sin\alpha\cos\alpha\,\frac{1}{\varepsilon}\frac{d\varepsilon y_0^{\circ}}{dx} \tag{4}$$
$$u_1 = -\frac{\partial u_0}{\partial \psi}\Big|_{\psi=\psi_0^{*}}\psi_1^{\circ} + \sin\alpha\,\frac{1}{\varepsilon}\frac{d\varepsilon y_0^{\circ}}{dx}$$

These relations are the consequence of the first three conditions (2) and serve to determine the arbitrary functions

which enter into the solution/ when determining the functions $\delta_0^*(\psi)$ and $\delta_1^*(\psi)$, it is convenient to use the specific form of the dependence of the energy of the gas of the incoming stream on the density and on the pressure, a dependence that can be specified either analytically, or in the form of tables. The fourth condition (2) is satisfied identically, owing to the suitable choice of the function $\psi_0^*(x)$. The last condition of (2) can be written, retaining the principal terms, in the following form

$$i\left(p_0, \frac{\rho_0}{\varepsilon}\right) - i\left(p_1^*, \rho_1^*\right) = \frac{1}{2} U^2 \sin^2\alpha \left(1 + \frac{2}{\nu}\varepsilon\right)$$

This condition serves to determine $\varepsilon(x)$. The value of $\varepsilon(x)$ can be refined after finding the first approximation, using the refined value of the density and pressure.

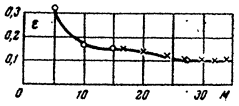

Fig. 2

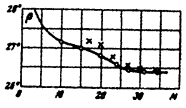

Fig. 3

The fact that the entropy and the heat content are specified as functions of the temperature and the pressure makes it necessary to use also the equation of state, but does not change the formulas obtained.

2. Flow of Stream of Air Around a Cone. By way of an example, of an application of the method detailed above, let us consider the problem of flow of a stream of air around a cone. In this case, the front of the shock wave is a straight line and ε = const. Using solution (3), and the boundary condition (4) for this case ($\nu = 2$), we have

$$u_0 = U\cos\alpha, \quad p_0 = p_1^* + \rho_1^* U^2 \sin^2\alpha, \quad \rho_0 = \rho_1^*$$

$$y_0 = \frac{2\psi}{x \sin 2\alpha \rho_1^* U}, \quad y_0^* = \frac{x \operatorname{tg}\alpha}{2}$$

$$r_0 = -\frac{\psi}{\rho_1^* x^2 \sin\alpha}$$

$$p_1 = -\frac{\psi^2 - \psi_0^{*2}}{\rho_1^{*2} x^4 \sin^2\alpha}$$

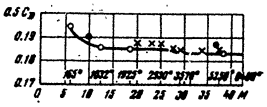

Fig. 4

Figs. 2 -- 4 show the results of the calculation for the case $\alpha = 25°$, $T_1^0 = 220°$, $p_1^0 = 0.1$ atmos.

The values of ε and T_0 were determined in the calculation from the following relations

$$\frac{\rho_1^*}{\varepsilon} = \rho(T_0, p_0), \qquad i(T_0, p_0) = i(T_1^*, p_1^*) = \frac{1}{2} U^2 \sin^2\alpha (1 + \varepsilon)$$

in which the values of the functions $\rho(T,p)$ and $i(T,p)$ were taken from tables /4, 6/.

The crosses on the same figures gave the values of the corresponding quantities, obtained as a result of the numerical calculation of the flow around cones with allowance for the change in the physical-chemical properties of the air at high temperatures.

These calculations were carried out subject to the only assumption that the change in the ratio $\gamma = c_p/c_v$ is small in the region between the shock wave and the surface of the cone (we were able to become acquainted with the results of these calculations at the Laboratory of Physics of Combustion of the Institute of Power Engineering of the Academy of Sciences, USSR).

Fig. 2 shows the dependence of the compression in the shock wave on the Mach number of the incoming stream. At Mach numbers on the order of 20, when the temperature behind the shock wave becomes on the order of 3,000° and the air begins to dissociate, the compression in the shock wave increases more rapidly with increasing Mach number than at lower temperatures.

Fig. 3 shows the dependence of the angle of half the spread of the shock wave, β, on the Mach number.

Fig. 4 shows the values of the coefficients of the resistance, calculated from the following formula

$$\frac{1}{2} c_D = \frac{p - p_1^*}{\rho_1^* U^2} = \left(1 + \frac{\varepsilon}{4}\right) \sin^2\alpha$$

Nonlinear Problems of Stability of Flat Panels at High Supersonic Speeds

V. V. Bolotin

Izvestiya Akakemii Nauk SSR, Otdeleniye Tekhnicheskikh Nauk, Mekhanika i Mashinostroyeniye /News of the Academy of Sciences USSR, Department of Technical Sciences, Mechanics and Machine Building/, No 1, Jan-Feb., 1959, pages 59-64.

The problems of stability of plates and shells, placed in a stream of a compressible gas, were heretofore considered in the linear formulation /1 -- 5/. For a subconic stream, and also for moderate supersonic Mach numbers, this assumption is apparently quite justified. However, at large supersonic velocities the aerodynamic nonlinearity becomes quite substantial. As was shown by V. V. Bolotin /6/ in many problems of theory of aero-elasticity, when taking into account the aerodynamic nonlinearity, there are observed solutions that differ from the unperturbed one, even at velocities less than critical. Among the solutions thus obtained, there are those that are stable with respect to sufficiently small disturbances.

These solutions can be realized if an elastic system, swept at subcritical speeds, is given a sufficiently large disturbance. Each real construction has such disturbances (defects in manufacture, deformations, caused by aerodynamic heating, vibrations under the influence of atmospheric turbulence and other non-stationary factors, etc.). Consequently, the critical velocity as determined by the methods of the linear theory of aeroelasticity turns out to be only the upper boundary of the critical velocities for real constructions (similar, for example, to the upper critical pressure in non-linear theory of elastic shells/7/).

It is the purpose of this article to investigate the stability of rectangular plates, swept with large supersonic speeds at a zero angle of attack. To determine the aerodynamic forces, we use an asymptotic formula of which, as shown in references/8 -- 9/, is valid when $M \gg 1$

$$p = p_\infty \left(1 + \frac{\varkappa - 1}{2} \frac{v}{a_\infty}\right)^{\frac{2\varkappa}{\varkappa - 1}} \qquad (1)$$

Here p is the gas pressure on the surface of the plate, p_∞ is the pressure of the undisturbed gas, v is the normal component of the velocity of the surface of the plate, a_∞ is the velocity of sound for the undisturbed gas, and $\varkappa$ is the polytropic exponent.

The linear approximation of formula (1) was used in references/2 -- 5/, and also in many other papers.

1. Let us consider an elastic plate which is rectangular in plan and has sides a and b. We assume that the plate is swept on both sides supersonic stream of gas with unperturbed velocities directed along the Ox axis and equal to respectively U_+ and U_- (Fig. 1). We shall assume that the plate is fastened in an absolutely rigid diaphragm, the plane of which coincides with the plate of the plane.

The deformations of the plate are described by the following equations

$$D\nabla^2\nabla^2 w = \frac{\partial^2\Phi}{\partial y^2}\frac{\partial^2 w}{\partial x^2} + \frac{\partial^2\Phi}{\partial x^2}\frac{\partial^2 w}{\partial y^2} - 2\frac{\partial^2\Phi}{\partial x\,\partial y}\frac{\partial^2 w}{\partial x\,\partial y} + q$$

$$\frac{1}{Eh}\nabla^2\nabla^2\Phi = \left(\frac{\partial^2 w}{\partial x\,\partial y}\right)^2 - \frac{\partial^2 w}{\partial x^2}\frac{\partial^2 w}{\partial y^2} \qquad (2)$$

where w (x,y,t) is the normal flexure and $\Phi(x,y,t)$ is a function that is connected with the fmx stresses in the mean surface by the following relations

$$N_x = \frac{\partial^2\Phi}{\partial y^2}, \qquad N_y = \frac{\partial^2\Phi}{\partial x^2}, \qquad N_{xy} = -\frac{\partial^2\Phi}{\partial x\,\partial y} \qquad (3)$$

where D is the cylindrical stiffness, h the thickness of the plate, E the modulus of elasticity, and ν the Poisson coefficient.

The sides of the plate will be considered to be freely supported

$$w = \frac{\partial^2 w}{\partial x^2} + \nu\frac{\partial^2 w}{\partial y^2} = 0 \ (x = 0,\ x = a), \qquad w = \frac{\partial^2 w}{\partial y^2} + \nu\frac{\partial^2 w}{\partial x^2} = 0 \ (y = 0,\ y = b) \qquad (4)$$

and, in addition, we assume that they are elastically fixed relative to axial displacements. This makes it possible to consider a continuous transition from a plate with the freely moving edges to a plate whose edges are stationary. Let c_x and c_y be the stiffness coefficients of the elastic couplings. We shall specify that the force boundary conditions on the edges be satisfied "in the mean"

$$\overline{N}_x = -c_x\overline{\Delta}_x, \qquad \overline{N}_y = -c_y\overline{\Delta}_y, \qquad \overline{N}_{xy} = 0 \qquad (5)$$

where $\overline{N}_x$, $\overline{N}_y$, and N_{xy} are the mean stresses on the edges, $\overline{\Delta}_x$ $\overline{\Delta}_y$ are the mean displacements of the edges.

For a plate subject to oscillations, the expression for the normal load component has the form

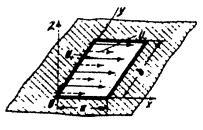

$$q = -\rho_0 h\frac{\partial^2 w}{\partial t^2} - 2\rho_0 h\varepsilon\frac{\partial w}{\partial t} + \Delta p \qquad (6)$$

Here ρ_0 is the density of the material of the plate, ε the damping coefficient, Δp the excess pressure of the gas. This pressure will be calculated using formula (1). If the plate is swept on one side, then $\Delta p = p_\infty - p_+$, where p_+ is determined for the velocity

$$v_+ = \frac{\partial w}{\partial t} + U_+ \frac{\partial w}{\partial x} \approx U_+ \frac{\partial w}{\partial x}$$

(it was shown, in particular, by Hedgepeth /5/ that it is possible to neglect the effect of non-stationarity at large supersonic velocities). Then

$$\Delta p = -\varkappa p_\infty \left[M \frac{\partial w}{\partial x} + \frac{\varkappa+1}{4} M^2 \left(\frac{\partial w}{\partial x}\right)^2 + \frac{\varkappa+1}{12} M^3 \left(\frac{\partial w}{\partial x}\right)^3 + \cdots \right] \quad (7)$$

where $M = U_+ / a_\infty$ is the Mach number for the unperturbed flow.

For the case when the plate is swept on both sides at equal velocities $U_+ = U_-$, the formula for the excess pressure becomes simpler, since the series will contain only odd powers of $\partial w / \partial x$

$$\Delta p = -2\varkappa p_\infty \left[M \frac{\partial w}{\partial x} + \frac{\varkappa+1}{12} M^3 \left(\frac{\partial w}{\partial x}\right)^3 + \cdots \right] \quad (8)$$

Thus, the problem reduces to an investigation of a system of nonlinear equations (2) in the case when the function q is determined by expressions (6), (7), and (8), and subject to boundary conditions (4) and (5). A particular case of this problem is the linear boundary problem, described by the equation

$$D\nabla^2\nabla^2 w + \rho_0 h \frac{\partial^2 w}{\partial t^2} + 2\rho_0 h\varepsilon \frac{\partial w}{\partial t} + \varkappa p_\infty M \frac{\partial w}{\partial x} = 0$$

with boundary conditions (4) or other linear homogeneous conditions, corresponding to other cases of supported mounting. In this [illegible] formulation, the problem was considered in many papers/2 -- 5/, in which it was shown that at certain sufficiently large values of $M = M_*$, the trivial solution $w \equiv 0$ becomes unstable with respect to small disturbances. Physically this corresponds to the occurrence of "panel flutter."

It will be shown below that under certain conditions the nonlinear system has solutions other than trivial and also at $M < M_*$. This means that oscillations of the "panel flutter" type can occur also at $M < M_*$, if the panels are subjected to a suitable initial disturbance. We shall make an estimate of the order of these disturbances below.

2. We shall seek a solution in the form of a series that satisfies the boundary conditions (4)

$$w(x, y, t) = \sum_{j=1}^{m} \sum_{k=1}^{n} q_{jk}(t) \sin \frac{j\pi x}{a} \sin \frac{k\pi y}{b} \quad (9)$$

where q_{jk} are the sought functions of time. Inserting (9) into the second equation of (2), we obtain the function Φ that satisfies the boundary conditions (5). We then insert the expression for Φ (which depends on the unknown functions q_{jk} as parameters) into the first equation. Applying the Galerkin method to this equation, we arrive at systems of ordinary differential equations

$$\frac{d^2 q_{jk}}{dt^2} + 2\varepsilon \frac{dq_{jk}}{dt} + \omega_{jk}^2 q_{jk} + f_{jk}(q_{11}, \ldots, q_{mn}, M) = 0 \quad \begin{pmatrix} j = 1, \ldots, n \\ k = 1, \ldots, m \end{pmatrix} \quad (10)$$

Here ω_{jk} are the frequencies of the small natural oscillations of the plate, and f_{jk} are certain nonlinear functions. The system (10) can be investigated further either using known approximate methods, or else by solving it with the aid of electronic computers. We shall employ both methods below.

An analysis of the corresponding linear problem shows /57 that the flutter motion near $M = M_*$ can be described in first approximation by an expression of the type

$$w(x, y, t) = q_1(t) \sin \frac{\pi x}{a} \sin \frac{\pi y}{b} + q_2(t) \sin \frac{2\pi x}{a} \sin \frac{\pi y}{b} \quad (11)$$

Introducing partial linear frequencies ω_1 and ω_2 and the dimensionless variables $\omega_1 t = \tau$, $q_1 / h = z_1$, $q_2 / h = z_2$, we obtain for the case of flow on one side only

$$z_1'' + \frac{\delta_1}{\pi} z_1' + z_1 + \mu\lambda \left[-\frac{\gamma}{\alpha} z_2 + \mu (a_{11} z_1^2 + a_{12} z_2^2) + \mu^2 z_1 (b_{11} z_1^2 + b_{12} z_2^2) \right] + L z_1 (c_{11} z_1^2 + c_{12} z_2^2) = 0 \quad (12)$$

$$z_2'' + \frac{\delta_2}{\pi} z_2' + \gamma^2 z_2 + \mu\lambda \left[\frac{\gamma}{\alpha} z_1 + \mu a_{21} z_1 z_2 + \mu^2 z_1 (b_{21} z_1^2 + b_{22} z_2^2) \right] + L z_2 (c_{21} z_1^2 + c_{22} z_2^2) = 0$$

The primes denote here differentiation with respect to the dimensionless time.

$$\delta_1 = \frac{2\pi\varepsilon}{\omega_1}, \quad \delta_2 = \frac{2\pi\varepsilon}{\omega_2}, \quad \gamma = \frac{4}{1+\alpha^2}, \quad \alpha = \frac{a}{b}, \quad \mu = M \frac{h}{a},$$

$$\lambda = \frac{4\varkappa p_\infty}{\pi^4 \omega_1^2 h^2} \cdot \frac{48}{\pi^4} \frac{1-\nu^2}{(1+\alpha^2)^2} \frac{\varkappa p_\infty}{E} \frac{a^4}{h^4}, \quad L = \frac{\pi^4 E h^2}{16 \rho_0 \omega_1^2 a^4} = \frac{3}{4} \frac{1-\nu^2}{(1+\alpha^2)^2}$$

$$a_{11} = \frac{2}{9}(\varkappa+1), \quad a_{12} = -\frac{51}{49}(\varkappa+1), \quad a_{21} = \frac{16}{45}(\varkappa+1)$$

$$b_{11} = b_{21} = \frac{1}{40}\pi^2(\varkappa+1), \quad b_{12} = -\frac{9}{20}\pi^2(\varkappa+1), \quad b_{22} = \frac{11}{20}\pi^2(\varkappa+1)$$

$$c_{11} = 1 + \alpha^4 + \frac{2(\beta_x + 2\nu\beta_x\beta_y + \alpha^4\beta_y)}{1-\nu^2\beta_x\beta_y}$$

$$c_{12} = c_{21} = 4(1+\alpha^4) + \frac{81\alpha^4}{(1+4\alpha^2)^2} + \frac{\alpha^4}{(9+4\alpha^2)^2} +$$

$$+\frac{2(4\beta_x+3\pi^2\beta_x\beta_y+\alpha^4\beta_y)}{1-\gamma^2\beta_x\beta_y}$$

$$c_{22}=16\frac{\vartheta_2}{\pi}+\alpha^4+\frac{2(16\beta_x+8\pi^2\beta_x\beta_y+\alpha^4\beta_y)}{(1-\gamma^2\beta_x\beta_y}\,,\quad \frac{1}{\beta_x}=1+\frac{Eh}{ac_x}\,,\quad \frac{1}{\beta_y}=1+\frac{Eh}{bc_y}$$

If the plate is swept on both sides at equal velocities, the system (12) assumes a simpler form

$$z_1''+\frac{\vartheta_1}{\pi}z_1'+z_1+\mu K\left[-\frac{2}{3}z_2+\mu^2z_2(b_{11}z_1^2+b_{12}z_2^2)\right]+$$
$$+Lz_1(c_{11}z_1^2+c_{12}z_1z_2)=0 \qquad (13)$$
$$z_2''+\frac{\vartheta_2}{\pi}z_2'+\gamma^2z_2+\mu K\left[\frac{2}{3}z_1+\mu^2z_1(b_{12}z_1^2+b_{22}z_2^2)\right]+$$
$$+Lz_2(c_{21}z_1^2+c_{22}z_2^2)=0$$

where K has a value twice as large as before.

We note that for the critical value μ_* in the foregoing approximation we obtain the simple formula

$$\mu_*=\frac{(3\gamma-1)}{2K(\delta_1+\delta_2)}\sqrt{\delta_1\delta_2}+O(\delta^2) \qquad (14)$$

3. We seek an approximate solution of the system (13) in among the class of periodic motions with finite amplitudes

$$z_1=A\cos\theta\tau+B\sin\theta\tau+\cdots,\qquad z_2=C\cos\theta\tau+\cdots \qquad (15)$$

Here A, B, C, and θ are certain unknown constants; the dots stand for the terms that contain harmonics. We consider the steady-state self-oscillation mode, and therefore the initial phase is of no importance. Inserting (15) into (13) and neglecting the terms that contain harmonics, we obtain the system of equations

$$(1-\theta^2)A+\frac{\vartheta_1\theta}{\pi}B-\frac{2}{3}\mu KC+\mu^3KC\left[\frac{1}{4}b_{11}(3A^2+B^2)+\frac{3}{4}b_{12}C^2\right]+$$
$$+LA\left[\frac{3}{4}c_{11}(A^2+B^2)+\frac{3}{4}c_{12}C^2\right]=0$$
$$(1-\theta^2)B-\frac{\vartheta_1\theta}{\pi}A+\frac{1}{2}\mu^3KABCb_{11}+LB\left[\frac{3}{4}c_{11}(A^2+B^2)+\frac{1}{4}c_{12}C^2\right]=0$$
$$(\gamma^2-\theta^2)C+\frac{2}{3}\mu KA+\mu^3KA\left[\frac{3}{4}b_{21}(A^2+B^2)+\frac{3}{4}b_{22}C^2\right]+ \qquad (16)$$
$$+LC\left[\frac{1}{4}c_{21}(3A^2+B^2)+\frac{3}{4}c_{22}C^2\right]=0$$
$$-\frac{\vartheta_2\theta}{\pi}C+\frac{2}{3}\mu KB+\mu^3KB\left[\frac{3}{4}b_{21}(A^2+B^2)+\frac{1}{4}b_{22}C^2\right]+\frac{1}{2}LABCc_{21}=0$$

An approximation solution of this system can be obtained by assuming that the damping is sufficiently small. Then $B^2 \ll A^2$, $C \sim A$, $\delta_1 B \ll A$, and $\delta_2 B \ll A$. Using the first two and the last equation, we can express A, B, and θ in term of C, after which, inserting the found values into the third equation, we obtain the resolving equation $\Delta(C)=0$, the roots of which are obtained graphically. Fig. 2 shows the behavior of the function $\Delta(C/A)$ for cylindrical flexure at $\mu=\mu_*$. For the calculations the values taken were K = 30.2, $\delta_1=\delta_2=0.05$ and $\gamma=1.44$. At these values we get $\mu_*=0.372$.

The results of the calculations are shown in Fig. 3. The most interesting result of these calculations is the fact that at sufficiently small β_x (in the example considered this occurs already at $\beta_x=0.4$), the steady state motion is possible at $\mu<\mu_*$. This is seen already in Fig. 2, where the branch of the equation $\Delta(C/A)$ goes into the upper half plane at values $\beta_x \leq 0.4$. The question of the stability of the obtained solutions was not considered theoretically; however, from the shape of the curves at $\beta_x \leq 0.4$, in analogy with the results for a nonlinear system with 1° of freedom, it is possible to conclude that these solutions are unstable (on the same basis one can say that the branches that go from the points $\mu=\mu_*$ to the right correspond to stable solutions). This conclusion was fully confirmed by an analysis of the corresponding equations with electronic analogue devices. Undoubtedly, in the region $\mu<\mu_*$, the physical system has also a stable periodic motion, due to all kinds of nonlinearities, which appear at large displacements (phenomena of breaks in the stream, sharp increase in the dissipation of energy when going out of the elastic stage of work of the material, etc.) These motions could not be obtained from equations of type (12) and (13). The unstable solutions thus obtained are nevertheless of some value, since they indicate the order of the disturbances, necessary in order to cause intense oscillations of the panel. The most sensitive to the initial disturbances are panels with freely displaced edges ($\beta_*=0$). Since the greatest flexure of the plate has an order of magnitude Ah, it is seen from Fig. 3 that in order for dangerous oscillations to occur at $\mu=0.9\mu_*$, it is enough to have a disturbance on the order of 0.5 h. If $\mu=0.8\mu_*$, the order of the necessary initial disturbance increases to h. When $\mu=0.5\mu_*$, it is necessary to have an initial disturbance of 2.5 h. As the stiffness of the longitudinal couplings increases, the sensitivity of the panel to flutter disturbance at subcritical velocities deminishes rapidly. Thus, combined work of the panel as a structural element appears to be favorable as regards its stability under large disturbances. If the disturbances are still sufficiently small, as it is assumed in linear theory, the flutter occurs in the vicinity

of $\mu=\mu_*$. At small β_x we shall have "stiff" excitation of the oscillations with rapid increase of the amplitude to large values. For panels, the edges of which are fastened as regards actual displacements, to the contrary, a slow increase will occur in the amplitude in the post critical region.

Analogous calculations were made also for a square panel under other principal parameters of the same order of magnitude. There is no qualitative difference between the results obtained and those given above for a panel of infinite span.

4. To check the obtained approximate solutions, and also to clarify the character of their stability, the systems of Eqs. (12) and (13) were solved on an electronic computer MN-2 (this work was carried out in the Laboratory of Mathematical Machines of the Moscow Power Institute, with N.I. Chelnokov and Yu. R. Shneyder participating). The solution was carried out for a cylindrical flexure, both in the case of a two-sided and single-sided flow. The values of the parameter μ (i.e., the reduced Mach number) and of the parameter β_x, which characterizes the magnitude of the elastic nonlinearity, were varied. The problem consisted of ascertaining the character of the perturbed solutions for different initial conditions. For all cases it was assumed that $z'_1(0)=z'_2(0)=0$, and the values of $z_1(0)$ and $z_2(0)$ were changed in such a way, that at given μ and β_x the limit was established between the damped and infinitely increasing solutions.

Fig. 4 shows the boundaries of the stability regions for the case $\beta_x=0$ in case of two-sided flow. The region of stability of the trivial solution was located below the origin; the limits of the region in the three other quadrants of the plane $z_1(0)$, $z_2(0)$ were not determined. It is seen from the curve that upon approaching the critical value $\mu_*=0.372$, the dimensions of the stability region diminish, and in the limiting case this region vanishes. The same curve shows the points $z_1(0)=A$, $z_2(0)=C$, corresponding to the values of the approximate solution (16) at $\tau=0$ (these points are denoted by circles).

Figs. 5 and 6 shows typical solutions near the boundary of the stability region. Fig. 5 corresponds to a case $\mu=0.3$, $\beta_x=0$. When $z_1(0)=-z_2(0)=1.15$, the initial disturbance, although slow, nevertheless is damped with time, although slowly. The small increase in the initial disturbance to $z_1(0)=-z_{20}(0)=1.22$ leads to a sharp change in the character of the oscillations: we have flutter motion with rapidly increasing amplitudes. An analogous behavior of the system is obtained when $\mu=0.15$ (Fig. 6). The changeover from stability to instability takes place here as the initial disturbance increases from values $z_1(0)=-z_2(0)=4.3$ to values $z_1(0)=-z_2(0)=4.4$.

Received 18 November 1958.

BIBLIOGRAPHY

1. Bolotin, V. V. Oscillations and Stability of an Elastic Cylindrical Shell in a Stream of Compressible Gas. Inzh. sb. (Engineering Collection) vol 24, 1956.
2. Movchan, A. A. On the Stability of a Panel Moving in a Gas, PMM (Applied Mathematics and Mechanics) vol 21, no 2, 1957.
3. Stepanov, R. D. On the Flutter of Shells and Panels Moving in a Gas Stream, PMM, vol 21, no 6, 1957.
4. Hedgepeth, J. On the Flutter of Panels at high Mach Numbers, J. Aeronaut. Sci., vol 23, no 6, 1957.
5. Hedgepeth, J. Flutter of Rectangular Freely Supported Panels at High Supersonic Speeds. Coll. Mekhanika (Mechanics) IL, no 2, 1958.
6. Bolotin, V. V. On Critical Velocities in Nonlinear Theory of Aeroelasticity. Dokl. vyssh. shkoly, ser. Mashinostroyeniye i priborostroyeniye (Trans. of the Higher Schools, Machine Building and Instrument Building Series), no 3, 1958.
7. Vol'mir, A. S. Gibkiye plastinki i obolochki (Flexible Plates and Shells), Gostekhizdat, 1956.
8. Il'yushin, A. A. Law of Plane Flow at High Supersonic Velocities, PMM, vol 20, no 6, 1956.
9. Ashley, H., and Zartarian, C. Piston Theory -- a New Aerodynamic Tool for the Aeroelastician. J. Aeronaut. Sci., vol 23, no 6, 1956.

Supersonic Flow Around Flat Quasitriangular Wings of Small Length

P. O. Zheludev

Izvestiya Akademii Nauk SSR, Otdeleniye Tekhnicheskikh Nauk, Mekhanika i Mashinostroyeniye /News of the Academy of Sciences USSR, Department Technical Sciences, Mechanics and Machine Building/, No. 3, May-June, Moscow, pages 202-203.

In reference /1/, there is given a method of finding the velocity potential in the second approximation in supersonic flow over slender bodies. We shall use this method to consider the flow over plane quasi-triangular wings of small elongation. The compled potential of the first approximation for such wings is written, after reference /2/, in the following form

$$w(\xi) = \alpha\left(\pm\sqrt{\xi^2 + a^2(x)} - \xi\right) \qquad (1)$$

Here, 2a (x) is the spread of the wing, the plus sign pertains to the upper half plane, and the minus sign to the lower half plane.

Since we seek a real solution near the surface of the wing, we expand (1) in series of positive powers of ξ

$$w(\xi) = \pm\alpha a(x)\left[1 + \frac{1}{2}\frac{\xi^2}{a^2(x)} + \ldots\right] - \alpha\xi$$

This series converges inside the circle $|\xi| \leq a(x)$, and terms in higher powers of $\xi/a(x)$ are discarded as being too small. Then the velocity potential of first approximation is written in the form

$$\varphi_0 = \pm\alpha a(x)\left[1 + \frac{1}{2}\frac{r^2}{a^2(x)}\cos 2\theta\right] - \alpha r\cos\theta$$

The boundary condition for the velocity potential of second approximation is written in the form

$$\frac{\partial\varphi_2}{\partial y} = \left(\frac{1}{r}\frac{\partial\varphi_2}{\partial\theta}\right)_{\theta=\pi/2} = \pm\alpha a'(x)\left[1 + \frac{r^2}{2a^2(x)}\right] \qquad (2)$$

After calculating the derivatives of θ_0 with respect to x, r, and θ, and integrating the equation by the method of iteration Eq. (3.5) of reference /1/, we obtain the particular solution in the following form

Upper half plane:

$$\varphi_{1+}' = \mathrm{Re}\left\{\frac{1}{4}\alpha\xi\bar{\xi}\left[(M_\infty^2-1)\left(a''(x) - \frac{a(x)a''(x) - 2a'^2(x)}{6a^2(x)}\xi^2\right) + M_\infty^2\frac{\alpha}{a(x)}\left(\frac{a'(x)-\alpha}{a(x)}\xi - \frac{a'(x)}{2a^2(x)}\xi\bar{\xi} + \frac{\alpha\xi^2}{3a^2(x)} + \alpha\right)\right]\right\} =$$
$$= \frac{1}{4}\alpha r^2\left\{\left[(M_\infty^2-1)a''(x) + M_\infty^2\frac{\alpha^2}{a(x)}\right] - \frac{1}{3}\left[(M_\infty^2-1)\frac{a(x)a''(x) - 2a'^2(x)}{2} - M_\infty^2\alpha^2\right]\frac{r^2}{a^2(x)}\cos 2\theta + M_\infty^2\frac{\alpha[a'(x)-\alpha]}{a^2(x)}r\cos\theta - \frac{1}{2}M_\infty^2\frac{\alpha a'(x)}{a^2(x)}r^2\right\} \qquad (3)$$

Lower half plane:

$$\varphi_{1-}' = \mathrm{Re}\left\{-\frac{1}{4}\alpha\xi\bar{\xi}\left[(M_\infty^2-1)\left((a''(x) - \frac{a(x)a''(x) - 2a'^2(x)}{6a^2(x)}\xi^2\right) + M_\infty^2\frac{\alpha}{a(x)}\left(\frac{a'(x)+\alpha}{a(x)}\xi + \frac{a'(x)}{2a^2(x)}\xi\bar{\xi} + \frac{\alpha\xi^2}{3a^2(x)} + \alpha\right)\right]\right\} =$$
$$= -\frac{1}{4}\alpha r^2\left\{\left[(M_\infty^2-1)a''(x) + M_\infty^2\frac{\alpha^2}{a(x)}\right] - \frac{1}{3}\left[(M_\infty^2-1)\frac{a(x)a''(x) - 2a'^2(x)}{2} - M_\infty^2\alpha^2\right]\frac{r^2}{a^2(x)}\cos 2\theta + M_\infty^2\frac{\alpha[a'(x)+\alpha]}{a^2(x)}r\cos\theta + \frac{1}{2}M_\infty^2\frac{\alpha a'(x)}{a^2(x)}r^2\right\} \qquad (4)$$

Since the functions (3) and (4) do not satisfy the boundary condition (2), we add to these the following harmonic functions:

Upper plane:

$$\varphi_{1+}'' = -\alpha^2 a'(x)r\cos\theta + \frac{1}{12}\alpha^2[a'(x)(M_\infty^2+2) - M_\infty^2\alpha]\frac{r^3}{a^2(x)}\cos 3\theta \qquad (5)$$

Lower half plane:

$$\varphi_{1-}'' = \alpha^2 a'(x)r\cos\theta - \frac{1}{12}\alpha^2[a'(x)(M_\infty^2+2) + M_\infty^2\alpha]\frac{r^3}{a^2(x)}\cos 3\theta \qquad (6)$$

The functions (5) -- (6) were obtained by representing them in the form of a series

$$\varphi_1'' = a_0''\ln r + \sum_{n=1}^{\infty} n\left(a_n''r^n\cos n\theta + b_n''r^n\sin n\theta\right) + c_1(x)$$

as is done in reference /1/.

Thus, the second-approximation is written as the sum $\varphi_2 = \varphi_1' + \varphi_1''$ in the form:

Upper half plane:

$$\varphi_{2+} = \frac{1}{4}\alpha r^2\left\{\left[(M_\infty^2-1)a'(x)+M_\infty^2\frac{a^2}{a(x)}\right]-\right.$$
$$-\frac{1}{3}\left[(M_\infty^2-1)\frac{a(x)a''(x)-2a'^2(x)}{2}-M_\infty^2\alpha^2\right]\frac{r^2}{a^2(x)}\cos 2\theta-$$
$$+M_\infty^2\frac{a|a'(x)-\alpha|}{a^2(x)}r\cos\theta-\frac{1}{2}M_\infty^2\frac{\alpha a'(x)}{a^2(x)}r^2\Big\}-$$
$$-\alpha^2 a'(x)r\cos\theta+\frac{1}{12}\alpha^2|a'(x)(M_\infty^2+2)-M_\infty^2\alpha|\frac{r^3}{a^3(x)}\cos 3\theta \qquad (7)$$

Hower half plane:

$$\varphi_{2-} = -\frac{1}{4}\alpha r^2\left\{\left[(M_\infty^2-1)a'(x)-M_\infty^2\frac{a^2}{a(x)}\right]-\right.$$
$$\frac{1}{3}\left[(M_\infty^2-1)\frac{a(x)a''(x)-2a'^2(x)}{2}-M^2{}_\infty\alpha^2\right]\frac{r^2}{a^2(x)}\cos 2\theta+$$
$$+M_\infty^2\frac{\alpha|a'(x)+\alpha|}{a^2(x)}r\cos\theta+\frac{1}{2}M_\infty^2\frac{\alpha a'(x)}{a^2(x)}r^2\Big\}+$$
$$+\alpha^2 a(x)r\cos\theta-\frac{1}{12}\alpha^2|a'(x)(M_\infty^2+2)+M_\infty^2\alpha|\frac{r^3}{a^3(x)}\cos 3\theta \qquad (8)$$

Let us derive an expression for the pressure coefficient c_p on a triangular wing. For such a wing, $a(x) = x/\mathrm{tg}\chi$, where χ is the sweep angle relative to the leading edges. In the first approximation, c_p is expressed in the form

$$c_p = 4\frac{\partial\varphi_{0+}}{\partial x} = \frac{4\alpha x}{\mathrm{tg}^2\chi\sqrt{(x/\mathrm{tg}\chi)^2-z^2}} \qquad (9)$$

Here z is the coordinate along the spread of the wing, and after calculating the derivatives with respect to x, r, and we obtain from (3.11)/1/ an expression for the pressure coefficient in the second approximation, in the following form

$$c_p = \frac{4\alpha x}{\mathrm{tg}\chi\sqrt{x^2-(z\,\mathrm{tg}\chi)^2}}-\frac{2M_\infty^2\alpha^2x^2}{\mathrm{tg}\chi\sqrt{[x^2-(z\,\mathrm{tg}\chi)^2]^3}}+$$
$$+\alpha\,\mathrm{tg}\chi\frac{x^2}{x^2}\left\{\left[(M_\infty^2-1)+M_\infty^2\alpha^2\mathrm{tg}^2\chi\right]\frac{x^2}{x^2}-\right.$$
$$-M_\infty^2\alpha^2+\frac{2M_\infty^2\alpha^2x^2\mathrm{tg}^2\chi}{x\sqrt{x^2-(x\mathrm{tg}\chi)^2}}\Big\}+\frac{4\alpha^2}{3\mathrm{tg}\chi}\left(1+\frac{z^2\mathrm{tg}^2\chi}{2x^2}\right) \qquad (10)$$

Expression (10), like the first approximation (9), gives infinite pressure peaks on the leading edges of the wing, i.e., it can be used to calculate the pressure on the wing when $z \neq a(x)$.

Received 10 December 1958.

BIBLIOGRAPHY

1. Zheludev, P. I. Supersonic Flow of Feathered and Unfeathered Slender Bodies of Revolution, Izv. AN SSSR, OTN, No. 9, 1958.

2. Supersonic Flow Past Slender Pointed Bodies, Quart. J. Mech. Appl. Math. V. 2, 75, 1949.

One Form of Equations of Supersonic Gas Flow

F. S. Churikov

Izvestiya Akademii Nauk SSR, Otdeleniye Tekhnicheskikh Nauk, Mekhanika i Mashinostroyeniye /News of the Academy of Sciences USSR; Department of Technical Sciences, Mechanics and Machine Building/, No. 3, May-June, Moscow, pages 204-206

1. It is known that in many important cases supersonic flow of gas is described by a system of two quasi-linear first-order partial differential equations of the hyperbolic type for two functions of two independent variables. Such cases include, for example, unsteady isentropic flow -- homogeneous and spherical, steady state flat irrotational isentropic flow, steady state three dimensional flow with axial symmetry, etc... /1/.

If we denote the independent variables by x, y, and the sought functions by u(x,y), and v(x,y), such a system can be written

$$L_1(x, y, u, v, u_x, u_y, v_x, v_y) = 0, \quad L_2(x, y, u, v, u_x, u_y, v_x, v_y) = 0 \qquad (1.1)$$

where L_1 and L_2 are linear functions with respect to the derivatives.

One of the methods of solving the problems of gas dynamics is based on the linearization of the system (1.1), which is attained either by transforming this system into an equivalent linear system, or by replacing it by an approximate linear system.

Let the system (1.1) be reduced, by some method or other, to a linear system; then, retaining the previous designations for the independent variables and the sought functions and assuming the ordinary conditions of solvability of the linear system are satisfied, the system can be solved with respect to the derivatives v_x and v_y (or with respect to the derivatives u_x and u_y) and written in the following form

$$v_x = a(x, y)v + l(x, y, u, u_x, u_y)$$
$$v_y = b(x, y)v + m(x, y, u, u_x, u_y) \qquad (1.2)$$

where l, m are linear functions of u, u_x, u_y. If the coefficients a(x,y), b(x,y), in (1.2) satisfy the condition

$$\frac{\partial a}{\partial y} = \frac{\partial b}{\partial x} \qquad (1.3)$$

then the system (1.2) can be replaced by one equivalent linear differential equation of second order and of the hyperbolic type, for the function u (or for the function v), which, after transformation to the characteristic coordinates ξ and η, will have the form

$$\frac{\partial^2 u}{\partial \xi\, \partial \eta} = A(\xi, \eta)\frac{\partial u}{\partial \xi} + B(\xi, \eta)\frac{\partial u}{\partial \eta} + C(\xi, \eta)u + D(\xi, \eta) \qquad (1.4)$$

Further simplification of Eq. (2.3), if at all possible, can be only by transforming the sought function.

We shall call the linear hyperbolic second-order equation for the function w compact, and we shall call the function w a compact function, if out of all the derivatives of first and second order it contains only a mixed derivative, i.e., it has the form

$$\frac{\partial^2 w}{\partial \xi\, \partial \eta} = a(\xi, \eta)w \qquad (1.5)$$

Eq. (1.4) can be converted to the form (1.5), if its coefficients of the first derivatives satisfy the condition

$$\frac{\partial A}{\partial \xi} = \frac{\partial B}{\partial \eta} \qquad (1.6)$$

Here the compact function w is determined from the relations

$$w = cu \exp\left(-\int A\, d\eta\right) \quad \text{or} \quad w = cu \exp\left(-\int B\, d\xi\right) \qquad (1.7)$$

if $\partial A / \partial \xi = \partial B / \partial \eta \neq 0$, or else from the relation

$$w = cu \exp\left(-\int A\, d\eta - \int B\, d\xi\right) \qquad (1.8)$$

if $\partial A / \partial \xi = \partial B / \partial \eta = 0$, where c is an arbitrary constant.

In particular if the coefficients A and B in Eq. (1.4) are either constant or satisfy the conditions $A = A(\eta)$, $B = B(\xi)$, such an equation is transformed into a compact equation.

Eq. (1.4), the coefficients of which satisfy condition (1.6) will henceforth be called reducible, and the equivalent system (1.2) will be called the reducible system.

It will be shown below that different linearized equations of gas dynamics are reducible and are therefore transformable into compact equations.

2. a) Supersonic unidimensional unsteady isentropic flow of gas is described by the following hyperbolic quasi-linear system of equations

$$\rho_t + u\rho_x + \rho u_x = 0,\quad u_t + uu_x + (c^2/\rho)\rho_x = 0 \tag{2.1}$$

where all the symbols have the usual meaning. If we interchange the roles of the independent variables x,t and functions u, r, and if the representative functions are subjected not only to the ordinary conditions of continuity and differentiability but to the supplementary condition

$$\frac{D(x,t)}{D(u,\rho)} \neq 0$$

Then the system (2.1) is transformed into the following equivalent linear system

$$x_u - ut_u + \rho t_\rho = 0,\qquad x_\rho - ut_\rho + (c^2/\rho)t_u = 0 \tag{2.2}$$

Condition (1.3) for the system (2.2) is satisfied and consequently the system can be replaced by one equivalent equation of second order.

Introducing the function $\Phi(u,\rho)$, which is connected with the x,t by the following relations[4]

$$\Phi_u = x - ut,\qquad \Phi_\rho = -\frac{c^2}{\rho}t$$

and also introducing a new variable S instead of ρ and the following symbols

$$S = \int_0^\rho \frac{c}{\rho}\,d\rho,\qquad p = a\rho^n,\qquad \frac{dp}{d\rho} = c^2$$

we obtain an equation for the function $\Phi(u,S)$, which after being transformed to characteristic coordinates, determined from the relations

$$\xi = S - u,\qquad \eta = S + u$$

becomes the well known Euler-Poisson-Darboux equation

$$\Phi_{\xi\eta} + \frac{k}{\xi+\eta}(\Phi_\xi + \Phi_\eta) = 0 \qquad \left(k = \frac{3-n}{2(n-1)}\right) \tag{2.3}$$

Condition (1.6) is satisfied for Eq. (2.3), and therefore, putting in accordance with (1.7)

$$w = c\Phi\exp\int\frac{k\,d\xi}{\xi+\eta}$$

we obtain after transformation

$$w_{\xi\eta} = -\frac{k(1-k)}{(\xi+\eta)^2}w \tag{2.4}$$

We note that transformation of Eq. (2.3) to the compact form displays the known case of its integrability in final form when k = 1.

b) The differential equations of plane vortex-free steady state isentropic supersonic flow of gas, as is known, can be written

$$\frac{\partial\varphi}{\partial x} = \frac{1}{\rho}\frac{\partial\psi}{\partial y},\qquad \frac{\partial\varphi}{\partial y} = -\frac{1}{\rho}\frac{\partial\psi}{\partial x} \tag{2.5}$$

where φ and ψ are respectively the potential and the stream function. This system is linearized if the variables x,y are replaced by the variables θ and S, where θ is the angle between the velocity vector q and the x axis, and S is determined from the relation

$$\frac{dS}{dq} = \frac{1}{q}\sqrt{\frac{q^2}{c^2} - 1}$$

and then the system (2.5) is transformed into the linear equivalent system

$$\frac{\partial\varphi}{\partial\theta} = -K\frac{\partial\psi}{\partial S},\qquad \frac{\partial\varphi}{\partial S} = K\frac{\partial\psi}{\partial\theta},\qquad K = \frac{1}{\rho^2}\left(\frac{q^2}{c^2} - 1\right) \tag{2.6}$$

where K depends only on S, and where c denotes the velocity of sound.

Condition (1.3) is satisfied for the system (2.6), and therefore this system is equivalent to one equation for the function φ, or else for the function ψ. After transformation to characteristic coordinates ξ and η, which we determine from the relations $S = \xi + \eta$ and $\theta = \eta - \xi$, these equations become

$$\frac{\partial^2\varphi}{\partial\xi\,\partial\eta} = F(S)\left(\frac{\partial\varphi}{\partial\xi} + \frac{\partial\varphi}{\partial\eta}\right) \tag{2.7}$$

$$\frac{\partial^2\psi}{\partial\xi\,\partial\eta} = -F(S)\left(\frac{\partial\psi}{\partial\xi} + \frac{\partial\psi}{\partial\eta}\right) \qquad \left(F(S) = F(\xi,\eta) = \frac{1}{4}\frac{d}{dS}\ln K\right) \tag{2.8}$$

Each of Eqs. (2.7) and (2.8) is reducible. Thus, for example, assuming according to (1.7)

$$w = c\psi\exp\int F(\xi,\eta)\,d\xi,$$

we obtain a compact equation corresponding to Eq. (2.8)

$$\frac{\partial^2 w}{\partial\xi\,\partial\eta} = \left(F^2 + \frac{\partial F}{\partial\eta}\right)w \tag{2.9}$$

Putting $F^2 + \partial F/\partial\eta = 0$ and integrating Eq. (2.9) subject to the condition $\partial F/\partial\xi = \partial F/\partial\eta$, we find the integral of Eq. (2.8)

$$\psi = \frac{1}{\xi + \eta}[f_1(\xi) + f_2(\eta)]$$

(where $f_1(\xi)$, $f_2(\eta)$ are arbitrary functions). This integral was found by the [illegible] method in reference/3/.

c) The equation for the stream function ψ considered by L.I. Sedov/2/

$$\frac{\partial^2\psi}{\partial\theta^2} + \frac{1}{\sigma}\frac{\partial\psi}{\partial\sigma} + \frac{\sigma}{A^2}\left(\frac{1}{\sigma^2} - 1\right)\frac{\partial^2\psi}{\partial\sigma^2} = 0 \qquad (2.10)$$

in the supersonic region at velocities close to the velocity of sound, is also reducible if it is transformed to variables ξ, η, which are determined from the formulas

$$\xi = \theta - \frac{\sqrt{\sigma}}{3A}(\sigma^2 - 1)^{3/4}, \qquad \eta = \theta + \frac{\sqrt{\sigma}}{3A}(\sigma^2 - 1)^{3/4}$$

The compact equation corresponding to Eq. (2.10) will have the form

$$\frac{\partial^2 w}{\partial\xi\,\partial\eta} = \frac{1}{36}\left[\frac{5}{(\xi-\eta)^2} - \frac{a_1^3}{(\xi-\eta)^{3/4}}\right]w \qquad (2.11)$$

where

$$w = \sigma\psi(\xi-\eta)^{3/4}\exp\left[\frac{a}{4}(\xi-\eta)^{3/4}\right], \qquad a_1^3 = \left(\frac{9A^3}{4\sigma}\right)^{3/4}$$

d) The Euler-Tricomi equation

$$\frac{\partial^2\psi}{\partial z^2} - z\frac{\partial^2\psi}{\partial\theta^2} = 0 \qquad (2.12)$$

at $z > 0$, after being transformed to the characteristic variables

$$\xi = \theta - \tfrac{2}{3}z^{3/2}, \qquad \eta = \theta + \tfrac{2}{3}z^{3/2}$$

corresponds to the following compact equation

$$\frac{\partial^2 w}{\partial\xi\,\partial\eta} = \frac{5}{36(\xi-\eta)^2}w \qquad (2.13)$$

if the compact function is put equal to $w = c\,(\xi-\eta)^{1/6}\psi$.

e) It is also possible to subject to an analogous transformation certain other equations, which are encountered both in gas dynamics and in other divisions of mathematical physics. It is known, for example, that the telegraphy equation

$$\frac{\partial^2 u}{\partial x^2} = a^2\frac{\partial^2 u}{\partial t^2} + b^2\frac{\partial u}{\partial t} + c^2 u \qquad (2.14)$$

where a, b, and c are constants, is transformed into the compact equation

$$\frac{\partial^2 w}{\partial\xi\,\partial\eta} = k^2 w \qquad (2.15)$$

Here $\xi = t - ax$, $\eta = t + ax$, $w = cu\exp\left[\frac{b^2}{4a^2}(\xi+\eta)\right]$

$k^2 = b^4 - 4a^2c^2 > 0$

Estimation of the Permissible Irregularity of Rotation of a Reversible Table for Testing Floated Integrating Gyroscopes for Drift

G. A. Slomyanskiy

Izvestiya Akademii Nauk SSR, Otdeleniye Tekhnicheskikh Nauk, Mekhanika i Mashinostroyeniye /News of the Academy of Sciences USSR, Department of Technical Sciences, Mechanics and Machine Building/, No. 3, May-June, Moscow, pages 211-212.

The angular drift velocity of a floated integrating gyroscope, ω_1, is called the absolute angular velocity, with which it is necessary to rotate the instrument about its input axis (measuring axis) y, in order to maintain the output signal of the gyroscope, the voltage U_-, constant in the absence of current in the control winding of the transmitter (torque transducer). In other words, this is the absolute angular velocity, with which it is necessary to rotate the instrument about its input axis y, in order to produce a gyroscopic torque equal in magnitude and opposite in direction to the noise torque M, acting on a float gyro unit about its axis of rotation x. Tests for drift, i.e., the determination of the angular drift velcoity, is carried out on a special rotary table/1/, shown schematically inthe figure. Located in housing 1 is a motor that drives shaft 2, to which is attached platform 3. By inclining the housing 1 about its suspension axis ξ, it is possible to set the shaft 2 vertically, horizontally, or at some other angle to the horizontal.

Shaft 2 is strictly perpendicular to the axis ξ. The axis ξ, in one method of testing, is placed perpendicular to the plane of the meridian, and in another method, it is placed in the plane of the meridian. Fastened on platform 3 is the tested float integrating gyroscope 4. Its input axis y is placed along or parallel to the axis of rotation of shaft 2, while the x axis is placed in a plane perpendicular to shaft 2. In some tests this axis occupies a horizontal position and in others a vertical one.

The axis z_0 is perpendicular to the axes x and y. Deviations of the axes of the gyroscope figure z from the axis z_0 (the angle β) can be only small. In certain cases tests for drift are made with the instrument occupying such a position, at which it is subjected to a transfer angular velocity ω_2, equal to the projection of the angular velocity of the daily rotation of the earth on the y axis.* In other

* All the angular velocities around the y axis will be considered positive if the direction of their vectors coincides with the positive direction of the y axis.

cases the instrument is placed in such a way, that the angular velocity of the daily rotation of the earth does not affect it.

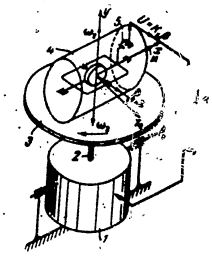

In the presence of a torque M and an angular velocity ω_2, in tests for drift, there appears a voltage U_- at the output of the angle transducer 5 of the gyroscope. This voltage is applied to amplifier 6, which feeds the drive motor of shaft 2. The motor is actuated and starts rotating the platform 3 with a certain relative angular velocity ω_3. Were the torque M to be equal to 0, and were the dependence of the velocity 3 on the voltage U_- to be strictly proportional, then we would have the equality $\omega_3 = -\omega_2$ at $K_1 = \text{const}$ (see figure). Under the same conditions, but with $M \neq 0$, the equality $\omega_3 = -\omega_2$ will not hold. In this case the absolute angular velocity $\omega_1 = \omega_2 + \omega_3$ will indeed be the sought drift velocity of the floated integrating gyroscope, due to the presence of a torque M (when $\omega_2 = 0$ we have $\omega_1 = \omega_3$). However, if the setup is such that when amplifier 6 is disconnected from the angle transducer 5 and if a certain voltage $U_+ = \text{const}$ is applied to the input of the amplifier, then the platform 3 rotates unevenly, then the drift velocity on it will be determined with a certain relative error ε. Let us calculate what the permissible value of unevenness in platform rotation should be at $U_+ = \text{const}$, in order for ε not to exceed a certain specified value. Let us denote by ω_3 the actual value of the relative angular velocity of the platform at $U = \text{const}$; by $\omega'_3 = -K_2 U_+$ ($K_2 = \text{const}$) we denote the ideal value of the relative angular velocity of the platform; let $\delta = (\omega_3 - \omega'_3)/\omega'_3$ be the relative error of the relative angular velocity of the platform, or, in other words, the unevenness in rotation of the platform.

Neglecting inertia, we assume that

$$\omega_3 = -K_2 U_+ (1 + \delta_{max} \sin \omega t) \qquad (1)$$

In this case $\delta = \delta_{max} \sin \nu t$, where δ_{max} is the maximum unevenness in rotation of the platform, which will be assumed to be a small quantity.

Assuming the gyroscope not to have any inertia, we can write its equation in the form

$$\frac{K_2}{K_1} \dot{U}_- = H(\omega_2 + \omega_3) - M \qquad (2)$$

where H is the intrinsic (kinetic) torque of the gyroscope, K_2 the specific damping torque in g-cm/(1/sec); K_1 the slope of the angle-transducer characteristic in v/rad.

Combining (1) and (2), and bearing in mind that $\omega_1 = M/H$ and $U_- = U_+$, we get

$$T\dot{\omega}_2 + \omega_2 = -(\omega_2 - \omega_1) + \delta_{max}\left[\frac{\nu T \cos \nu t}{1 + \delta_{max} \sin \nu t}\omega_2 - (\omega_2 + \omega_3 - \omega_1)\sin \nu t\right] \qquad (3)$$

where $$T = \frac{K_2}{HK_1}$$

Neglecting in Eq. (3) the term $\delta_{max} \sin \nu t$ compared with unity, in view of the smallness of δ_{max}, and making use of expansion in powers of small parameter/2/ for integration of this equation, with the small parameter being in our case δ_{max}, we find that in the steady state

$$\omega_2 = -(\omega_2 - \omega_1)\left[1 + \frac{\delta_{max}\nu T}{1 + \nu^2 T^2}(\cos \nu t + \nu T \sin \nu t)\right] \qquad (4)$$

The relative error in the determination of the drift is $\varepsilon = (\omega_1 - \omega_1)/\omega_1$, where $\omega_1 = \omega_2 + \omega_3$ is the measured value of the angular drift velocity. Using expression (4), we get

$$\varepsilon = \left(1 - \frac{\omega_2}{\omega_1}\right)\frac{\delta_{max}\nu T}{1 + \nu^2 T^2}(\cos \nu t + \nu T \sin \nu t)$$

From this, replacing the expression in the last bracket by its maximum value, we obtain the following formula for an estimate of the maximum permissible unevenness in platform rotation

$$\delta_{max} < \frac{|\varepsilon|}{\nu T}\frac{1 + \nu^2 T^2}{|1 - \omega_2/\omega_1|} \qquad (5)$$

Considering that in drift tests $\omega_{2max} = 15°/hr$ and assuming $\omega_1 = 0.01°/hr$, we can readily see that for acceptable operation of the rotary table the product νT should be considerably less than unity. Consequently, we can write (for $\omega_2 \neq 0$)

$$\delta_{max} < \frac{|\varepsilon|}{\nu T}\left|\frac{\omega_1}{\omega_2}\right|$$

Received 6 February 1959

BIBLIOGRAPHY

1. Slonimskiy, G. A., Priyadilov Yu. N. Poplavkovyye giroskopi i ikh primeneniye (Floated Gyroscopes and Their Applications), Oborongiz, 1958.

2. Krylov, A. N., Lektsii o priblizhennykh vychisleniyakh (Lectures on Approximate Calculations), Izd. AN SSSR, L. p 344, 1953.

All-Union Conference on Static Stability of Turbomachinery

Ye. I. Boldyrev

Izvestiya Akademii Nauk SSR, Otdeleniye Tekhnicheskikh Nauk Mekhanika i Mashinostroyeniye [News of the Academy of Sciences USSR Mechanics and Machine Building] No. 3 May-June Moscow pages 213-214.

From 9 through 12 February 1959, there was held in Leningrad an All-Union Conference on Problems of Static Strength of Turbine Machinery, called together by the Commission on Strength of Gas Turbines at the Institute of Mechanics Academy of Sciences USSR (Chairman of Commission Academician Yu. N. Rabotnov) and by the Leningrad Technical Council on T Turbine Construction.

Participating in the conference were approximately 250 representatives of the scientific institutions, higher institutions of learning, and plants of Moscow, Leningrad, Kiev, Khar'kov, Chelyabinsk, Novosibirsk, and other cities. Twenty-two papers were delivered.

The paper by V. P. Rabinovich (Central Scientific Research Institute of Technology and Machinery) and Yu. N. Rabotnov (Institute of Hydrodynamics, Academy of Sciences USSR) "Strength of Turbine Disks Under Conditions of Creep", was devoted to the results of an investigation of the influence of plastic properties of materials on strength of the turbine disk, operating under creep conditions.

As a result of the investigations it has been shown that as the plasticity of the material is decreased, the deformation of the disk is decreased, and this decrease is greater than in specimens. There is also a change in the character of their failure, a reduction in the strength of the disk, and the disk design based on mean stresses becomes unreliable.

Along with this, for any plasticity (within the limits of the investigations) of the material and for any character of failure, the condition $\sigma_i = \sigma_{long}$ for the failure of the disk remains in force, i.e., the disk fails when the maximum stress reaches the long-term ultimate strength.

For any plasticity of the material, the stresses and deformations of the disks are reliably determined from the aging theory as formulated by Yu. N. Rabotnov.

It is shown that a reduction in the strength of the disks with decreasing plasticity is connected with the reduction in the degree of

redistribution of the stresses.

A.D. Kovalenko (Institute of Structural Mechanics, Academy of Sciences Ukrainian S S R), in a paper "Thermal Stresses in a Disk of Symmetrical Profile in a Three-Dimensional Temperature Field" considered the problem of thermal stresses in a thin disk of radially-variable stiffness, in the case of a three-dimensional temperature field, when the temperature varies along the radius, periphery, and thickness of the disk. It is assumed here that the ordinary process of non-stationary heat exchange takes place, at which the rate of change of temperature is small compared with the velocity of sound.

The introduction of generalized thermal deformations has made it possible to subdivide this problem into two: the problem of the asymmetrical thermal elongation (concering the plane-stressed state) of the disk and the problem of the asymmetrical thermal flexure of the disk.

The use of a static-geometrical analogy has permitted an investigation of only one resolving equation instead of the two that describe the problems of elongation and bending of the disk.

Analytical solutions have been found in hypergeometric functions for a wide class of disk profiles.

Ye. R. Plotkin (All-Union Heat Engineering Institute) in a paper "Investigation of the Strength of an Experimental Diaphragm of Welded Construction with Reinforcing Ribs" has reported the results of an experimental investigation of the strength of a welded diaphragm with narrow blades and reinforcing ribs.

Ya. A. Shustorovich (Leningrad Metal Plant) lectured on the topic "Calculation of Disks in Accordance with Their Bearing Ability."

B. F. Thorr (Central Scientific Research Institute of Aircraft Engines imeni P.I. Baranov) in a paper "Calculation of Turbine Parts for Creep in Variable Temperature" has developed a method for calculating turbine parts for creep under variable temperature.

The paper by A.V. Amel'yanchik (Central Scientific Research Institute of Aircraft Engines imeni P.I. Baranov) was devoted to the calculation of disks and shells using mathematical computers.

The paper by Ye. I. Molchanov (All-Union Heat Engineering Institute) "Investigation of Temperature Fields in Operating Blades of Gas Turbines" was devoted to a procedure of calculation of temperature fields, occurring in rotors of gas turbines; these calculations

were carried out with a hydraulic integrator under non-stationary conditions.

I. A. Birger (Central Scientific Institute for Aviation Engines imeni P.I. Baranov) in a paper "Method of Variable Parameters of Elasticity in Problems of the Theory of Plasticity" developed an approximate method for solving many problems in the theory of plasticity, based on representation of the equations of plasticity of Henky in the form of ordinary Hooke equations. The elasticity parameters were found in general to depend on the stress state at the point. The calculation was carried out by the method of successive approximation, and the original approximation was assumed to be the elastic solution.

The method was used to calculate blades, disks, and shells of rotation.

In a second paper, "Calculation of Structurally-Orthotropic Shells of Rotation" I.A. Birger developed a method for calculating shells of rotation with very frequent reinforcement by means of longitudinal and annular ribs. The parameters of elasticity of the shell and the temperature deformation vary arbitrarily along the thickness of the shell.

Formulas were given for the stresses in the case of plane deformation of a cylindrical shell with longitudinal reinforcement.

To calculate shells in the region of plasticity or creep (in accordance with the aging theory), the method of variable elasticity parameters is used.

The paper by B. Ya. Britvar (Leningrad Metal Plant) was devoted to problems of joining austenitic blades of gas turbines to pearlite rotors.

L. M. Kachanov (Leningrad State University), in a paper "On an Approximate Solution of Problems of Creep" dwelled on an examination of the steady-state creep of a body at specified stresses on the surface in a power-law variation of the creep. He introduced the concept of an ideally creeping body. The solution of the problem of minimum additional scattering is sought in the form of a linear combination of an "elastic" distribution of stresses and a distribution of stresses in an ideally creeping body. The conditions under which the stressed state in an ideally creeping body coincides with the stressed state in the corresponding problem for an ideally plastic body are indicated.

M.A. Radtsig (Central Scientific Research Institute for Boilers and Turbines imeni Polzunov) delivered a paper, "Calculation of Certain Parts of Steam and Gas Turbines Under Creep Conditions."

The paper by B. Ye. Sivchikov (LKVVIA imeni A.F. Mozhayskiy), "Investigation of Blades of Turbines by the Photoelasticity Method" was devoted to the results of an experimental investigation of the stressed state of rotating blades of gas turbines under conditions of their elastic stretching and uniform heating. A study of the stresses was carried out on natural models of many blades of gas turbine engines. The procedure of determining the stresses did not differ in principle from the procedure used to investigate three-dimensional stressed states using the "freezing" of the deformations.

I.A. Oding and Z.G. Fridman (Institute of Metallurgy Academy of Sciences U S S R, imeni A.A. Baykov) in a paper, "Influence of Scale Factor on Long-Term Strength" reported the results of an experimental investigation of the influence of the scale factor, connected with the influence of the surface layer on the surface of a metal in creep. It is shown that the scale factor influences considerably the plasticity and the service life of samples, and reduces their values with increasing thickness of the sample.

The paper by I.A. Oding and V.N. Geminov (Institute of Metallurgy Academy of Sciences U S S R imeni A.A. Baykov) was devoted to problems of temperature-forced dependence of long-term strength.

B.V. Zver'kov (Central Scientific Research Institute for Boilers and Turbines imeni Polzunov) in a paper "Creep of Tubes Under Complex Loads" reported the results of a study of the creep of tubes under complex loads.

The paper by V.S.Chernina (Central Scientific Research Institute for Boilers and Turbines), "Problems of Calculation of Welded Unequal Pipes and Welded Journals of Turbine Rotors" was devoted to the results of work at the Central Scientific Research Boiler and Turbine Institute imeni Polzunov towards creating methods of calculating welded unequal pipes and welded journals of turbine rotors. The author considers elastic-plastic deformation of a welded inhomogeneous tube for two cases: ideal plasticity and linear strengthening of the material. The residual temperature and working stresses in welded journals of a turbine rotor are determined for various loading conditions.

R. N. Sizova (Central Scientific Research Institute of Aircraft Engines imeni P.I. Baranov) delivered a communication "Summation of Tendency to Damage During Testing for Long-Term Strength Under Conditions of Multiple Overloads."

Z.I. Rozenblyum (Central Boiler and Turbine Institute imeni Polzunov) lectured on the subject "On the Strength of Welded Non-homogeneous Disk of a Gas Turbine."

A.D. Kovalenko, and L.A. Il'in (Institute of Structural Mechanics Academy of Sciences, U.S.S.R.) delivered a paper on the topic "Investigation of the Stressed State of Covered Working Rotors of Centrifical Compressors.

In the adopted resolution, the conference noted that during the last years considerable progress was achieved in work on the determination of static strength of elements of turbine machinery. Methods have been developed for the design of disks and rotors under conditions of prolonged operation, experimental research has been done and is being continued on the strength of disks, and this research essentially justifies the computation procedure that has been developed. Effective methods have been produced for determining heat stresses in turbine parts, particularly in constructions with reinforcing elements. High speed electronic computers have found application in computation practice. The availability of such machines extends the possibility of employing more accurate and more complicated computation methods, which reflect quite well the physical properties of the material, the features of the construction, and the operating conditions. On the other hand, any of the existing computational methods can be brought to such a state, that they can be employed in the daily practice of the construction bureaus of the plants.

The conference calls attention of the scientific workers to the need for developing specific sufficiently simple methods, suitable for rapid mastery on the part of the plant workers, on the compilation of tables and nomograms that facilitate calculations.

The conference proposes that the use of modern computational techniques in the design of turbine machinery should be extended more and more and recommends a considerable increase in the use of computing machines in the computation practice of the construction bureaus, involving in this project the available computational centers.

In the field of statistical strength, the most urgent problems at the present time are those connected with the study of strength of parts under conditions of non-stationary temperature modes and variable loads, and also the search for optimum structural forms and technological procedures (composite rotors, disks of radial turbine machines, the use of welding, etc.).

The conference calls attention to the need of reinforcing the theoretical and particularly experimental research in these directions.

The conference notes the known strengthening work in the field of research of creep and ultimate strength of materials and constructions, but the scope of these works is still considered insufficient and lagging as regards the requirement of the rapidly developing construction of power machinery.

The investigations performed have resulted in certain material for establishing criteria of strength, but until now there are now well founded norms of strength for the principal parts and units of turbine machinery, operating with high parameters.

The conference considers it necessary to carry out planned and systematic work on the formulation of strength norms.

Coordination Conference on Stability of Gas Turbines

Izvestiya Akademii Nauk SSR, Otdeleniye Tekhnicheskikh Nauk Mekhanika i Mashinostroyeniye [News of the Academy of Sciences USSR Mechanics and Machine Building], No. 3, May-June, Moscow, page 215

Ye. . . Kolodyrev

A coordination conference on the strength of gas turbines, called together by the Commission on Gas Turbines of the Institute of Mechanics Academy of Sciences USSR, was held on 6 -- 7 January 1959, at the Institute of Mechanics Academy of Sciences USSR.

Participating in the conference were workers from plants of turbine-building industry, scientific-research institutes of the industry, and of the academies of sciences of the country, as well as of the higher institutions of learning in Moscow, Leningrad, Kiev, Novosibirsk, and Chelyabinsk.

Papers were delivered and discussed on the performance of the plans during 1958, and also for the plans of1959, in the field of strength of turbine machines, performed on the part of the principal scientific research institutes and plants.

The coordination conference noted the following:

1. For successful operation of the groups that have been created by the Commission on Coordination and of the scientific-research work in various directions in the field of strength of turbine machinery, it is necessary to assign these projects to the institutes in which specialists that head the groups are working.

2. In spite of the numerous resolutions of the preceding conferences (the Leningrad Conference on the Long-Term Static Strength of Turbine Machinerey -- November 1957, the Leningrad Conference on Dynamic Strength -- April 1958, and the Leningrad Conference on Tensometry -- May 1958), the Gosplan of the USSR has thus far not solved the problem of organizing in the USSR an enterprise on the production of tensometric apparatus for the investigation of static and dynamic deformations under normal and high temperatures.

3. The program of the Conference on Static Strength of Turbine Machinery, which should be held in Leningrad in February 1959, was discussed.

The coordination conference has resolved:

1. To assign the working groups that are incorporated in the Commission on Strength of Gas Turbines, which carry out the direct coordination work in their fields, to the institutes and plants in which the leaders of the groups work.

2. To request again of the Gosplan of the USSR to organize a specialized enterprise on the production of tensometric transducers and apparatus associated with them.

3. To request the leaders of the organizations, associated with the problem of strength of turbine machinery, to send to the commission (Moscow, Leningradskiy prospekt, 7, Institute of Mechanics Academy of Sciences USSR) notes concerning the work performed, in order that the commission be able to submit them to all the interested organizations as well as plans of work on the problem of strength.

1107

E N D

STAT